© 2019 by Bo Han. All rights reserved.

APPLICATIONS OF CONFORMAL FIELD THEORIES IN TOPOLOGICAL PHASES OF MATTER

BY

BO HAN

DISSERTATION

Submitted in partial fulfillment of the requirements
for the degree of Doctor of Philosophy in Physics
in the Graduate College of the
University of Illinois at Urbana-Champaign, 2019

Urbana, Illinois

Doctoral Committee:

Professor Taylor Hughes, Chair
Professor Michael Stone, Director of Research
Assistant Professor Thomas Faulkner
Professor Lance Cooper

Abstract

This dissertation discusses some applications of conformal field theories (CFTs) in topological phases of matter.

The first part is devoted to a discussion of coupled wire constructions of some novel quantum Hall systems. Through a theoretical coupled wire model, we construct strongly correlated electronic *integer* quantum Hall states with filling factor $\nu = 16$. The edge state is a bosonic chiral $(E_8)_1$ CFT, which is closely related to topological paramagnets in (3+1)d. As a distinguishing feature, these states support electric and thermal Hall transport violating the Wiedemann-Franz law as $(\kappa_{xy}/\sigma_{xy}) \,/\, \left[\left(\pi^2 k_B^2 T\right)/3e^2\right] < 1$. We further construct two descendant non-Abelian quantum Hall states at filling $\nu = 8$, each carrying bosonic chiral $(G_2)_1$ or $(F_4)_1$ edge theories, and hosting Fibonacci anyonic excitations in the bulk. Finally, we discover a new notion of particle-hole conjugation based on the E_8 state that relates the G_2 and F_4 Fibonacci states, which is reminiscent of similar physics in half-filled Landau level.

The second part is focused on the surface topological orders of 3D bulk topological systems. Symmetry-protected and symmetry-enriched topological (SPT/SET) phases in three dimensions are quantum systems that support non-trivial two-dimensional surface states. These surface states develop finite excitation energy gaps when the relevant symmetries are broken. On the other hand, one-dimensional gapless modes can populate along interfaces that separate adjacent gapped surface domains with distinct symmetry-breaking orders. A surface strip pattern in general reduces the low-energy SPT/SET surface degrees of freedom onto a 2D array of gapless 1D channels. These channels can be coupled to one another by quasiparticle tunneling, and these inter-wire interactions collectively provide an effective description of the surface state. In this part, we study a general class of symmetry-preserving or breaking SPT/SET surface states that admit finite excitation energy gaps and Abelian topological orders via the coupled wire construction. In particular, we focus on the prototype Abelian surface topological orders that fall under the ADE classification of simply-laced Lie algebras. We also elaborate on the emergent symmetry and duality properties of the coupled wire models.

The third part is to discuss the relation between the conformal boundary state and (2+1)d SPT phases.

We propose a diagnostic tool for detecting nontrivial symmetry-protected topological (SPT) phases protected by a symmetry group G in $2+1$ dimensions. Our method is based on directly studying the $1+1$-dimensional anomalous edge conformal field theory (CFT) of SPT phases. We claim that if the CFT is the edge theory of an SPT phase, then there must be an obstruction to cutting it open. This obstruction manifests as the non-existence of boundary states in the CFT that preserves both the conformal symmetry and the global symmetry G. We discuss the relation between edgeability and gappability in the presence of G. We study several examples including time-reversal symmetric topological insulators, $\mathbb{Z}_N$ symmetric bosonic SPT phases, and $\mathbb{Z}_2 \times \mathbb{Z}_2$ symmetric topological superconductors.

To my parents and friends.

Acknowledgments

First of all, I would like to thank my advisor Michael Stone for his scientific guidance, generous support, and constant encouragement. I have learned a lot of mathematics and physics from discussions with him and from his personal notes that he shared with me after each discussion. He has taught me to work on problems that I am particularly obsessed with, rather than those that people are most interested in. I will always remember that and try to keep it in the rest of my life.

I would like to thank my collaborator, Shinsei Ryu, who brought me into the world of conformal field theories and showed me how interesting and beautiful it is in itself and how useful it is as a tool to study various problems in condensed matter and high energy theories.

I would like to thank my collaborator, Jeffrey Teo, who has always been patient to me and taught me many things on topological phases of matter, especially on conformal field theories and coupled wire models.

I would like to thank Lance Cooper, for helping me through the hard time I had during my PhD study in UIUC. Whenever I was in a dilemma, I went to talk to him.

I would like to thank Taylor Hughes, Thomas Faulkner and Lance Cooper for being the committee members of my thesis defense and their support on my thesis.

I would like to thank my collaborators and friends, Chang-Tse Hsieh and Xueda Wen, who have helped me substantially on my research and the completion of my PhD study. I have benefited a lot from discussions and conversations with them.

I have benefited greatly from collaborations, discussions and interactions with my collaborators and colleagues in and out UIUC. To name a few of them: AtMa Chan, Xiao Chen, Thomas Faulkner, Zihe Gao, Taylor Hughes, Ady Stern, Apoorv Tiwari, Huajia Wang, Yuxuan Wang, Wenchao Xu, Peng Ye, Mao-Chuang Yeh, Beni Yoshida, Jitong Yu, Tianci Zhou, Ye Zhuang.

Finally, I would like to express my sincere gratitude to my parents, Yu Han and Yuzhu Guo for their endless love and support, with which I believe that I can overcome any difficulty I meet.

Table of Contents

List of Figures viii

Chapter 1 Introduction 1

Chapter 2 Coupled wire construction of Quantum Hall systems 7
2.1 Novel quantum Hall state 8
2.1.1 E_8 quantum Hall state 8
2.1.2 G_2 and F_4 Fibonacci quantum Hall states 13
2.2 Particle-hole conjugation 15

Chapter 3 Coupled wire models of surface topological orders 16
3.1 Summary of results 18
3.2 General coupled wire construction of surface gapping interactions 20
3.2.1 $SO(6)$ and $U(4)$ as illustrative examples 22
3.3 Review of free Dirac fermion/3d QED duality 35
3.4 D-series: SO(N) surface theory 39
3.4.1 Surface massless Majorana fermions in a coupled wire model 39
3.4.2 Gapping potentials for surface Majorana fermions 42
3.4.3 Duality transformation of the Hamiltonian and the symmetry 47
3.5 A-series: U(N) surface theory 49
3.5.1 Surface gapless Dirac Hamiltonian via coupled wire construction and decomposition . 49
3.5.2 Gapping terms for surface Dirac fermions 51
3.5.3 Duality transformation 60
3.6 E-series surface theory 61
3.6.1 $E_7 \times SU(2)$ 65
3.6.2 $E_6 \times SU(3)$ 67

Chapter 4 Boundary conformal field theories and symmetry protected topological phases 71
4.1 Introduction 71
4.1.1 SPT phases and quantum anomalies 71
4.1.2 Edgeability 72
4.1.3 Gappability 73
4.1.4 Working Principles 74
4.2 An introduction to BCFT 75
4.3 Edge theories of (2 + 1)d time-reversal symmetric topological insulators 78
4.4 More general SPT phases in (2 + 1)d 83
4.4.1 Canonical quantization 83
4.4.2 Ishibashi states 85
4.4.3 Equivalence between the Ishibashi condition and Haldane's null vector condition . . . 87
4.4.4 Symmetry analysis 88
4.4.5 Example: $\mathbb{Z}_2$ symmetric bosonic SPT 89
4.4.6 Generalization to $\mathbb{Z}_N$ cases 93

4.4.7 General symmetry groups . . . 95
4.5 (2+1)D topological superconductors . . . 96
4.5.1 Quantization and boundary states . . . 96
4.5.2 Boundary states and the $\mathbb{Z}_8$ classification . . . 99
4.5.3 Boundary conditions, gapping potentials and triality . . . 101

Chapter 5 Conclusions and outlook . . . 104

Appendix A Details of Chapter 2 . . . 110
A.1 E8 Quantum Hall state and momentum commensurability conditions . . . 110
A.2 A G2 x F4 conformal embedding into E8 . . . 112
A.2.1 From E_8 to $SO(16)$ . . . 112
A.2.2 From $SO(16)$ to $G_2 \times F_4$ . . . 114
A.3 G2 and F4 quantum Hall states momentum commensurability conditions . . . 118
A.4 Fibonacci primary field representations in the G2 and F4 WZW CFTs at level 1 . . . 118

Appendix B Details of Chapter 3 . . . 123
B.1 Gapping conditions for K-matrix formalism . . . 123
B.1.1 Gapping terms for the general K-matrix theory . . . 123
B.1.2 Gapping conditions in different basis . . . 124
B.2 Simply-laced Lie algebras and their representations . . . 125

References . . . 129

List of Figures

1.1 Adopted from Ref. [1]. Some experimental setup and data for IQHE. 2
1.2 Adopted from Ref. [2]. Some experimental setup and data for FQHE. The sample for this experiment is a 500 Å wide modulation-doped GaAs/AlGaAs quantum well of size about 5 mm × 5 mm. 2
1.3 Adopted from Ref. [3]. (a) Landau levels with the finite size effect. The intersections between the Fermi energies and the Landau levels represent the chiral modes on the boundary. (b) Classical picture of the cyclotron motion of electrons in the bulk and on the edge. l_0 is the magnetic length. (Illustration: Alan Stonebraker/stonebrakerdesignworks.com). 3
1.4 Adopted from Ref. [4]. (a) 1D array of quantum wires placed on the 2D plane. The magnetic field is perpendicular to the plane. (b) The interwire and intrawire scattering processes at some fractional filling factor. 4

2.1 Coupled-wire model of the E_8 quantum Hall state at filling $\nu = 16$. Black lines represent bundles with 11 electron wires, each carrying a counter-propagating pair of Dirac fermions, in the presence of a magnetic flux (green). Yellow boxes represent an unimodular basis transformation U ($\det(U) = 1$) restructuring $U(11)_1 \to U(3)_1 \times (E_8)_1$. The recombined fermionic $U(3)_1$ triplets and the bosonic $(E_8)_1$ are coupled through intra-bundle and inter-bundle backscatteings $\mathcal{H}_{\text{intra}}$ and $\mathcal{H}_{\text{inter}}$ defined in (2.9) and (2.10). The 2D bulk is fully gapped leaving just the chiral $(E_8)_1$ modes at the edges. 9
2.2 The coupled wire model (2.13) for the F_4 Fibonacci quantum Hall state at filling $\nu = 8$. . . . 13

3.1 Coupled wire description of a topological surface state. (a) Emergence of surface channels through alternating symmetry breaking. (b) Gapless surface state resulting from uniform competing inter-channel backscattering $\mathcal{H}_{\text{bc}}$. (c) Surface gapping through channel bipartition and non-competing inter-channel dimerization $\mathcal{H}_{\text{dimer}}$. 18
3.2 A string of "quasi-local" operators (3.19) creates a pair of fractional surface excitations in the form of a kink and anti-kink pair of the sine-Gordon order parameter $\langle 2\boldsymbol{\Theta}_{y-1/2}(x)\rangle$. 27
3.3 A $hc/2e$ flux vortex in the topological superconducting bulk associates to a string of vertex operators on the surface (represented by the blue stars) and create a pair of π-kink excitations (red dots). 30
3.4 Duality transformation of the sine-Gordon term on the u-plane. $\hat{D}$ is the duality operator. Under $\hat{D}$, points on the circle with radius $|u|$ is reflected with respect to the real axis. P, Q are self-dual points. P describes a gapless point, which can be seen in Fig. 3.5(c). Other points on the circle describe gapped phases. 34
3.5 The ground state expectation values of $\langle 2\boldsymbol{\Theta}_{y+1/2}\rangle$ that minimize the sine-Gordon Hamiltonian (3.43) for (a) $\vartheta = 0$, (b) $\vartheta = -3\pi/5$ and (c) $\vartheta = \pi$. The plots are taken over the fundamental region in $\mathbb{R}^3$ modulo the Haldane dual lattice $\mathcal{L}_{\boldsymbol{\Theta}}^{SU(4)}$ in (3.41). The sine-Gordon Hamiltonian generically has a finite energy gap and a single minimum for $-\pi < \vartheta < \pi$. At $\vartheta = \pi$, there are gapless Goldstone modes on the boundary of the fundamental region. 35
3.6 Pictorial illustration of the duality transformation in Eq. (3.50) or (3.51). Two flux quanta from $+\infty$ and $-\infty$ attached to each pair of wires. 36

4.1 Edgeability and gappability of conformal field theories are closely related – they both diagnose if they must be realized as a boundary of (topological) systems in one higher dimensions. Hence, edgeability and gappability are both related to quantum anomalies. 73
4.2 We claim that one cannot "cut" or "make a boundary" while preserving G symmetry for certain CFTs and certain symmetry implementations. These symmetry implementations correspond precisely to $(2+1)$d G-symmetric SPT phases and the corresponding CFTs are their edge theories. 74
4.3 An illustration of the Cardy condition; a consistency condition for conformal boundary states. For boundary states that preserve conformal symmetry, the open channel partition function $Z_{\text{open}} := \text{Tr}_{\mathcal{H}_{\text{open}}}\left[e^{-(2\pi i/\tau)H_{\text{open}}}\right]$ must equal the amplitude for a "Cardy" state $\mathcal{A} = \langle B|e^{2\pi i\tau H_{\text{closed}}}|B\rangle$. 77

A.1 The Dynkin diagram of E_8 and the charge assignment q (in units of e) of the simple roots $(E_{E_8})^{\sigma}_{y\boldsymbol{\alpha}_I}$, for $I = 1, \ldots, 8$. Uncolored entries are electrically neutral. 111

"When nothing seems to help, I go and look at a stonecutter hammering away at his rock perhaps a hundred times without as much as a crack showing in it. Yet at the hundred and first blow it will split in two, and I know it was not that blow that did it, but all that had gone before."

— *Jacob Riis*

Chapter 1

Introduction

Since the discovery of topological insulators (TIs) and superconductors (TSCs) over the past decade [5, 6], topological phases of matter have drawn the attention of both condensed matter and high energy physicists. They are attractive not only because they present exotic properties in theory, but also because some of these phenomena can be verified in materials. They introduce new frontiers in previously well-studied physical concepts, such as quantum phase transitions in condensed matter physics and quantum anomalies in high energy physics.

Topological phases are quantum phases that do not adiabatically connect to trivial ones. The ground states of these phases are quantum mechanically entangled to an extent that any deformation path connecting a topological state and a trivial state must go through a quantum phase transition where the bulk excitation energy gap closes. For example, a topological insulating phase must be separated from a normal insulating phase by a gapless Dirac/Weyl (semi)metallic phase or critical point [7]. This is intimately related to the fact that, generically in three dimensional real space, a topological material and a normal one are distinctly separated by an anomalous two dimensional surface. For example, the gapless Dirac surface state provides a definitive measurable signature of a topological insulator [8]. Some topological phases require the presence of symmetries. For example, topological insulators rely on time reversal symmetry, which protects the Kramers degeneracy of the surface Dirac point, and charge conservation, which disallows pairing. In general, symmetries provide a finer classification of topological phases by forbidding deformation paths that violate them. These phases are referred to as symmetry-protected or symmetry-enriched topological (SPT/SET) phases depending on whether the 3D bulk material supports integral or fractional quasiparticle excitations. On the other hand, conformal field theories (CFTs) have wide applications in different fields, ranging from mathematical physics [9, 10], high energy physics [11], to condensed matter physics.

Before we discuss specific topics, I would like to introduce some background information about the development of topological systems.

Quantum Hall systems

Quantum Hall systems provide one of the biggest platforms for topological phases of matter. Since the discoveries more than 30 years ago of the integer quantum Hall effect (IQHE) [12] and fractional quantum Hall effect (FQHE) [13] in experiments, substantial theoretical and experimental work has appeared. There are many excellent references on QHE, to list a few, Ref. [14, 15, 16]. Fig. 1.1,1.2 below show some of the characteristic experimental results of QHE.

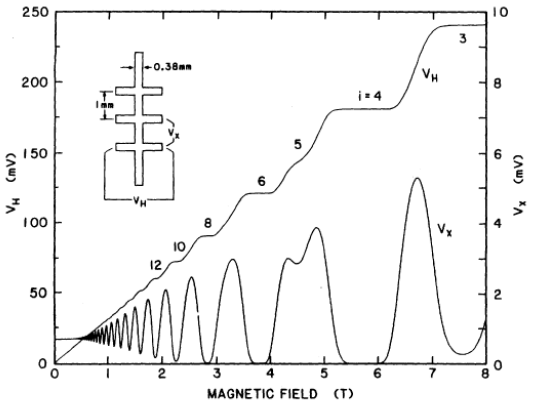

Fig. 1. Recording of V_H and V_x versus magnetic field for a GaAs device cooled to 1.2 K. The current is 25.5 μA.

Figure 1.1: Adopted from Ref. [1]. Some experimental setup and data for IQHE.

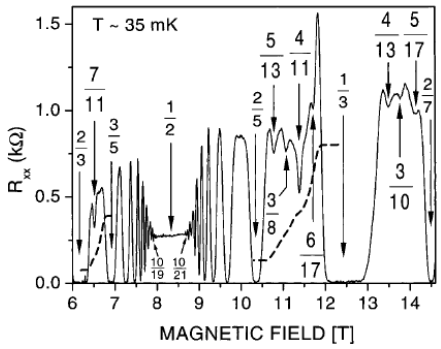

FIG. 1. R_{xx} in the regime $2/3 > \nu > 2/7$ at $T \sim 35$ mK. Major fractions are marked by arrows. Dashed traces are the Hall resistance R_{xy} around $\nu = 7/11$ and $\nu = 4/11$.

Figure 1.2: Adopted from Ref. [2]. Some experimental setup and data for FQHE. The sample for this experiment is a 500 Å wide modulation-doped GaAs/AlGaAs quantum well of size about 5 mm $\times$ 5 mm.

There are some characteristic properties for QHE. For instance, the IQHE regime exhibits:

- integral filling factors;
- disorder, no interactions;
- finite energy gap for excitations;
- local excitations in the bulk and local gapless edge modes.

Fig. 1.3 shows some characteristics of IQHE.

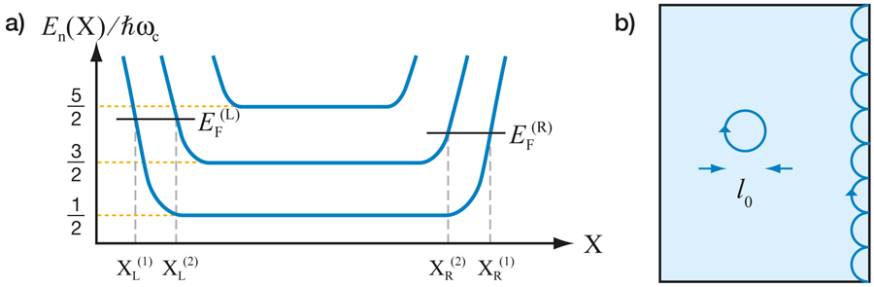

Figure 1.3: Adopted from Ref. [3]. (a) Landau levels with the finite size effect. The intersections between the Fermi energies and the Landau levels represent the chiral modes on the boundary. (b) Classical picture of the cyclotron motion of electrons in the bulk and on the edge. l_0 is the magnetic length. (Illustration: Alan Stonebraker/stonebrakerdesignworks.com).

Correspondingly, the FQHE regime exhibits:

- fractional rational filling factors;
- disorder and interactions;
- finite energy gap for excitations;
- anyonic excitations in the bulk and anyonic gapless edge modes.

Ref. [17] has a nice effective field theory description of QHE, in terms of K-matirx formalism and chiral Luttinger liquids.

In this dissertation, we will introduce some new quantum Hall systems that are combinations of IQHE and FQHE in the sense that they have properties from both IQHE and FQHE. For instance, these new states have integer filling factors but they are intrinsically strongly interacting. Detailed constructions and analysis will be presented in Chapter 2 with coupled wire models, which is introduced in the following subsection.

Coupled wire construction

The coupled wire construction was first introduced in Ref. [18] to study the Abelian fractional quantum Hall effect (FQHE). The basic idea is to start from arrays of 1D quantum wires aligned parallel on the 2D plane, which is shown in Fig. 1.4 below. The magnetic field is turned on perpendicular to the plane. Then each wire is described by a Luttinger liquid Hamiltonian and the interwire gapping interactions are turned on. The result of this setup is that there is a gapped 2D bulk and 1D gapless modes on the boundary wires, which describe precisely the same topological properties of the corresponding FQHE, including the edge states and bulk quasiparticle excitations. The coupled wire construction was later generalized to non-Abelian FQHE in Ref. [4] and other (2+1)D systems, such as dualities [19, 20], surface topological orders [21, 22, 23] and (3+1)D systems like Dirac semimetals [24].

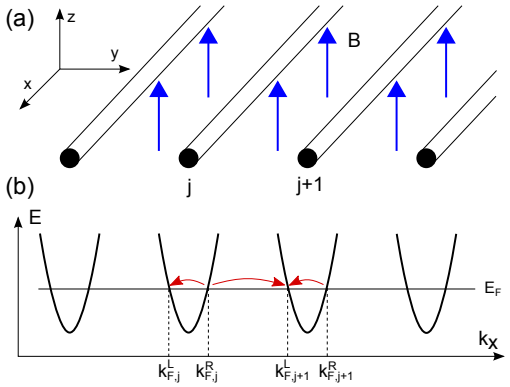

Figure 1.4: Adopted from Ref. [4]. (a) 1D array of quantum wires placed on the 2D plane. The magnetic field is perpendicular to the plane. (b) The interwire and intrawire scattering processes at some fractional filling factor.

The benefit of the coupled wire construction is that it has the desirable property that the Hamiltonian of the system can be written down explicitly with the microscopic degrees of freedom of the system, compared with the pure field theoretic analysis. We can construct the interactions and the excitations explicitly. Their properties can be studied with conformal field theory (CFT), which is a powerful tool in discussing 2D spacetime systems. The bulk-boundary correspondence is manifest in this concrete construction.

In this dissertation, in addition to the construction of novel quantum Hall systems, we will discuss surface topological orders (STOs) of some topological systems with the coupled wire construction. These STOs can be constructed from current algebras of ADE classifications in Lie algebra language. Microscopic Hamiltonians, ground states, quasiparticle excitations and duality properties will be detailed in Chapter 3.

Symmetries in topological systems

A symmetry is an important part of a topological system. One of the most famous examples is the time-reversal invariant topological insulators in both 2D [25, 26] and 3D [27, 28, 29] systems. The nontrivial phase is protected by both time-reversal and U(1) symmetries. If we break either of these symmetries explicitly or spontaneously, the resulting phase can be adiabatically connected to a trivial phase. For fermion systems, at the free fermion level, topological phases have been classified in different spacetime dimensions according to Altland-Zirnbauer (AZ) ten-fold symmetry classes, based on time-reversal symmetry, particle-hole symmetry and chiral symmetry, in physics language. [30, 31, 32] After that some more symmetries are added into the classification scheme. More details can be found in Ref. [33]. However, when interactions are taken into account, the classification would collapse for some cases. [34, 35] The reduction of the classification in the presence of interactions was conjectured correctly to be related with global anomalies in Ref. [36] and studied systematically in Ref. [37]. During the same period of time, a new concept was born, namely, "symmetry protected topological phases" or "SPT phases" in short, which is more relevant to this dissertation. SPT phases have been discussed for both bosonic and fermionic systems. There are some characteristic properties for SPT phases, for instance, in d spatial dimensions,

- the system has a finite energy gap for all excitations in the bulk;
- the system is invariant under some symmetry group G that is neither explicitly nor spontaneously broken;
- there is a unique ground state on all closed d-manifolds for a particular topological phase;
- Two inequivalent phases cannot be adiabatically connected without breaking the symmetry G or closing the energy gap;
- if there is a nonempty boundary, the boundary theory cannot be a trivial gapped theory.

Here a trivial state means a product state or an atomic insulator. SPT phases were first discussed for 1D Haldane spin chains in Ref. [38]. Then they were generalized to different dimensions and classified by different schemes, like group cohomology [39], cobordism group [40], K-matrix formalism [41], to list a few. The study of SPT phases deepens our understanding between condensed matter physics and high energy physics, especially the relation between quantum phases and quantum anomalies.

In this dissertation, we analyze and classify SPT phases in (2+1)D systems from the perspective of the boundary conformal field theory (BCFT). The basic idea is to start from the (1+1)D CFT with a well-defined boundary state. Then we will check the consistency between the global symmetry and the Cardy condition,

which is a consistency requirement for BCFT. Then we use the bulk-boundary correspondence to diagnose and classify the (2+1)D SPT phases. Details will be presented in Chapter 4.

To summarize the Introduction, we discuss some applications of CFTs on topological phases of matter. The structure of the dissertation is as follows. Chapter 2 introduces the coupled wire construction of some novel quantum Hall systems and their interesting properties. Chapter 3 continues the coupled wire model on the surface of (3+1)D topological systems and studies their surface topological orders (STOs). Chapter 4 discusses the detection and classification of SPT phases with boundary conformal field theories (BCFTs). We conclude the dissertation and discuss some of the future work in Chapter 5. Some details of the calculations and background knowledge are relegated in Appendix A and B.

Chapter 2

Coupled wire construction of Quantum Hall systems

This chapter is largely based on Ref. [42]. Ordinarily, the indistinguishability of quantum particles is embodied by either bosonic or fermionic statistics. In two dimensions, however, the complexity of quantum many-body interference phenomena is brought to a new level of depth as anyon statistics becomes a possibility [43, 44, 45]. The magnetic-quenched kinetic energy of the lowest Landau level in a (2+1)D electron gas makes fractional quantum Hall fluids the paradigmatic anyonic system [14]. The remaining Coulomb interactions establish long-range entanglement in these phases, where topological order develops with gapless charge and energy transporting edge-modes and whose bulk excitations display anyonic behavior.

While a sensitive competition among phases is ubiquitous in fractional quantum Hall systems, less diversity is discussed at integral quantum Hall (IQH) plateaus, prompting the question: can interactions drive topological phase transitions in Hall fluids at integral magnetic filling fractions? Here we answer this query in the affirmative, providing explicit examples based on exactly solvable coupled-wire constructions [18] and showing that such transitions are traceable by changes in the Wiedemann-Franz law [46].

To direct our construction towards a noteworthy scenario, we take the point of view that while all anyons are remarkable, not all anyons are equally remarkable. The class of non-Abelian anyons is characterized by a degenerate Hilbert space which can be navigated by adiabatic particle exchanges. These (braiding) operations offer a promising approach to encode and manipulate gates for quantum information. With such goal in mind, one of the most distinguished is the τ anyon of Fibonacci topological order [45, 47], obeying the fusion rule $\tau \times \tau = \mathbb{I} + \tau$ and offering a venue for universal (braiding-based) topological quantum computing. Previous attempts at building models for Fibonacci topological order included the $\nu = 12/5$

fractional quantum Hall phase of Read and Rezayi [48], a trench construction between $\nu = 2/3$ fractional quantum Hall and superconducting states [49], and a recent interacting Majorana model based on a tricritical Ising coset construction [50]. Contrasting with these previous proposals, we set here to build a model for Fibonacci order in homogeneous systems (no heterostructures), in terms of regular complex fermions and, most importantly, at integral magnetic filling fractions.

Fibonacci topological order can be found in Wess-Zumino-Witten (WZW) conformal field theories (CFTs) based on the Lie groups G_2 and F_4 at level 1 [51, 49] (c.f. Appendix A). Remarkably, an embedding exists from $(G_2)_1 \times (F_4)_1$ into a larger $(E_8)_1$ WZW CFT [52]. The E_8 group corresponds to the largest exceptional Lie algebra [53] and is the starting point of our discussion. Due to its internal algebraic structure [1], $(E_8)_1$ only corresponds to trivial topological order, not supporting fractional excitations, similar to IQH plateaus. This suggests the existence of an incompressible fluid, here constructed and dubbed the E_8 *quantum Hall state*, that competes with some IQH phase. Indeed, the E_8 quantum Hall state is found to develop at filling fraction $\nu = 16$, and its $(E_8)_1$ edge CFT displays a chiral central charge $c_{E_8} = 8$ [54, 55, 11] with even-charged bosonic edge modes. It is set apart from the standard $\nu = 16$ IQH liquid with $c = 16$ and fermionic edge modes. Finally, explicitly building the mentioned conformal embedding, we partition the E_8 state into two new G_2 and F_4 quantum Hall states with chiral central charges $c_{G_2} = 14/5$ and $c_{F_4} = 26/5$. These display topological order while remaining at integer filling fraction $\nu = 8$, with even charged edge modes. We end up by showing that these two Fibonacci phases are related by an unconventional particle-hole conjugation based on an unifying description coming from the Lie group E_8.

2.1 Novel quantum Hall state

2.1.1 E_8 quantum Hall state

We begin with an array of electron wire bundles (Fig. 2.1 black lines) with vertical positions $\mathsf{y} = dy$, d being their displacement and y an integer label. Each bundle contains N wires carrying, at the Fermi level, left (L) and right (R) moving fermions whose annihilation operators admit a bosonized representation

$$c^{\sigma}_{ya}(\mathsf{x}) \sim \exp\left[i\left(\Phi^{\sigma}_{ya}(\mathsf{x}) + k^{\sigma}_{ya}\mathsf{x}\right)\right], \tag{2.1}$$

forming a $U(N)_1$ WZW theory. Here, $a = 1, \ldots, N$ indexes the wires, x is the coordinate along them, $\sigma = R, L = +, -$ is the propagation direction and k^{σ}_{ya} is the Fermi momentum of each channel. The bosonic

[1] namely, the minimal even unimodularity of its root lattice

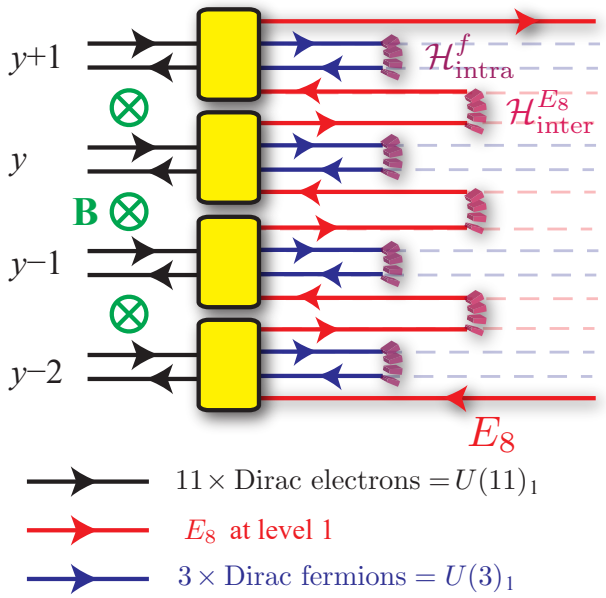

Figure 2.1: Coupled-wire model of the E_8 quantum Hall state at filling $\nu = 16$. Black lines represent bundles with 11 electron wires, each carrying a counter-propagating pair of Dirac fermions, in the presence of a magnetic flux (green). Yellow boxes represent an unimodular basis transformation U ($\det(U) = 1$) restructuring $U(11)_1 \to U(3)_1 \times (E_8)_1$. The recombined fermionic $U(3)_1$ triplets and the bosonic $(E_8)_1$ are coupled through intra-bundle and inter-bundle backscatteings $\mathcal{H}_{\text{intra}}$ and $\mathcal{H}_{\text{inter}}$ defined in (2.9) and (2.10). The 2D bulk is fully gapped leaving just the chiral $(E_8)_1$ modes at the edges.

variables obey the commutation relations

$$\left[\partial_{\mathsf{x}}\Phi^{\sigma}_{ya}(\mathsf{x}), \Phi^{\sigma'}_{y'a'}(\mathsf{x}')\right] = 2\pi i\sigma\delta^{\sigma\sigma'}\delta_{aa'}\delta_{yy'}\delta(\mathsf{x}-\mathsf{x}'). \tag{2.2}$$

To couple the fermions of different bundles and introduce a finite excitation energy gap, while leaving behind gapless chiral $(E_8)_1$ edges, two ingredients are necessary: (i) a basis transformation that extracts the $(E_8)_1$ degrees of freedom from $U(N)_1$ (Fig. 2.1 yellow boxes) and (ii) backscattering interactions between L- and R-movers of different bundles to gap out all low energy channels throughout the bulk (Fig. 2.1 dashed arcs).

Regarding ingredient (i), it suffices to generate the eight simple roots basis of the E_8 root lattice. These assume, under bosonization, the general ansatz [54]

$$[E_{E_8}]^{\sigma}_{y\boldsymbol{\alpha}_I} \sim \exp\left[i\left(\tilde{\Phi}^{\sigma}_{yI}(\mathsf{x}) + \tilde{k}^{\sigma}_{yI}\mathsf{x}\right)\right], \; I = 1, ..., 8. \tag{2.3}$$

Here $\boldsymbol{\alpha}_I$ is a simple root vector of E_8 so that

$$\left[\partial_{\mathsf{x}}\tilde{\Phi}^{\sigma}_{yI}(\mathsf{x}),\tilde{\Phi}^{\sigma'}_{y'I'}(\mathsf{x}')\right]=2\pi i\sigma\delta^{\sigma\sigma'}K^{E_8}_{II'}\delta_{yy'}\delta(\mathsf{x}-\mathsf{x}'),\tag{2.4}$$

and $K^{E_8}_{II'}=\boldsymbol{\alpha}_I\cdot\boldsymbol{\alpha}_{I'}$ is the Cartan matrix of E_8. The challenge here is to represent the E_8 roots as products of electron operators, so that their bosonized variables are related to the electronic ones by an integer-valued transformation $\tilde{\Phi}^{\sigma}_{yI}=U^{\sigma\sigma'}_{Ia}\Phi^{\sigma'}_{ya}$. As a consistency condition from (3.5) and (2.4), $\sigma''U^{\sigma\sigma''}_{Ia}U^{\sigma'\sigma''}_{I'a}=\sigma\delta^{\sigma\sigma'}K^{E_8}_{II'}$. From (2.1), the E_8 roots momenta and charges are related to the fermionic ones similarly: $\tilde{k}^{\sigma}_{yI}=U^{\sigma\sigma'}_{Ia}k^{\sigma'}_{ya}$ and $\tilde{q}^{\sigma}_{I}=U^{\sigma\sigma'}_{Ia}q^{\sigma'}_{a}$, respectively. Such a basis transformation exists, but is not unique, and requires, in particular, $N>8$ wires. To fix a solution, we demand the extra modes to correspond to a trivial fermionic sector. This way, one of the simplest constructions contains $N=11$ wires, decomposing into a E_8 and three $U(1)$ sectors [2]. In practice, we write

$$U=\begin{pmatrix}U^{++} & U^{+-}\\ U^{-+} & U^{--}\end{pmatrix}\tag{2.5}$$

as unimodular matrix, decomposing $U\eta U^T=K^{E_8}\oplus\mathbf{I}_3\oplus(-K^{E_8})\oplus(-\mathbf{I}_3)$, where $\eta^{\sigma\sigma'}=\sigma\delta^{\sigma\sigma'}$. For our particular construction,

[2] In fact, a solution exists for $N=9$ wires also, where the E_8 quantum Hall phase develops at filling fraction $\nu=32$, higher than our present solution. Also, the Dynkin labels 4, 5, 6 and 8 in this construction are neutral, leaving an SO(8) subsector with trivial x-momenta. A main consequence is that the embedding of G_2 currents also carry trivial momenta, and Fibonacci phases can never be stabilized.

$$(U^{++}|U^{+-}) = (U^{--}|U^{-+}) = \tag{2.6}$$

$$\left(\begin{array}{cccccccccc|ccccccccccc}
-1 & -1 & -1 & & & & & & & & & & & & & & & & & & -1 \\
 & & 1 & 1 & & & & & & & & & & & & & & & & & \\
 & & & -1 & 1 & & & & & & & & & & & & & & & & \\
 & & & & -1 & 1 & & & & & & & & & & & & & & & \\
 & & & & & -1 & -1 & & & & & & & & & & & & & & \\
 & & & & & & 1 & 1 & & & & & & & & & & & & & \\
 & & & & & & & -1 & 1 & & & & & & & & & & & & \\
 & & -1 & 1 & 1 & 1 & & & & & & & & & & & & & & 1 & -1 \\
 & & & & & & & & & 1 & 1 & 1 & & & & & & & & & \\
 & & & & & & & & & 3 & -5 & -2 & -1 & -2 & 2 & 2 & 2 & -2 & 2 & 2 & & \\
2 & & 1 & -1 & -1 & -1 & 1 & -1 & -1 & & & & & & & & & & & -1 & 3
\end{array}\right)$$

where the rows and columns of $U^{\sigma\sigma'}$ are respectively labeled by $I, a = 1, \ldots, 11$. Rows $I = 1$ to 8 associate to the simple roots of E_8, whose charge assignment is $(\tilde{q}_{I=1,\ldots,8}) = (-4, 2, 0, 0, -2, 2, 0, 2)$. Rows 9 to 11 correspond to recombined (spin $|h| = 1/2$) Dirac fermions $f^{\sigma}_{yn} \sim \exp\left[iU^{\sigma\sigma'}_{I=8+n,a}(\Phi^{\sigma'}_{ya} + k^{\sigma'}_{ya}\mathsf{x})\right]$, for $n = 1, 2, 3$, that generate $U(3)_1$. They are also integral products of the original electrons and carry odd electric charges $(\tilde{q}_{n=1,..,3}) = (3, 1, 1)$.

Returning now to ingredient (ii), electron backscattering interactions generally require momentum commensurability to stabilize oscillatory factors [56]. To tune these phases, and break time-reversal as necessary in a quantum Hall fluid, we introduce a magnetic field perpendicular to the system (Fig. 2.1 green crosses). The Fermi momenta of the electron channels become spatially dependent as

$$k^{\sigma}_{ya} = \frac{eB}{\hbar c}\mathsf{y} + \sigma k_{F,a}, \tag{2.7}$$

according to the Lorenz gauge $A_x = -B\mathsf{y}$ and where $k_{F,a}$ are the bare Fermi momenta in the absence of field. The associated magnetic filling fraction can be expressed as

$$\nu = \frac{\frac{1}{2\pi}\sum_a 2k_{F,a}}{Bd/\phi_0} = \frac{\hbar c}{eBd}\sum_a 2k_{F,a}, \tag{2.8}$$

where $\phi_0 = hc/e$ is the magnetic flux quantum.

At this point we introduce the wire-coupling interactions

$$\mathcal{H}^{y,f}_{\text{intra}} = u_{\text{intra}} \sum_{n=1}^{3} {f^R_{yn}}^\dagger f^L_{yn} + h.c., \tag{2.9}$$

$$\mathcal{H}^{y+1/2,E_8}_{\text{inter}} = u_{\text{inter}} \sum_{I=1}^{8} {[E_{E_8}]^R_{y,\boldsymbol{\alpha}_I}}^\dagger [E_{E_8}]^L_{y+1,\boldsymbol{\alpha}_I} + H.c.. \tag{2.10}$$

From (2.3), and the corresponding bosonization of f^σ_{yn}, (2.9) and (2.10) carry the expected momentum-dependent oscillating factors $e^{ik\text{x}}$ which average out in the thermodynamic limit. Demanding the vanishing of these oscillations, i.e. requiring the backscattering interactions to conserve momentum, fixes a unique choice of ratios between the bare $k_{F,a}$. Most remarkably, this identically fixes $\nu = 16$ (c.f.Appendix A).

Under the conditions above, and in a periodic geometry with N_l bundles, the intra- and inter-bundle backscattering Hamiltonians introduce $11 \times N_l$ independent sine-Gordon terms satisfying the Haldane's nullity condition [57]. At strong coupling, the coupled-wire model therefore possesses a finite energy excitation gap.

The E_8 quantum Hall phase carries distinctive phenomenology. Opening the periodic boundary conditions leaves behind, at low energies, eight chiral E_8 boundary modes along the top and bottom edges, as illustrated in Fig. 2.1. As consequence of the discrepancy between the magnetic filling factor and the number of E_8 edge modes, we predict an unconventional Wiedemann-Franz law [46] for the E_8 quantum Hall phase. A general set of gapless edge modes, as in regular IQH states, carries the differential thermal and electric conductances (or, equivalently, Hall conductances) [58, 59, 60, 61, 62]

$$\kappa_{xy} = c\frac{\pi^2 k_B^2}{3h}T, \quad \sigma_{xy} = \nu\frac{e^2}{h}, \tag{2.11}$$

where e is the electric charge, h is Planck's constant, k_B is Boltzmann constant, c is the chiral central charge and T is the temperature. For a standard IQH state, $c = \nu$ identic to the number of chiral Dirac electron edge channels. A deviation away from $c/\nu = 1$ indicates the onset of a strongly-correlated many-body phase. Here, the E_8 quantum Hall phase carries 8 chiral edge bosons and therefore $c_{E_8} = 8$, while $\nu = 16$ is necessary to stabilize the phase. This leads to a modified Wiedemann-Franz law, where $c_{E_8}/\nu = 1/2$.

We note in passing that the E_8 state is topologically related to a thin slab of a 3D $e_f m_f$ topological paramagnet with time-reversal symmetry-breaking top and bottom surfaces [63, 64]. Like a topological insulator, hosting a 1D chiral Dirac channel with $(c, \nu) = \pm(1, 1)$ along a magnetic surface domain wall, the $e_f m_f$ topological paramagnet supports a neutral chiral E_8 interface with $(c, \nu) = \pm(8, 0)$ between adjacent time-reversal breaking surface domains with opposite magnetic orientations [6, 5, 65, 33]. Comparing $(c, \nu) =$

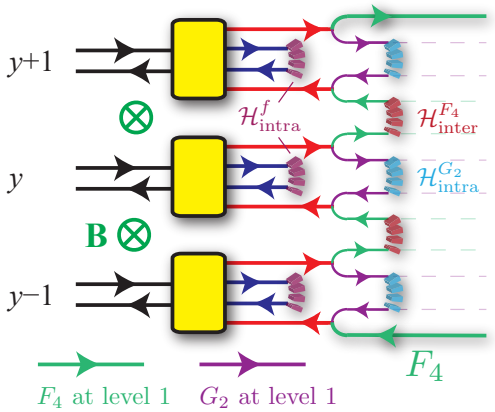

Figure 2.2: The coupled wire model (2.13) for the F_4 Fibonacci quantum Hall state at filling $\nu = 8$.

$(8, 16) = (16, 16) - (8, 0)$, the charged edge modes of the E_8 quantum Hall state are therefore equivalent to the neutral E_8 topological paramagnet surface interface up to 16 chiral Dirac channels, which exists on the edge of the conventional $\nu = 16$ IQH state. In fact, the matrices K^{E_8} and $\mathbf{I}_{16} \oplus (-K^{E_8})$ are related by a charge preserving stable equivalence [66]. Finally, the unimodularity of the E_8 lattice entails that all primary fields of the edge E_8 CFT are integral products of the simple roots (2.3), which are even products of electron operators. Hence, ignoring any edge reconstruction, the edge modes of the E_8 state support *only* evenly charged bosonic gapless excitations.

2.1.2 G_2 and F_4 Fibonacci quantum Hall states

The E_8 state constructed above serves as a stepping stone for building a coupled wires model of phases carrying $(G_2)_1$ or $(F_4)_1$ WZW CFTs at the edges. These correspond to phases with Fibonacci topological order. To build these models, we proceed with a conformal embedding of $G_2 \times F_4$ into E_8, guaranteed by the relationship among central charges $c_{E_8} = 8 = 14/5 + 26/5 = c_{G_2} + c_{F_4}$ [54, 52]. The conformal embedding is carried out by an explicit choice of the generators of F_4 and G_2, denoted by $[E_{F_4}]^{\sigma}_{y,\boldsymbol{\alpha}}$ and $[E_{G_2}]^{\sigma}_{y,\boldsymbol{\alpha}}$, where $\boldsymbol{\alpha}$ are vectors in the F_4 or G_2 root lattices Δ_{F_4} or Δ_{G_2}, respectively. This embedding is also not unique, and is chosen by a particular decomposition $SO(7) \times SO(9) \subseteq SO(16) \subseteq E_8$ that relies on refermionizing the E_8 generators into bilinear products of 8 non-local Dirac fermions. Subsequently, a specific choice is made to embed G_2 into $SO(7)$ and extend $SO(9)$ into F_4. This construction is presented in detail in Appendix A. The found operators are linear combinations of the E_8 generators, which are even products of electron operators, and therefore carry even electric charge and spin 1.

Similar to the E_8 state, the coupled wire models for the F_4 and the G_2 quantum Hall phases are based on an array of 11-wire bundles. Fig. 2.2 shows the schematics of the backscattering terms in the F_4 quantum

Hall Hamiltonian. The G_2 state can be described using a similar diagram by switching the roles of G_2 and F_4. The models are written with the intra-bundle backscattering (2.9), which leaves behind a counter-propagating pair of E_8 modes per bundle. The $\mathcal{G} = F_4$ or G_2 currents are then dimerized within or between bundles according to

$$\begin{aligned}\mathcal{H}^{y,\mathcal{G}}_{\text{intra}} &= u_{\text{intra}} \sum_{\boldsymbol{\alpha}\in\Delta_{\mathcal{G}}} [E_{\mathcal{G}}]^{R}_{y,\boldsymbol{\alpha}}{}^{\dagger} [E_{\mathcal{G}}]^{L}_{y,\boldsymbol{\alpha}} + h.c. \\ \mathcal{H}^{y+1/2,\mathcal{G}}_{\text{inter}} &= u_{\text{inter}} \sum_{\boldsymbol{\alpha}\in\Delta_{\mathcal{G}}} [E_{\mathcal{G}}]^{R}_{y,\boldsymbol{\alpha}}{}^{\dagger} [E_{\mathcal{G}}]^{L}_{y+1,\boldsymbol{\alpha}} + h.c.\end{aligned} \tag{2.12}$$

The F_4 and G_2 quantum Hall states consist, respectively, of the ground states of the following models,

$$\mathcal{H}[F_4] = \sum_{y=1}^{N_l} \left(\mathcal{H}^{y,f}_{\text{intra}} + \mathcal{H}^{y,G_2}_{\text{intra}}\right) + \sum_{y=1}^{N_l-1} \mathcal{H}^{y+1/2,F_4}_{\text{inter}}, \tag{2.13}$$

$$\mathcal{H}[G_2] = \sum_{y=1}^{N_l} \left(\mathcal{H}^{y,f}_{\text{intra}} + \mathcal{H}^{y,F_4}_{\text{intra}}\right) + \sum_{y=1}^{N_l-1} \mathcal{H}^{y+1/2,G_2}_{\text{inter}}. \tag{2.14}$$

The momentum-conservation conditions have to be reimplemented to the many-body interactions in either (2.13) or (2.14). Each phase is stabilized by its own distribution of electronic momenta k^{σ}_{ya} (c.f.Appendix A), but both have the same magnetic filling $\nu = 8$. At strong coupling, $\mathcal{H}[F_4]$ ($\mathcal{H}[G_2]$) gives rise to a finite excitation energy gap in the bulk, but leaves behind a gapless chiral F_4 (G_2) WZW CFT at level 1 at the boundary. As a consequence, the Wiedemann-Franz law is again unconventional in these phases, displaying $c_{F_4}/\nu = 13/20$ and $c_{G_2}/\nu = 7/20$.

According to the bulk-boundary correspondence, the anyon content of the F_4 and G_2 phases can be read from their boundary theories. In addition to the vacuum 1, each edge carries a Fibonacci primary field $\bar{\tau}$ for $(F_4)_1$ and τ for $(G_2)_1$, with conformal scaling dimensions 3/5 and 2/5 respectively. Each consists of a collection of operators, known as a super-selection sector, that corresponds to the 26 dimensional (7 dimensional) fundamental representation of F_4 (G_2) that rotates under the WZW algebra. Our construction allows an explicit parafermionic representation of these fields (c.f. Appendix A). Here, we notice that since the current operators $[E_{F_4}]_{\boldsymbol{\alpha}}$ are even combinations of electrons, the Fibonacci operators within a super-sector differ from each other by pairs of electrons, and therefore correspond to the same anyon type. Moreover, they all have even electric charge and therefore the gapless chiral edge CFT only supports even charge low-energy excitations. An analogous analysis follows for the G_2 case.

2.2 Particle-hole conjugation

The G_2 and F_4 Fibonacci states at $\nu = 8$ half-fill the E_8 quantum Hall state, which has $\nu = 16$. Remarkably, they are related under a notion of particle-hole (PH) conjugation that is based on E_8 bosons instead of electrons. A similar generalization of PH symmetry has been proposed for parton quantum Hall states [67]. The PH conjugation manifests in the edge CFT as the coset identities $(G_2)_1 = (E_8)_1/(F_4)_1$ and $(F_4)_1 = (E_8)_1/(G_2)_1$, which reflect the equality $T_{G_2} + T_{F_4} = T_{E_8}$ between energy-momentum tensors (c.f. Appendix A). The coset $E_8/\mathcal{G}$ can be understood as the subtraction of the WZW sub-algebra $\mathcal{G}$ from E_8. The coset identities are direct consequences of the conformal embedding $(G_2)_1 \times (F_4)_1 \subseteq (E_8)_1$.

The conventional PH symmetry of the half-filled Landau level has been studied in the coupled wire context [19, 68, 20, 69]. Here, the E_8-based PH conjugation has a microscopic description as well. It is represented by an anti-unitary operator $\mathcal{C}$ that relates the E_8 bosonized variables between the two Fibonacci states

$$\begin{aligned} \mathcal{C}\tilde{\Phi}^R_{y,I}\mathcal{C}^{-1} &= \tilde{\Phi}^L_{y,I} - q_I \times /2 \\ \mathcal{C}\tilde{\Phi}^L_{y,I}\mathcal{C}^{-1} &= \tilde{\Phi}^R_{y-1,I} - q_I \times /2 \end{aligned} \tag{2.15}$$

while leaving the recombined Dirac fermions unaltered, $\mathcal{C} f^\sigma_{yn}\mathcal{C}^{-1} = f^\sigma_{yn}$. Since the E_8 root structure is unimodular the PH conjugation (2.15) is an integral action of the fundamental electrons, $\mathcal{C} c_J \mathcal{C}^{-1} = \prod_{J'} (c_{J'})^{m^J_{J'}}$, where $m^J_{J'}$ are integers, J, J' are the collections of indices y, a, σ, and the product is finite and short-ranged so that it only involves nearest neighboring bundles $|y - y'| \leq 1$. The PH conjugation switches between intra- and inter-bundle interactions of the G_2 and F_4 currents, exchanging the two Fibonacci phases $\mathcal{C}\mathcal{H}[F_4]\mathcal{C}^{-1} = \mathcal{H}[G_2]$ and $\mathcal{C}\mathcal{H}[G_2]\mathcal{C}^{-1} = \mathcal{H}[F_4]$. Lastly, the coupled wire description artificially causes the PH conjugation to be non-local. Similar to an antiferromagnetic symmerty, $\mathcal{C}^2$ unitarily translates the E_8 currents from y to $y-1$.

We have some comments on the particle-hole conjugate. In general, when the chiral central charge $c \in 8\mathbb{Z}$, there exist some "trivial" theories, like the E_8 state that we construct. [70, 71] By "trivial", it means that the bulk is topologically trivial, without even fermionic excitations. Let's call it "1". Then if there exists some $CFT \subset$ "1", then we can obtain $\overline{CFT} = \frac{\text{"1"}}{CFT}$ by some particle-hole conjugation operation $\mathcal{C}$. Note that $\mathcal{C}$ is not unique. There can be different definitions of particle-hole conjugation. In this sense, the particle-hole conjugate of a state is not unique unless the particle-hole operation is specified. It has been discussed in high energy physics and mathematical physics, like string theories, monster groups, Niemeier lattices [70, 71], although the term "particle-hole" conjugate is not used. To our understanding, they are closely related.

Chapter 3

Coupled wire models of surface topological orders

This chapter is largely based on Ref. [72]. This chapter will not focus on the distinction between SPT and SET, and its general results will be applicable to both situations.

The surface of an SPT/SET state can obtain a finite excitation energy gap by (a) breaking the relevant symmetry, or (b) developing a surface topological order that supports fractional surface quasiparticle excitations that are absent in the bulk. For example, the Dirac surface state of a topological insulator can acquire a finite Dirac mass by breaking time reversal or a superconducting pairing gap by breaking charge conservation. On the other hand, it can gain a many-body energy gap while preserving all symmetries. However, the symmetric surface must carry topological order, such as the T-Pfaffian, that supports quasiparticle and charge fractionalization [73, 74, 75, 76]. The main focus of this chapter is to develop an exactly solvable model technique in describing a collection of prototype classes of Abelian SPT/SET surface states.

We will focus on three classes of surface states that corresponds to the ADE classification of simply-laced Lie algebra [54]. These simple affine Lie algebras at level 1 were explored as conformal field theories that effectively describes the $1+1$D boundary edge states of $2+1$D Abelian topological phases [77, 78]. In this chapter, we discover a relationship between the ADE classification and SPT/SET surface states. The A-class corresponds to a series of charge $U(1)$ conserving gapped surface states that live on the symmetry breaking boundary surfaces of topological (crystalline) insulators [79] or fractional topological insulators [80]. The D-class corresponds to a series of superconducting gapped surface states of topological superconductors [30, 32]. The E-class corresponds to three exceptional surface states of a topological paramagnet [63, 64]. For simplicity, we only consider Abelian surface topological orders, whose quasiparticle excitations can be

fractional but cannot support non-local quantum information storage. The non-simply-laced simple Lie algebras in the B, C, F, G series corresponds to non-Abelian surface topological orders, and will not be addressed in this chapter.

We will explore these correspondences using the exactly solvable coupled-wire model technique on the surface SPTs/SETs. In general, coupled wire models may have several advantages compared with the more conventional pure field theoretic approaches. One can write down microscopic many-body interacting Hamiltonians explicitly in terms of local electronic degrees of freedom. In many situations, these Hamiltonians can be theoretically designed in a way so that they are exactly solvable and do not require a mean-field approximation. In addition, one can also perform explicit symmetry and duality transformations on the local fields and study the topological properties of the ground states, quasiparticle excitations as well as their braiding statistics.

Generalizing sliding Luttinger liquid theories [81, 82, 83, 84, 85], the coupled wire construction was first developed in Ref. [18] to study the Laughlin [86] and Haldane-Halperin hierarchy [87, 88] fractional quantum Hall (FQH) states. Later this construction was applied to non-Abelian FQH states [4, 89, 90, 91, 92], anyon systems [77, 93, 23], spin liquids [94], studies on duality [19] and many other areas in two spatial dimensions. Recently, the coupled wire construction has also been applied to study three spatial dimensional Abelian and non-Abelian topological systems [95, 96, 97], Dirac (semi)metals [24], Weyl (semi)metals [98], Dirac superconductors [99] and other strongly correlated fractional topological systems [100].

The application of the coupled-wire technique on the surface of an SPT/SET relies on an anisotropic reduction of low-energy surface degrees of freedom onto a 2D array of parallel 1D wires. The simplest example were demonstrated on the surface a topological insulator [101] with a magnetic surface stripe order with alternating magnetic orientations (see figure 3.1). The Dirac surface state becomes massive in the interior of each magnetic strip. This leaves behind chiral Dirac channels with alternating propagating directions that live along the interfaces between strips where the magnetic order flips. A similar construction was also applied to the surface of topological superconductors [21]. In this chapter, instead of deriving from the 3D bulk of an SPT/SET, we begin with the assumption that an array of chiral channels – each described by certain conformal field theory (CFT) related to one of the ADE affine Lie algebras at level 1 – can be generated by similar alternating symmetry-breaking stripe order on the surface of an SPT/SET. This assumption can be verified in the three prototype examples of topological (crystalline) insulators, superconductors and paramagnets mentioned above. On the other hand, it may also be applicable to other more exotic types of SPT/SET such as fractional topological insulators and superconductors.

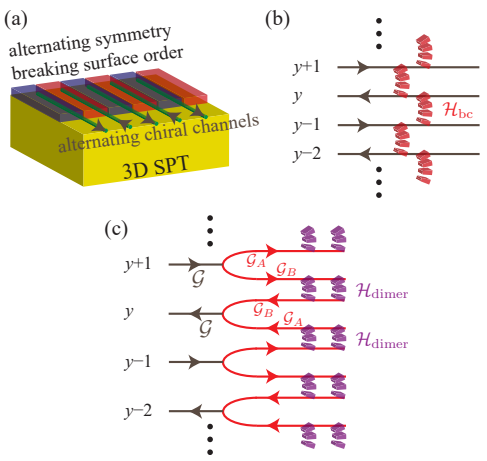

Figure 3.1: Coupled wire description of a topological surface state. (a) Emergence of surface channels through alternating symmetry breaking. (b) Gapless surface state resulting from uniform competing inter-channel backscattering $\mathcal{H}_{\rm bc}$. (c) Surface gapping through channel bipartition and non-competing inter-channel dimerization $\mathcal{H}_{\rm dimer}$.

3.1 Summary of results

Figure 3.1 summarizes the coupled wire models that describes the surface ADE topological orders of SPTs/SETs. The surface state of a generic SPT/SET gains a finite excitation energy gap in the interior of each symmetry-breaking strip. The remaining gapless degrees of freedom are localized along 1D interfaces between adjacent strips with distinct symmetry-breaking orders. The low-energy degrees of freedom along each interface are effectively described by a conformal field theory (CFT), or more precisely, an affine Kac-Moody current algebra (also known as an affine Lie algebra [54] or Wess-Zumino-Witten (WZW) theory [55, 11]). In single-body mean-field topological band insulators and superconductors, the gapless modes along these line interfaces, or line defects in general, were completely classified [102]. Such an interface host a number of copies of chiral Dirac (or Majorana) fermions that propagate in a single-direction and is described a $U(N)_1$ (resp. $SO(N)_1$) current algebra. However, our surface wire construction does not only restrict to the non-interacting case. It also applies to general SPTs/SETs such as fractional topological insulators, which lead to fractional surface Parton Dirac $U(N)_1/\mathbb{Z}_N$ orbifold channels [103, 67], and topological paramagnets, which lead to surface E_8 channels [104].

In this chapter, we explore the possible surface interactions that lead to non-trivial Abelian surface topological orders regardless of whether the interactions preserve or break the relevant symmetries of the underlying SPT/SET. In other words, the surface topological orders are not necessarily anomalous and for some cases, are realizable in non-holographic pure 2D systems. Instead, we are interested in surface states that facilitate non-trivial quasiparticle fractionalization through surface many-body interactions. The coupled wire

construction provides an exact solvable description of such interactions. The oscillating symmetry-breaking surface stripe order requires the propagating directions of the gapless interface channels to alternate. The gapping interactions are theoretically constructed (see figure 3.1(c)) by first decomposing the current algebra $\mathcal{G}$ along each interface channel into two decoupled fractional components

$$\mathcal{G} \sim \mathcal{G}_A \times \mathcal{G}_B, \tag{3.1}$$

and subsequently backscattering the two current components to adjacent interfaces in opposite directions

$$\mathcal{H} = u \sum_{y \text{ even}} \mathbf{J}^y_{\mathcal{G}_A} \cdot \mathbf{J}^{y+1}_{\mathcal{G}_A} + u \sum_{y \text{ odd}} \mathbf{J}^y_{\mathcal{G}_B} \cdot \mathbf{J}^{y+1}_{\mathcal{G}_B}. \tag{3.2}$$

The collection of backscattering interaction between fractional Kac-Moody currents is a 2+1D generalization of the 1+1D AKLT spin chain [105, 106], and leads to fractional gapped quasiparticle excitations. We apply the models to the A, D and E series, where the decomposition (3.1) is given by (3.105) for the A classes, (3.72) for the D classes, and (3.141) for exceptional E classes.

In addition to the exactly solvable model, the coupled wire construction also provides an explicit description of symmetries and dualities. Although time reversal symmetry is necessarily broken by each chiral channel, the array of channels with alternating propagating directions collectively recovers an emergent antiferromagnetic time reversal (AFTR) symmetry, which accompanies local time reversal with a half-translation $y \to y + 1$. We will elaborate on how the AFTR symmetry is preserved in the D class and how it is broken in the A and E classes. On the other hand, duality is also a central theme in theoretical physics. It is a powerful technique that relates distinct theories with no a priori common origins. For example, the order and disorder (i.e. low and high temperature) phases of the 2D classical Ising model are related by the Kramers-Wannier duality. [107] Duality provides a field theoretical mapping between weakly and strongly interacting phases. Recently, there has been some work on non-supersymmetric dualities at the field theoretical level [108, 109, 110, 111]and the concept of duality has also been established in a coupled wire description of composite Dirac fermions [19]. In this chapter, we perform similar constructions to the gapped surface ADE topological orders. Although it is mentioned in Introduction, Table 3.1 summarizes the 3d bulk SPT/SET phases corresponding to the ADE classifications of surface topological orders discussed in this chapter. For a coupled wire construction of these 3d bulk systems, we will discuss it elsewhere.

The outline of this chapter is as follows. In Sec. 3.2, we explicitly demonstrate the coupled wire construction in two simple and specific examples, and elaborate on the central themes that can be systematically carried over to the general scenarios. Sec. 3.3 briefly reviews the coupled wire derivation of the duality

Classification	3d bulk SPT/SET	Section in this chapter
Class A	TCI, FTI	Sec. 3.5
Class D	TSC	Sec. 3.4
Class E	TP, E_8 QH [42]	Sec.3.6

Table 3.1: 3d bulk SPT/SET topological phases corresponding to the surface topological orders of ADE classifications discussed in this chapter. TCI=topological crystalline insulator, FTI=fractional topological insulator, TSC= topological superconductor, TP=topological paramagnet [63, 64], QH = quantum Hall.

between free Dirac fermion and QED_3 proposed in Ref. [19]. Sec. 3.4 reviews the coupled wire models for surface Majorana fermions discussed in Ref. [21] and discuss their duality properties. Next, we introduce the topological orders and duality properties of the A and E classes systematically in Sec. 3.5 and 3.6 respectively. Appendix B.1 is a brief review of the Haldane's nullity gapping condition [112] for bosonized sine-Gordon models. Appendix B.2 contains the relevant background information of the ADE classifications and their representations.

3.2 General coupled wire construction of surface gapping interactions

The coupled wire construction provided exactly solvable many-body interacting models of surface states of symmetry protected topological (SPT) phases. Examples include the T-Pfaffian surface state of a topological insulator [101], and the $SO(3)_3$-like surface state of a topological superconductor [21]. These surface states preserve the relevant symmetries of the SPT phase. The T-Pfaffian surface state [74, 73, 75, 76] preserve time-reversal and charge conservation, while the $SO(3)_3$-like superconducting surface preserve time-reversal [113]. They arise as a consequence of strong many-body interaction beyond the single-body mean field description. The massless Dirac (Majorana) fermion on the surface of a topological insulator (resp. superconductor) cannot acquire a single-body mass term without breaking the relevant symmetries. In general, the surface state of a SPT phase can only develop a finite excitation energy gap while preserving symmetries by many-body interactions that introduce additional surface topological order. This allows fractional quasiparticle surface excitations to emerge that carry fractional properties, such as electric charge and exchange statistics. For example, the T-Pfaffian surface state supports excitations with fractionally quantized electric charge in units of $e/4$.

The coupled wire description of topological surface states is based on an anisotropic surface arrangement where the relevant symmetries emerge in the long wavelength low energy limit. The surface of a topological insulator (superconductor) can be mimicked by an array of 1D chiral Dirac (resp. Majorana) channels with

alternating propagating directions (see figure 3.1). Electronic quasiparticles propagate continuously along each channel and tunnel discretely from one wire to the next. The inter-channel tunneling amplitude is suppressed by an energy barrier, which comes from symmetry breaking interactions that remove or integrate out low-energy electronic degrees of freedom in the surface strips between channels. For example, the symmetry breaking interactions are given by the Dirac (Majorana) mass on the surface of a topological insulator (resp. superconductor). The symmetry breaking interactions correspond to order parameters, such as magnetization or pairing phase. These symmetry breaking order parameters alternate from strips to strips (see figure 3.1(a)). For example, the surface magnetization flips between adjacent strips. Consequently, the 1D interface, where the Dirac mass changes sign, bounds the chiral Dirac mode in low-energy. Similarly, the pairing phase conjugates from one strip to the next, and therefore the interface between adjacent surface strips hosts the chiral Majorana mode. Symmetry is restored in an "antiferromagnetic" manner because the order parameters are conjugated by the symmetry between neighboring strips and the propagating directions are reversed by the symmetry between neighboring channels.

The coupled wire Hamiltonian consists of the kinetic energy of each chiral channel $\mathcal{H}^{y}_{\text{KE}}$ and backscattering coupling potentials $\mathcal{H}^{y+1/2}_{\text{bc}}$ between neighboring channels, where each channel is labeled by an integer y that represents its vertical position in the array (see figure 3.1(b) and (c)). The antiferromagnetic symmetry requires the inter-channel backscatterings to have uniform strength. In other words, symmetry forbids inter-channel dimerization, where counter-propagating channels are pairwise coupled. Under a dimerization where the strength of $\mathcal{H}^{y+1/2}_{\text{bc}}$ alternates between even and odd y, the surface state acquires a symmetry breaking energy gap. Similar to the Su-Schrieffer-Heeger model [114], there are two topologically distinct gapped phases – one where $\mathcal{H}^{y+1/2}_{\text{bc}}$ is stronger for even y and channels are paired between $y = 2n$ and $2n + 1$, and the other where $\mathcal{H}^{y+1/2}_{\text{bc}}$ is stronger for odd y and channels are paired between $y = 2n - 1$ and $2n$. The critical point that separates these two phases has uniform $\mathcal{H}^{y+1/2}_{\text{bc}}$ (see figure 3.1(b)). It preserves the relevant symmetry and has vanishing energy gap. For example, the array of chiral Dirac (Majorana) channels under uniform inter-channel coupling recovers the massless Dirac (resp. Majorana) fermions on the surface of a topological insulator (resp. superconductor).

The uniform backscattering model that preserves the antiferromagnetic symmetry is gapless because adjacent backscattering terms compete. Moreover, the antiferromagnetic symmetry forbids any channel dimerization. On the other hand, if each channel can be fractionalized and bipartitioned into two decoupled components, then they can be backscattered and dimerized in opposite directions (see figure 3.1(c)). This is a higher dimensional analogue of the Haldane integral spin chain [115, 116] and the AKLT spin chain [105, 106], where the integral spin on each site is fractionalized into a pair of half-integral spins and they are

independently dimerized with neighboring ones. The backscattering of these fractional degrees of freedom are now non-competing because they act on orthogonal Hilbert spaces. Moreover, the antiferromagnetic symmetry is preserved if the dimerization strength $\mathcal{H}_{\text{dimer}}^{y+1/2}$ is uniform. The channel fractionalization is stabilized by the many-body inter-channel backscattering $\mathcal{H}_{\text{dimer}}^{y+1/2}$, which are combination of products of local electronic operators.

In this chapter, we consider a variety of SPT phases, whose surface state can be mapped into an array of integral electronic channels. The SPT phase could be protected by certain combinations of global symmetries such as time-reversal and local symmetries represented by a continuous group. Instead of elaborating on the 3D SPT phases, we target surface topological order and begin with the general assumption that the surface array of chiral channels is supported by some unknown 3D SPT bulk. In particular, we focus on situations where these channels can be bosonized. Before inter-channel coupling, each channel can be described in low-energy by a conformal field theory (CFT), which falls under the ADE classification of affine Lie algebra [54] at level one. The A-series consists of the Lie algebras $A_r = SU(r+1)$, where r is the rank of the algebra. The D-series consists of $D_r = SO(2r)$, and the E-series consists of the exceptional E_6, E_7 and E_8. These algebras form the fractional degrees of freedom under the bipartition of channels. Their general construction will be discussed in upcoming sections. In this section, we present the main ideas in the coupled wire construction by demonstrating the $A_3 = SU(4)$ and $D_3 = SO(6)$ case.

3.2.1 $SO(6)$ and $U(4)$ as illustrative examples

In this subsection, we take the $SO(6)$ and $U(4)$ surface models as examples to illustrate the coupled wire construction. In particular, we demonstrate the inter-channel backscattering sine-Gordon interactions. The ground state of each of these interactions exhibits an angle order parameter, which is the ground state expectation value of the angle variable in the sine-Gordon potential. These angle order parameters can take discrete values in a lattice, which will be referred to as the "Haldane's dual lattice". We also present the fractional gapped excitations that corresponds to deconfined kinks of the sine-Gordon interactions. These excitations can be created or destroyed by bosonized vertex operators, whose exponents lie also in the dual lattice.

We begin with the $SO(6)_1$ model. This model can be supported by the surface of a class DIII topological superconductor [30, 32] with topological index $N = 12$. The surface carries 12 massless Majorana fermions, which cannot be turned massive without breaking time reversal symmetry. The surface state can be mimicked by a coupled wire model previously provided in Ref. [21]. An antiferromagnetic surface pair density wave – where the surface is decorated by an array of parallel strips with alternating time-reversal breaking pairing

phases $\varphi = \pm\pi/2$ – supports an array of chiral Majorana interfaces. Each is sandwiched between adjacent strips with time-reversal conjugate Majorana mass, and carries 12 chiral Majorana $\psi_y^1, \ldots, \psi_y^{12}$, where y labels the interface.

We group the Majorana fermions in two collections $\psi_y^{A,i} = \psi_y^i$ and $\psi_y^{B,i} = \psi_y^{6+i}$, for $i = 1, \ldots, 6$. Each collection generates a $SO(6)$ Wess-Zumino-Witten (WZW) algebra (also known as Kac-Moody or affine Lie algebra) at level one. The algebra consists of current operators

$$J_y^{C,jk} = i\psi_y^{C,j}\psi_y^{C,k} \tag{3.3}$$

for $1 \leq j < k \leq 6$ and $C = A, B$. We first pair Majorana fermions into Dirac fermions $c_y^{C,j} = (\psi_y^{C,2j-1} + i\psi_y^{C,2j})/\sqrt{2}$, for $j = 1, 2, 3$, and bosonize each Dirac fermion $c_y^{C,j} \sim e^{i\phi_y^{C,j}}$. The bosonized variables follow the action with Lagrangian density

$$\mathcal{L}_0 = \sum_y \sum_{C=A,B} \left[\frac{(-1)^y}{2\pi} \sum_{j=1}^{3} \partial_t \phi_y^{C,j} \partial_x \phi_y^{C,j} + \sum_{j,j'=1}^{3} V_{jj'} \partial_x \phi_y^{C,j} \partial_x \phi_y^{C,j'} \right], \tag{3.4}$$

where $V_{jj'}$ is a non-universal velocity matrix. The alternating sign $(-1)^y$ signifies the alternating propagating directions of the channels. The action dictates the equal-time commutation relation

$$\left[\phi_y^{C,j}(x), \partial_{x'} \phi_{y'}^{C',j'}(x') \right] = 2\pi i \delta^{CC'} \delta^{jj'} \delta_{yy'} \delta(x - x') \tag{3.5}$$

or equivalently the time-ordered correlation function

$$\phi_y^{C,j}(z) \phi_{y'}^{C',j'}(z') = -\delta^{CC'} \delta^{jj'} \delta_{yy'} \log(z - z') + \ldots \tag{3.6}$$

up to non-singular terms and Klein factors, where $z \sim \tau + i(-1)^y x$ is the (anti)holomorphic complex space-time parameter.

The current operators (3.3) can be expressed in terms of the bosonized variables. There are 3 Cartan generators

$$H_y^{C,j} = i\partial\phi_y^{C,j} \sim c_y^{C,j\dagger} c_y^{C,j} = i\psi_y^{C,2j-1} \psi_y^{C,2j} \tag{3.7}$$

that form a maximal set of mutually commuting Hermitian operators. In addition, there are 12 roots

$$E_y^{C,\boldsymbol{\alpha}} = \exp\left(i\alpha_j \phi_y^{C,j}\right), \tag{3.8}$$

which act as ladder operators on the root lattice. The root vectors $\boldsymbol{\alpha} = (\alpha_1, \alpha_2, \alpha_3)$ all have integral entries $\alpha_j = 0, \pm 1$ and length square $|\boldsymbol{\alpha}|^2 = 2$ so that there are two and only two non-zero entries. Each vertex operator $E_y^{C,\boldsymbol{\alpha}}$ can be expressed as a complex quadratic combination of Majorana fermions (3.3). The Cartan generators and roots therefore generate the complexified $SO(6)$ WZW algebra for each channel y and sector $C = A, B$. One can pick a set of three linearly independent simple roots

$$R_{SO(6)} = \begin{pmatrix} -- & \boldsymbol{\alpha}^1 & -- \\ -- & \boldsymbol{\alpha}^2 & -- \\ -- & \boldsymbol{\alpha}^3 & -- \end{pmatrix} = \begin{pmatrix} 0 & 1 & 1 \\ 1 & -1 & 0 \\ 0 & 1 & -1 \end{pmatrix}. \tag{3.9}$$

All 12 roots can be expressed as integral linear combination of the simple ones. The choice of simple roots recovers the Cartan matrix of $SO(6)$ by the inner product

$$K_{SO(6)} = R_{SO(6)} R_{SO(6)}^T = \begin{pmatrix} 2 & -1 & 0 \\ -1 & 2 & -1 \\ 0 & -1 & 2 \end{pmatrix}. \tag{3.10}$$

The roots also generate and lie inside a face-centered cubic lattice FCC $= \mathrm{span}_{\mathbb{Z}}\{\boldsymbol{\alpha}^1, \boldsymbol{\alpha}^2, \boldsymbol{\alpha}^3\}$ in three dimension. We refer to this as the root lattice.

Now we introduce the inter-channel backscattering sine-Gordon potential

$$\begin{aligned} \mathcal{H}_{\text{dimer}} &= -\frac{u}{2} \sum_y \sum_{\boldsymbol{\alpha}} E_y^{A,\boldsymbol{\alpha}} E_{y+1}^{B,-\boldsymbol{\alpha}} \\ &= -u \sum_y \sum_{\boldsymbol{\alpha}} \cos\left(\boldsymbol{\alpha} \cdot 2\boldsymbol{\Theta}_{y+1/2}\right), \end{aligned} \tag{3.11}$$

where $2\Theta_{y+1/2} = (2\Theta^1_{y+1/2}, 2\Theta^2_{y+1/2}, 2\Theta^3_{y+1/2})$ and $2\Theta^j_{y+1/2} = \phi_y^{A,j} - \phi_{y+1}^{B,j}$. In a periodic cylinder geometry with $L = 2l$ channels, there are $3L$ counter-propagating pairs of bosons and there are also $3L$ linearly independent sine-Gordon angle variables $\boldsymbol{\alpha} \cdot 2\boldsymbol{\Theta}_{y+1/2}$. The angle variable satisfy the "Haldane nullity"

gapping condition [112]

$$\left[\boldsymbol{\alpha}\cdot 2\boldsymbol{\Theta}_{y+1/2}(x), \boldsymbol{\alpha}'\cdot 2\boldsymbol{\Theta}_{y'+1/2}(x')\right] = 0. \tag{3.12}$$

There are actually $12L$ sine-Gordon terms because there are 12 roots in $SO(6)$. However, only $3L$ of them are linearly independent, but the redundant sine-Gordon terms do not compete. Collectively, they pin the angle variables

$$\boldsymbol{\alpha}\cdot\left\langle 2\boldsymbol{\Theta}_{y+1/2}\right\rangle \in 2\pi\mathbb{Z} \tag{3.13}$$

in the ground state, for all root vectors $\boldsymbol{\alpha}$. Since the roots generate a FCC lattice, eq.(3.13) requires the ground state expectation values of the angle variables $\left\langle 2\boldsymbol{\Theta}_{y+1/2}\right\rangle$ to lie in the body-centered cubic (BCC) reciprocal lattice

$$\begin{aligned}\mathcal{L}_{\boldsymbol{\Theta}} &\equiv \{2\boldsymbol{\Theta} : \boldsymbol{\alpha}\cdot 2\boldsymbol{\Theta} \in 2\pi\mathbb{Z}\} \\ &= 2\pi\mathrm{BCC} = \mathrm{span}_{\mathbb{Z}}\left\{2\pi\boldsymbol{\beta}_1, 2\pi\boldsymbol{\beta}_2, 2\pi\boldsymbol{\beta}_3\right\},\end{aligned} \tag{3.14}$$

$$R^{\vee}_{SO(6)} = \begin{pmatrix} -- & \boldsymbol{\beta}_1 & -- \\ -- & \boldsymbol{\beta}_2 & -- \\ -- & \boldsymbol{\beta}_3 & -- \end{pmatrix} = \begin{pmatrix} 1/2 & 1/2 & 1/2 \\ 1 & 0 & 0 \\ 1/2 & 1/2 & -1/2 \end{pmatrix}. \tag{3.15}$$

Here, $\boldsymbol{\beta}_I = \frac{1}{2}\varepsilon_{IJK}\boldsymbol{\alpha}^J\times\boldsymbol{\alpha}^K / \left[\boldsymbol{\alpha}^1\cdot(\boldsymbol{\alpha}^2\times\boldsymbol{\alpha}^3)\right]$ are the simple dual roots so that $\boldsymbol{\alpha}^I\cdot\boldsymbol{\beta}_J = \delta^I_J$. In Lie algebra language, $\boldsymbol{\beta}_I$ are called *fundamental weights*. In the following discussion, we use the terms "simple dual roots", "primitive reciprocal vectors" and "fundamental weights" interchangeably. We refer to the lattice $\mathcal{L}_{\boldsymbol{\Theta}}$ of simultaneous minima of the sine-Gordon potentials as the "Haldane's dual lattice". In Lie algebra language, $\mathrm{span}_{\mathbb{Z}}\{\boldsymbol{\beta}_1,\boldsymbol{\beta}_2,\boldsymbol{\beta}_3\}$ are called weight lattice. To comply with physics community, we use "Haldane's dual lattice" in the following discussions.

The inter-channel backscattering interactions (3.11) therefore freeze the angle-variables and introduce an finite excitation energy gap. Deconfined excitations are of the form of kinks where the expectation value $\left\langle 2\boldsymbol{\Theta}_{y+1/2}(x)\right\rangle$ jumps discontinuously along x from one lattice value to another. They can be represented using fractional vertex operators

$$V_y^{C,\boldsymbol{\gamma}}(x_0) = \exp\left[i\gamma_j\phi_y^{C,j}(x_0)\right] \tag{3.16}$$

that corresponds to a primary field of $SO(6)_1$, where $\boldsymbol{\gamma} = (\gamma_1,\gamma_2,\gamma_3)$ can take non-integral entries. For

example, the vertex operator $V_y^{A,\boldsymbol{\gamma}}(x_0)$ creates a kink for $\langle 2\boldsymbol{\Theta}_{y+1/2}(x)\rangle$ at x_0 because

$$\begin{aligned} &V_y^{A,\boldsymbol{\gamma}}(x_0)^\dagger 2\partial_x \Theta^j_{y+1/2}(x) V_y^{A,\boldsymbol{\gamma}}(x_0) \\ &= 2\partial_x \Theta^j_{y+1/2}(x) + i\left[\gamma_k \phi_y^{A,k}(x_0), 2\partial_x \Theta^j_{y+1/2}(x)\right] \\ &= 2\partial_x \Theta^j_{y+1/2}(x) - 2\pi(-1)^y \gamma_j \delta(x_0 - x) \end{aligned} \tag{3.17}$$

from the equal-time commutation relation (3.5). Integrating the above equation x near x_0, we see the vertex operator creates a discontinuity for $\langle 2\boldsymbol{\Theta}_{y+1/2}(x)\rangle$, where it jumps by $-2\pi\boldsymbol{\gamma}$ from $x < x_0$ to $x > x_0$. The excitation is deconfined if the angle-variable on both sides of x_0 minimizes all the sine-Gordon potentials in (3.11). Otherwise, it will cost a linearly diverging energy to pull apart from its anti-partner. This restricts the jump of height of the kink $2\pi\boldsymbol{\gamma}$ to also live in the Haldane's dual lattice $\mathcal{L}_{\boldsymbol{\Theta}}$. In other words, deconfined excitations are represented by vertex operators $V_y^{C,\boldsymbol{\gamma}}$ (3.16) where $\boldsymbol{\gamma}$ lives in the BCC lattice (3.14). Similarly, we have

$$V_y^{B,\boldsymbol{\gamma}}(x_0)^\dagger 2\partial_x \Theta^j_{y-1/2}(x) V_y^{B,\boldsymbol{\gamma}}(x_0) = 2\partial_x \Theta^j_{y-1/2}(x) + 2\pi(-1)^y \gamma_j \dot{(}x_0 - x). \tag{3.18}$$

It shows that if $\boldsymbol{\gamma}$ is one of the reciprocal vectors in the BCC lattice (3.14), then $V_y^{C,\boldsymbol{\gamma}}$ creates a deconfined quasiparticle excitation in the form of a kink of the sine-Gordon angle order parameter $\langle 2\boldsymbol{\Theta}_{y-1/2}(x)\rangle$.

It is crucial to recognize that in general the kink excitations may be *fractional*, in which case they must come in kink and anti-kink pairs. The notion of "quasi-locality" is set by the 3D SPT/SET bulk, which may already support long-range entangled topological order and carry non-trivial quasiparticle and quasi-string excitations. We will address this issue soon after the description of $SO(6)$ primary fields and Wilson strings below. At the moment, we consider "quasi-local" surface vertex operators that consists of a product of both the A and B sectors. We see that the combination $V_y^{A,\boldsymbol{\gamma}}(x_0) V_y^{B,\boldsymbol{\gamma}}(x_0)$ creates a kink-antikink pair in $\langle 2\boldsymbol{\Theta}_{y+1/2}(x)\rangle$ and $\langle 2\boldsymbol{\Theta}_{y-1/2}(x)\rangle$. The kink and anti-kink can be separated vertically by applying the string of vertex operators

$$\chi^{A,\boldsymbol{\gamma}}_{y,y'}(x_0) = \prod_{y''=y}^{y'} V_{y''}^{A,\boldsymbol{\gamma}}(x_0) V_{y''}^{B,\boldsymbol{\gamma}}(x_0), \tag{3.19}$$

on the ground state, where $y' > y$. This create a kink and anti-kink pair in $\langle 2\boldsymbol{\Theta}_{y'+1/2}(x)\rangle$ and $\langle 2\boldsymbol{\Theta}_{y-1/2}(x)\rangle$ without creating extra kinks in between (see figure 3.2). This is because the effect of $V_{y''}^{A,\boldsymbol{\gamma}}(x_0)$ and $V_{y''+1}^{B,\boldsymbol{\gamma}}(x_0)$ cancel. Physically what happens is that a pair of kink-antikink excitations are created in each wire in between

and consequently the quasiparticle is transported, which is explicitly shown in Eq. (3.17) and (3.18) In this sense, these excitations are deconfined along the y direction. It should be noticed that the kink-anti-kink pair can only be created by the operator string (3.19), which is constructed by the series of "quasi-local" operators $V^{A,\boldsymbol{\gamma}}_{y''}(x_0)V^{B,\boldsymbol{\gamma}}_{y''}(x_0)$. They cannot be created by $V^{A,\boldsymbol{\gamma}}_{y'}(x_0)V^{B,\boldsymbol{\gamma}}_{y}(x_0)$ alone without a string in between because of surface locality. We will address the surface "quasi-localilty" later.

The quasiparticle kinks can be moved in the x-direction by applying

$$\rho_y(x,x_0) = e^{i\int_{x_0}^{x}\gamma_j\partial_{x'}\phi^{C,j}_y(x')}, \tag{3.20}$$

which moves a quasiparticle excitation from x_0 to x on the same wire, without creating extra kinks in between. Together with (3.19), they describe the two-dimensional local motion of the quasiparticle kinks.

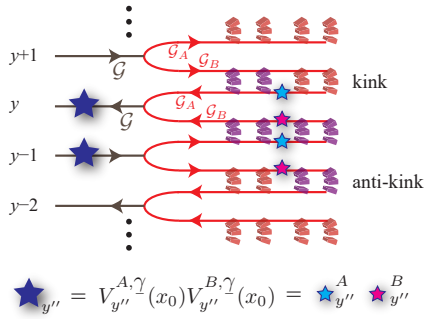

Figure 3.2: A string of "quasi-local" operators (3.19) creates a pair of fractional surface excitations in the form of a kink and anti-kink pair of the sine-Gordon order parameter $\langle 2\boldsymbol{\Theta}_{y-1/2}(x)\rangle$.

These deconfined excitation operators form representations of the $SO(6)_1$ affine Lie algebra. They obey the operator product expansion with the current generators (3.7) and (3.8)

$$\begin{aligned} H^{C,j}_y(z)V^{C,\boldsymbol{\gamma}}_y(z') &= \frac{\gamma_j}{z-z'}V^{C,\boldsymbol{\gamma}}_y(z') + \dots, \\ E^{C,\boldsymbol{\alpha}}_y(z)V^{C,\boldsymbol{\gamma}}_y(z') &= (z-z')^{\boldsymbol{\alpha}\cdot\boldsymbol{\gamma}}V^{C,\boldsymbol{\alpha}+\boldsymbol{\gamma}}_y(z') + \dots. \end{aligned} \tag{3.21}$$

In particular, primary fields are vertex operators with bounded singularities $\boldsymbol{\alpha}\cdot\boldsymbol{\gamma} \geq -1$. More precisely, each primary field is represented by a super-selection sector of vertex operators $\{V^{C,\boldsymbol{\gamma}^1}_y, \dots, V^{C,\boldsymbol{\gamma}^r}_y\}$ that transform under

$$E^{C,\boldsymbol{\alpha}}_y(z)V^{C,\boldsymbol{\gamma}^a}_y(z') = \frac{(E^{\boldsymbol{\alpha}}_\rho)^a_b}{z-z'}V^{C,\boldsymbol{\gamma}^b}_y(z') + \dots \tag{3.22}$$

where $E^{\boldsymbol{\alpha}}_\rho$ is the r-dimensional irreducible matrix representation of the root $E^{\boldsymbol{\alpha}}$ of $SO(6)$. The current

operators $E^{\boldsymbol{\alpha}}$ are therefore raising and lowering operators that rotate $V^{\boldsymbol{\gamma}} \to V^{\boldsymbol{\alpha}+\boldsymbol{\gamma}}$ if $\boldsymbol{\alpha}\cdot\boldsymbol{\gamma} = -1$. The singular factor $1/(z-z')$ reflects the unit scaling dimension of the current operators, and higher order non-singular terms are non-universal.

The $SO(6)$ affine Lie algebra at level 1 has four primary fields labeled by $1, \psi, s_+, s_-$. They corresponds to the trivial, vector, even and odd spinor representations of $SO(6)$ respectively. We now show their corresponding super-sectors of vertex operators. The primary field ψ at wire y and sector $C = A, B$ is generated by $\{e^{\pm i\phi_y^{C,1}}, e^{\pm i\phi_y^{C,2}}, e^{\pm i\phi_y^{C,3}}\}$, which form the 6-dimensional vector representation of $SO(6)$. These vertex operators can also be decomposed into real and imaginary components $e^{i\phi_y^{C,j}} = \psi_y^{C,2j-1} + i\psi_y^{C,2j}$, where $\psi_y^{C,1}, \ldots, \psi_y^{C,6}$ are Majorana fermions with spin (i.e. conformal scaling dimension) $h_\psi = 1/2$. The even/odd twist primary fields $s_\pm$ are generated by $e^{i\boldsymbol{\varepsilon}\cdot\boldsymbol{\phi}/2}$, where $\boldsymbol{\varepsilon} = (\varepsilon_1, \varepsilon_2, \varepsilon_3)$ and $\varepsilon_j = \pm 1$. $\boldsymbol{\varepsilon}$ is even (odd) if $\varepsilon_1\varepsilon_2\varepsilon_3 = +1$ (resp. -1). The collection of even (odd) vertices form the even (resp. odd) spinor representation of $SO(6)$. These vertices operators have spin $h_{s_\pm} = 3/8$.

Using eq.(3.17), the vector primary field ψ_y^A at x_0 creates an 2π kink of the sine-Gordon angle variable so that

$$\langle 2\boldsymbol{\Theta}_{y+1/2}(x_0+\delta)\rangle - \langle 2\boldsymbol{\Theta}_{y+1/2}(x_0-\delta)\rangle = -2\pi(-1)^y \mathbf{e}_j, \tag{3.23}$$

where the expectation values are taken with respect to the excited state $e^{i\phi_y^{A,j}(x_0)}|GS\rangle$. On the other hand, the spinor primary fields $(s_\pm)_y^A$ at x_0 creates a π kink where

$$\langle 2\boldsymbol{\Theta}_{y+1/2}(x_0+\delta)\rangle - \langle 2\boldsymbol{\Theta}_{y+1/2}(x_0-\delta)\rangle = -\pi(-1)^y \boldsymbol{\varepsilon}. \tag{3.24}$$

Since the "heights" of the kinks, which are given by the right hand side of the two equations above, belong to the Haldane's dual lattice $\mathcal{L}_{\boldsymbol{\Theta}}$ (see eq.(3.14)), the primary fields correspond to deconfined excitations that only cost a finite amount of energy to create and do not cost energy to move.

At this point, it is essential to address the surface "quasi-locality"' and take into account the 3D bulk SPT/SET state that supports the surface state. The 12 Majorana fermions $\psi_y^{A,1}, \ldots, \psi_y^{A,6}$ and $\psi_y^{B,1}, \ldots, \psi_y^{B,6}$ associates a $SO(12)_1$ WZW algebra along each wire y. The primary fields in the $SO(12)_1$ CFT are quasi-particle excitations that are supported by the 3D bulk, and should *not* be treated as fractional excitations allowed by the surface gapping interactions. For the purpose of describing the surface topological order, primary fields in $SO(12)_1$ should be regarded as "quasi-local" in the sense that such an excitation can be present without having a partner on the surface. This is because its partner can exist in the 3D bulk. On the other hand, the surface backscattering potential (3.11) allows additional fractional excitations that must

come in pairs on the boundary surface. These are quasiparticles that do not connect to any bulk excitations.

The $SO(12)_1$ WZW algebra that associates to the "quasi-local" primary field excitations is generated by the Cartan operators $H_y^{A,j}$, $H_y^{B,j}$ defined in (3.7) as well as the the 60 roots

$$E_y^{\boldsymbol{\lambda}} = \exp\left[i\left(\lambda_j^A \phi_y^{A,j} + \lambda_j^B \phi_y^{B,j}\right)\right] \tag{3.25}$$

where the root vectors $\boldsymbol{\lambda} = (\lambda_1^A, \lambda_2^A, \lambda_3^A, \lambda_1^B, \lambda_2^B, \lambda_3^B)$ have integral entries $\lambda_j^C = 0, \pm 1$ and length square $|\boldsymbol{\lambda}|^2 = 2$ so that there are two and only two non-zero entries. The simple roots can be chosen to be

$$R_{SO(12)} = \begin{pmatrix} -- & \boldsymbol{\lambda}^1 & -- \\ -- & \boldsymbol{\lambda}^2 & -- \\ \vdots & \vdots & \vdots \\ -- & \boldsymbol{\lambda}^5 & -- \\ -- & \boldsymbol{\lambda}^6 & -- \end{pmatrix} = \begin{pmatrix} 1 & -1 & 0 & \dots & 0 & 0 \\ 0 & 1 & -1 & \dots & 0 & 0 \\ \vdots & \vdots & \vdots & \ddots & \vdots & \vdots \\ 0 & 0 & 0 & \dots & 1 & -1 \\ 0 & 0 & 0 & \dots & 1 & 1 \end{pmatrix}. \tag{3.26}$$

The "quasi-local" surface excitations that connect to the 3D bulk are represented by the vertex operator

$$V_y^{\mathbf{l}}(x_0) = \exp\left[i\left(l_j^A \phi_y^{A,j}(x_0) + l_j^B \phi_y^{B,j}(x_0)\right)\right] \tag{3.27}$$

where the weight vectors $\mathbf{l} = (l_1^A, l_2^A, l_3^A, l_1^B, l_2^B, l_3^B)$ satisfy

$$\boldsymbol{\lambda} \cdot \mathbf{l} \in \mathbb{Z} \tag{3.28}$$

for all $SO(12)$ roots $\boldsymbol{\lambda}$. The weight vectors are integral combinations of the simple dual roots or fundamental weights

$$R_{SO(6)}^{\vee} = \begin{pmatrix} -- & \mathbf{l}_1 & -- \\ \vdots & \vdots & \vdots \\ -- & \mathbf{l}_6 & -- \end{pmatrix} = \begin{pmatrix} 1 & 0 & 0 & 0 & 0 & 0 \\ 1 & 1 & 0 & 0 & 0 & 0 \\ 1 & 1 & 1 & 0 & 0 & 0 \\ 1 & 1 & 1 & 1 & 0 & 0 \\ \frac{1}{2} & \frac{1}{2} & \frac{1}{2} & \frac{1}{2} & \frac{1}{2} & -\frac{1}{2} \\ \frac{1}{2} & \frac{1}{2} & \frac{1}{2} & \frac{1}{2} & \frac{1}{2} & \frac{1}{2} \end{pmatrix}, \tag{3.29}$$

which obey $\lambda^I \cdot \mathbf{l}_J = \delta_J^I$. The entries of a general weight vector $\mathbf{l}$ is either all integers or all half-integers.

It is useful to notice that there is a tensor product structure (referred to as conformal embedding or level

rank duality in the CFT context [54])

$$SO(12)_1 \supseteq SO(6)_1 \times SO(6)_1 \tag{3.30}$$

that splits the "quasi-local" $SO(12)_1$ primary fields (3.27) into the fracrtional $SO(6)_1^A$ and $SO(6)_1^B$ components

$$V_y^{\mathbf{l}}(x_0) \sim \exp\left(il_j^A \phi_y^{A,j}(x_0)\right) \exp\left(il_j^B \phi_y^{B,j}(x_0)\right) = V_y^{A,\mathbf{l}_A} V_y^{B,\mathbf{l}_B}. \tag{3.31}$$

In particular, if $\boldsymbol{\gamma} = (\gamma_1, \gamma_2, \gamma_3)$ lies inside the BCC Haldane dual lattice (3.14), then the combination $V_y^{A,\boldsymbol{\gamma}} V_y^{B,\boldsymbol{\gamma}}$ is a $SO(12)_1$ primary field and therefore represents a "quasi-local" excitation that connects to the 3D bulk. This shows that the vertex operator string (3.19) composes of "quasi-local" excitations. For example, in the class DIII topological superconductor case, a $hc/2e$ flux vortex inside the bulk corresponds to the vertex $V_y^{\boldsymbol{\varepsilon}}$ for each layer y that interests flux vortex, where $\varepsilon = (1/2, \ldots, 1/2)$. It associates to the vertex operator string $\prod_{y=y_0}^{y_1} V_y^{\boldsymbol{\varepsilon}}$ on the surface, and create a pair of π-kink quasiparticle excitations (see figure 3.3). Each vertex operator $V_y^{\boldsymbol{\varepsilon}}$ is "quasi-local" as it connects to the bulk, but the π-kink excitations are fractional. They are supported by the surface backscattering interactions and can only exist on the boundary surface.

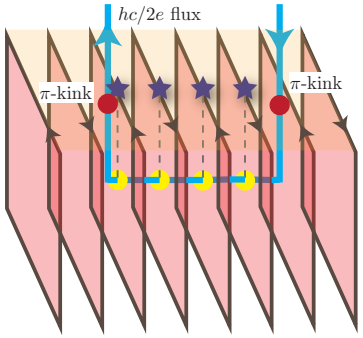

Figure 3.3: A $hc/2e$ flux vortex in the topological superconducting bulk associates to a string of vertex operators on the surface (represented by the blue stars) and create a pair of π-kink excitations (red dots).

Next, we illustrate the $U(4)_1$ model. The array of wire is now supported on the surface of some three dimensional symmetry protected topological state (see figure 3.1(a)), and each wire hosts eight Dirac fermions. The 3D SPT state can be a topological crystalline insulator [79] with mirror Chern number 8 that supports 8 massless surface Dirac cones. It can be a topological paramagnet [63, 64] that supports 8 neutral Dirac fermion along a time reversal breaking domain wall. Alternatively, it can also be a fractional bosonic topo-

logical insulator where a local boson is fractionalized into 8 parton Dirac fermions and the surface hosts 8 parton Dirac cones. In this chapter, we do not focus on the origin of the wire array, but instead we concentrate on its symmetric gapping interactions.

Here, the 8 Dirac fermions of each wire is decomposed into two groups $c_j^A = c_j \sim e^{i\phi_j^A}$ and $c_j^B = c_{4+j} \sim e^{i\phi_j^B}$, for $j = 1, 2, 3, 4$. Each sector is described by a $U(4)$ Kac-Moody conformal field theory at level 1. The bosonized variables follow the action with Lagrangian density

$$\mathcal{L}_0 = \sum_y \sum_{C=A,B} \left[\frac{(-1)^y}{2\pi} \sum_{j=1}^{4} \partial_t \phi_y^{C,j} \partial_x \phi_y^{C,j} + \sum_{j,j'=1}^{4} V_{jj'} \partial_x \phi_y^{C,j} \partial_x \phi_y^{C,j'} \right], \tag{3.32}$$

where $V_{jj'}$ is a non-universal velocity matrix. We further decompose each sector $C = A, B$ into

$$U(4)_1 \sim U(1)_4 \times SU(4)_1. \tag{3.33}$$

$U(1)_4$ represent the diagonal component and is generated by the bosonized variable

$$4\phi_{\rho,y}^C = \boldsymbol{\alpha}^0 \cdot \boldsymbol{\phi}_y^C = \phi_y^{C,1} + \ldots \phi_y^{C,4}, \tag{3.34}$$

where $\boldsymbol{\alpha}^0 = (1, 1, 1, 1)$. Although in this chapter we do not focus on charge conservation, for the charge preserving SPT states, the $U(1)_4$ sector is solely responsible for electric charge transport. The $SU(4)$ Kac-Moody current algebra at level 1 is generated by the 3 Cartan generators

$$H_y^{C,j} = i\partial\phi_y^{C,j} - i\partial\phi_y^{C,j+1} \tag{3.35}$$

for $j = 1, 2, 3$, and the 12 roots

$$E_y^{C,\boldsymbol{\alpha}} = \exp\left(i\alpha_j \phi_y^{C,j}\right) \tag{3.36}$$

where the root vectors $\boldsymbol{\alpha} = (\alpha_1, \alpha_2, \alpha_3, \alpha_4) \in \Delta_{SU(4)}$ has entries $\alpha_j = 0, \pm 1$, length square $|\boldsymbol{\alpha}|^2 = 2$ and is traceless $\alpha_1 + \alpha_2 + \alpha_3 + \alpha_4 = 0$. The $SU(4)_1$ represents electrically neutral degrees of freedom if the SPT state preserves charge symmetry. It also completely decoupled from $U(1)_4$ as all the roots $\boldsymbol{\alpha}$ are orthogonal to $\boldsymbol{\alpha}^0$.

One can pick the simple roots of $SU(4)$ to be

$$R_{SU(4)} = \begin{pmatrix} -- & \boldsymbol{\alpha}^1 & -- \\ -- & \boldsymbol{\alpha}^2 & -- \\ -- & \boldsymbol{\alpha}^3 & -- \end{pmatrix} = \begin{pmatrix} 1 & -1 & 0 & 0 \\ 0 & 1 & -1 & 0 \\ 0 & 0 & 1 & -1 \end{pmatrix}. \tag{3.37}$$

This recovers the Cartan matrix of $SU(4)$

$$K_{SU(4)} = R_{SU(4)} R^T_{SU(4)} = \begin{pmatrix} 2 & -1 & 0 \\ -1 & 2 & -1 \\ 0 & -1 & 2 \end{pmatrix}, \tag{3.38}$$

which is identical to that of $SO(6)$ (see eq.(3.10)). Consequently, as an affine Lie algebra or a Kac-Moody algebra, $SU(4)$ and $SO(6)$ are equivalent. For instance, they have the identical dimension $d = 15$ and rank $r = 3$. The root structures of the two are also isomorphic except the $SO(6)$ roots are presented in three dimensions whereas the $SU(4)$ ones are presented in a 3D orthogonal complement of $(1, 1, 1, 1)$ in four dimensions. The equivalence implies the $SU(4)$ roots span a face-centered cubic root lattice FCC = $\text{span}_{\mathbb{Z}}\{\boldsymbol{\alpha}^1, \boldsymbol{\alpha}^2, \boldsymbol{\alpha}^3\}$.

The inter-channel backscattering sine-Gordon potential (see also figure 3.1(a)) is

$$\begin{aligned} \mathcal{H}_{\text{dimer}} &= \mathcal{H}^{U(1)_4} + \mathcal{H}^{SU(4)_1}, \\ \mathcal{H}^{U(1)_4} &= -u \sum_y \cos\left(4\phi^A_{\rho,y} - 4\phi^B_{\rho,y+1}\right) \\ &= -u \sum_y \cos\left(2\Theta^1_{y+1/2} + \ldots + 2\Theta^4_{y+1/2}\right), \\ \mathcal{H}^{SU(4)_1} &= -\frac{u}{2} \sum_y \sum_{\boldsymbol{\alpha}} E^{A,\boldsymbol{\alpha}}_y E^{B,-\boldsymbol{\alpha}}_{y+1} \\ &= -u \sum_y \sum_{\boldsymbol{\alpha}} \cos\left(\boldsymbol{\alpha} \cdot 2\boldsymbol{\Theta}_{y+1/2}\right), \end{aligned} \tag{3.39}$$

where $2\Theta_{y+1/2} = (2\Theta^1_{y+1/2}, 2\Theta^2_{y+1/2}, 2\Theta^3_{y+1/2}, 2\Theta^4_{y+1/2})$ and $2\Theta^j_{y+1/2} = \phi^{A,j}_y - \phi^{B,j}_{y+1}$. Similar to the $SO(6)_1$ Hamiltonian (3.11), the backscattering term here also introduces a finite excitation energy gap. The angle variables of the sine-Gordon Hamiltonian obey the Haldane nullity gapping condition (c.f. (3.12)). The $SU(4)$ current-current backscattering provides more than enough gapping terms, and linearly dependent redundant terms are non-competing if $u > 0$. The ground state expectation values of the angle variables

$\langle 2\boldsymbol{\Theta}_{y+1/2}\rangle$ belongs in the "Haldane's dual lattice"

$$\mathcal{L}_{\boldsymbol{\Theta}} \equiv \left\{2\boldsymbol{\Theta} : \boldsymbol{\alpha}\cdot 2\boldsymbol{\Theta}, \boldsymbol{\alpha}^0\cdot 2\boldsymbol{\Theta} \in 2\pi\mathbb{Z}\right\} \tag{3.40}$$

so that the sine-Gordon energy (3.39) is minimized. The dual lattice can be decomposed into two orthogonal components

$$\begin{aligned} \mathcal{L}_{\boldsymbol{\Theta}} &= \mathcal{L}^{U(1)}_{\boldsymbol{\Theta}} + \mathcal{L}^{SU(4)}_{\boldsymbol{\Theta}}, \\ \mathcal{L}^{U(1)}_{\boldsymbol{\Theta}} &= \mathrm{span}_{\mathbb{Z}}\{2\pi\boldsymbol{\beta}_0\}, \\ \mathcal{L}^{SU(4)}_{\boldsymbol{\Theta}} &= 2\pi\mathrm{BCC} = \mathrm{span}_{\mathbb{Z}}\{2\pi\boldsymbol{\beta}_1, 2\pi\boldsymbol{\beta}_2, 2\pi\boldsymbol{\beta}_3\}, \end{aligned} \tag{3.41}$$

where the primitive reciprocal vectors of $\mathcal{L}^{U(1)}_{\boldsymbol{\Theta}}$ and $\mathcal{L}^{SU(4)}_{\boldsymbol{\Theta}}$ are

$$\begin{aligned} \boldsymbol{\beta}_\mu &= \frac{1}{3!}\varepsilon_{\mu\nu\lambda\sigma}\frac{\boldsymbol{\alpha}^\nu\wedge\boldsymbol{\alpha}^\lambda\wedge\boldsymbol{\alpha}^\sigma}{\boldsymbol{\alpha}^0\cdot(\boldsymbol{\alpha}^1\wedge\boldsymbol{\alpha}^2\wedge\boldsymbol{\alpha}^3)}, \\ \boldsymbol{\beta}_0 &= \frac{1}{4}(1,1,1,1), \\ R^\vee_{SU(4)} &= \begin{pmatrix} -- & \boldsymbol{\beta}_1 & -- \\ -- & \boldsymbol{\beta}_2 & -- \\ -- & \boldsymbol{\beta}_3 & -- \end{pmatrix} = \frac{1}{4}\begin{pmatrix} 3 & -1 & -1 & -1 \\ 2 & 2 & -2 & -2 \\ 1 & 1 & 1 & -3 \end{pmatrix}. \end{aligned} \tag{3.42}$$

Similar to the $SO(6)_1$ case, the deconfined excitations of the sine-Gordon model (3.39) are kinks of the angle variables where $\langle 2\boldsymbol{\Theta}_{y+1/2}\rangle$ jumps discontinuously from one value to another in $\mathcal{L}_{\boldsymbol{\Theta}}$. The kinks can be created by fractional vertex operators $V^{C,\boldsymbol{\gamma}}_y = \exp\left[i\gamma_j\phi^{C,j}_y\right]$ (c.f. (3.16)), where in this case the fractional lattice vectors are four dimensional $\boldsymbol{\gamma} = (\gamma_1,\gamma_2,\gamma_3,\gamma_4)$. Excitations can be decomposed into $U(1)_4$ and $SU(4)_1$ components that associates to kinks of $\mathcal{H}^{U(1)}$ and $\mathcal{H}^{SU(4)}$ in (3.39) respectively. For $U(1)_4$, the primary fields $[n]_\rho$ are vertex operators $e^{in\phi^C_{\rho,y}} = e^{in(\phi^{C,1}_y+\ldots+\phi^{C,4}_y)/4}$, where n is an integer. They carry spins (or conformal scaling dimensions) $h_{[n]_\rho} = n^2/8$.

For $SU(4)_1$, certain vertex operators can be grouped together into super-selection sectors $\{V^{C,\boldsymbol{\gamma}^1}_y,\ldots,V^{C,\boldsymbol{\gamma}^r}_y\}$ and corresponds to a primary field of $SU(4)_1$. Vertices of each super-sector transform among each other under the $SU(4)_1$ affine Lie algebra (c.f. (3.22)). As $SU(4)_1$ and $SO(6)_1$ are equivalent, there is a one-to-one correspondence between the primary fields. Using the same notation in $SO(6)_1$, the primary fields $1,\psi,s_+,s_-$ of $SU(4)_1$ corresponds to the trivial, vector, fundamental and anti-fundamental representations of $SU(4)$. The primary field ψ corresponds to the super-sector of 6 vertex operators $e^{i\boldsymbol{\gamma}^\psi\cdot\boldsymbol{\phi}^C_y}$, where $\boldsymbol{\gamma}^\psi = (1,1,-1,-1)/2$ or any permutation of the entries. The super-sector of the primary field $s_\pm$ consists of the 4 vertex operators

$e^{i\boldsymbol{\gamma}^{s_\pm}\cdot\boldsymbol{\phi}_y^C}$, where $\boldsymbol{\gamma}^{s_\pm} = \pm(3,-1,-1,-1)/4$ or any permutation of the entries. The spins (i.e. conformal scaling dimensions) of the primary fields are $h_\psi = 1/2$ and $h_{s_\pm} = 3/8$, which unsurprisingly match that of the primary fields of $SO(6)_1$.

Before we end this section, let us take a closer look at the sine-Gordon terms for $SU(4)_1$ sector. Usually we take $u > 0$ such that the sine-Gordon terms are pinned at their respective minima to gap out the system from the renormalization group (RG) analysis. What if $u < 0$ or even u is a complex parameter? This is related to the duality properties of ADE surface topological orders discussed later. So let us study the general structure of sine-Gordon terms when $u = |u|e^{i\vartheta}$ is complex valued. The general sine-Gordon is

$$\begin{aligned}\mathcal{H}^{SU(4)_1} &= -\frac{|u|}{2}\sum_y \sum_{\boldsymbol{\alpha}\in\Delta_+} \left(E_y^{A,\boldsymbol{\alpha}} E_{y+1}^{B,-\boldsymbol{\alpha}} e^{i\vartheta} + E_y^{A,-\boldsymbol{\alpha}} E_{y+1}^{B,\boldsymbol{\alpha}} e^{-i\vartheta}\right) \\ &= -|u|\sum_y \sum_{\boldsymbol{\alpha}\in\Delta_+} \cos\left(\boldsymbol{\alpha}\cdot 2\boldsymbol{\Theta}_{y+1/2} + \vartheta\right),\end{aligned} \tag{3.43}$$

where Δ_+ is the set of positive roots. In this case, we find that as long as $\vartheta \neq \pi$, the system is gapped; when $\vartheta = \pi$ the system becomes gapless. Reversing the sign of $\boldsymbol{\Theta}_{y+1/2}$ is equivalent to taking the complex conjugate of u, namely,

$$2\boldsymbol{\Theta}_{y+1/2} \to -2\boldsymbol{\Theta}_{y+1/2} \Leftrightarrow u \to u^* \Leftrightarrow \vartheta \to -\vartheta, \tag{3.44}$$

which is also equivalent to a reflection with respect to the real axis in the u complex plane. The duality transformation on the u-plane is shown in Fig. 3.4. Since $SO(6)_1$ has the same root structure as $SU(4)_1$, the above analysis also works for $SO(6)_1$ theory. The ground state structure is shown in Fig. 3.5.

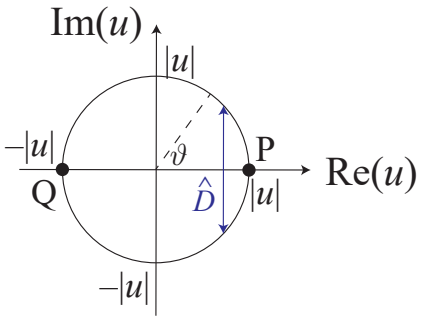

Figure 3.4: Duality transformation of the sine-Gordon term on the u-plane. $\hat{D}$ is the duality operator. Under $\hat{D}$, points on the circle with radius $|u|$ is reflected with respect to the real axis. P, Q are self-dual points. P describes a gapless point, which can be seen in Fig. 3.5(c). Other points on the circle describe gapped phases.

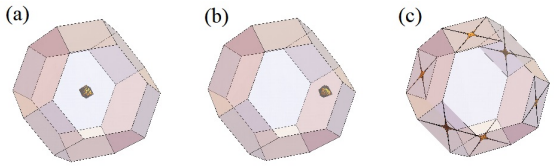

Figure 3.5: The ground state expectation values of $\langle 2\mathbf{\Theta}_{y+1/2}\rangle$ that minimize the sine-Gordon Hamiltonian (3.43) for (a) $\vartheta = 0$, (b) $\vartheta = -3\pi/5$ and (c) $\vartheta = \pi$. The plots are taken over the fundamental region in $\mathbb{R}^3$ modulo the Haldane dual lattice $\mathcal{L}_{\mathbf{\Theta}}^{SU(4)}$ in (3.41). The sine-Gordon Hamiltonian generically has a finite energy gap and a single minimum for $-\pi < \vartheta < \pi$. At $\vartheta = \pi$, there are gapless Goldstone modes on the boundary of the fundamental region.

3.3 Review of free Dirac fermion/3d QED duality

In this section, we review the coupled wire derivation of the free Dirac fermion/QED$_3$ duality following Ref. [19, 20]. Written explicitly, the duality says

$$\begin{aligned} S_{\text{Dirac}} &= \int dx^3 \; i\bar{\Psi}\gamma^\mu(\partial_\mu - iA_\mu)\Psi \\ &\updownarrow \\ S_{\text{QED}_3} &= \int dx^3 \; i\bar{\tilde{\Psi}}\gamma^\mu(\partial_\mu - ia_\mu)\tilde{\Psi} + \frac{1}{4\pi}\epsilon_{\mu\nu\rho}A_\mu\partial_\nu a_\rho, \end{aligned} \tag{3.45}$$

where a_μ is a dynamical $U(1)$ gauge field and A_μ is a background $U(1)$ field. Since in 2+1d, a single copy of Dirac fermion with unit charge suffers from the traditional "parity" anomaly, the duality is better understood to hold at the surface of a 3+1d topological insulator. We add quotation marks for "parity" because strictly speaking, parity is in the connected component of the rotation group in 2+1d. Therefore, the anomaly is better called as an anomaly of time-reversal symmetry T or reflection symmetry R. Detailed clarifications can be found in Ref. [117]. Several derivations have been given from the field-theoretic perspectives. Specifically, what they have done is to start from the conjectured fermion/boson duality, which is the duality between a single free Dirac fermion and a complex boson coupled to a dynamical $U(1)$ gauge field at the $O(2)$ Wilson-Fishier fixed point with quartic interactions. [110, 111] Then they perform flux attachment to the original duality to obtain the fermion/fermion duality. The same can be performed at the coupled wire level, which may be clearer in the sense that one can see the explicit interactions at the microscopic level. We now review it below.

Let us start from the array of 1D chiral electron wires, each aligned along x-direction. The Hamiltonian

can be written as

$$H = \sum_y \int dx\ v_x(-1)^y \psi_y^\dagger(-i\partial_x)\psi_y - v_y(-1)^y(\psi_y^\dagger\psi_{y+1} + \text{h.c.}), \tag{3.46}$$

where in Eq. (3.46) y is the wire label along y-direction. Wires labeled by even y carry right-moving electrons and odd y carry left-moving electrons. The first term in Eq. (3.46) describes the kinetic energy of electrons and the second term describes uniform inter-wire hopping between neighboring wires (see figure 3.1(b)). Using a two-component spinor $\Psi(x,y) = (\psi_{2y}(x), \psi_{2y+1}(x))^T$, Eq. (3.46) can be rewritten in the continuum limit as

$$H = \int dxdy\Psi^\dagger[v_x\sigma^z(-i\partial_x) + v_y\sigma^y(-i\partial_y)]\Psi, \tag{3.47}$$

where the sum $\sum_y$ is replaced by $\int dy$. Eq. (3.47) therefore recovers the effective Hamiltonian for a single copy of Dirac fermion in 2+1d. Now let us bosonize the Dirac fermion on each wire by $\psi_y = e^{i\phi_y}$, where ϕ_y is a chiral boson field satisfying the commutation relation

$$[\phi_y(x), \phi_{y'}(x')] = \delta_{yy'}(-1)^y i\pi\text{sgn}(x-x') + i\pi\text{sgn}(y'-y), \tag{3.48}$$

where $\text{sgn}(s) = s/|s|$ and $\text{sgn}(0) = 0$. The first and second terms of Eq. (3.48) give the correct anticommutation relations of fermions in the same wire and between different wires, respectively. Written in terms of boson fields, the original Dirac action in Eq. (3.45) becomes

$$S_{\text{Dirac}} = \sum_y \int dxdt\ \big[\frac{i(-1)^y}{4\pi}\partial_x\phi_y\partial_t\phi_y + \frac{v_x}{4\pi}(\partial_x\phi_y)^2 + v_y(-1)^y\cos(\phi_y - \phi_{y+1})\big]. \tag{3.49}$$

Under renormalization group (RG) flow, this theory remains gapless due to the competition between neighboring sine-Gordon terms.

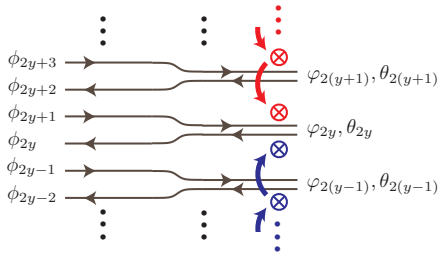

Figure 3.6: Pictorial illustration of the duality transformation in Eq. (3.50) or (3.51). Two flux quanta from $+\infty$ and $-\infty$ attached to each pair of wires.

Now let us perform the duality transformation

$$\tilde{\phi}_y(x) = \sum_{y'} \mathrm{sgn}(y-y')(-1)^{y'}\phi_{y'}(x) \equiv \sum_{y'} D_{yy'}\phi_{y'}(x). \tag{3.50}$$

This duality transformation (3.50) is a flux attachment (see figure 3.6). Using the non-chiral basis between wire $2y$ and $2y+1$, $\varphi_{2y}, \theta_{2y} = (\phi_{2y} \pm \phi_{2y+1})/2$, Eq. (3.50) is equivalent to

$$\tilde{\psi}^\dagger_{2y/2y+1} \sim \psi^\dagger_{2y+1/2y} \prod_{y'>y} e^{2i\theta_{2y'}} \prod_{y'<y} e^{-2i\theta_{2y'}}, \tag{3.51}$$

where $e^{2i\theta_{2y}}$ brings a 2π phase slip in φ_{2y}. Eq. (3.51) can be understood as bringing two fluxes from positive and negative infinities to the fermion at wire $2y/2y+1$. One can check that under duality (3.50), the equal-time commutation relation only changes by a sign

$$[\tilde{\phi}_y(x), \tilde{\phi}_{y'}(x')] = -[\phi_y(x), \phi_{y'}(x')]. \tag{3.52}$$

Physically it means that the dual fermions $e^{i\tilde{\phi}_y}$ have opposite chiralities with the original ones. After duality transformation, the original action (3.49) for the Dirac fermion becomes

$$\tilde{S}_{\mathrm{Dirac}} = \sum_y \int dxdt \left\{ \frac{-i(-1)^y}{4\pi}\partial_x\tilde{\phi}_y\partial_t\tilde{\phi}_y + \frac{v_x}{4\pi}(\partial_x D^{-1}_{yy'}\tilde{\phi}_{y'})^2 + v_y(-1)^y \cos\left(\tilde{\phi}_y - \tilde{\phi}_{y+1}\right)\right\}. \tag{3.53}$$

One can see that in the dual action (3.53), the first and last terms have the same form as the original action (3.49). However, the second term is highly non-local. To resolve this, one introduces two Lagrangian multipliers $\tilde{a}_{0,y}, \tilde{a}_{1,y}$ on each wire and rewrite Eq. (3.53) as

$$\tilde{\mathcal{L}}_{\mathrm{Dirac}} = \sum_y \frac{-i(-1)^y}{4\pi}\partial_x\tilde{\phi}_y\partial_t\tilde{\phi}_y + \mathcal{L}_{\mathrm{QED}_3}, \tag{3.54}$$

where

$$\begin{aligned}
\mathcal{L}_{\mathrm{QED}_3} &= \mathcal{L}_0 + \mathcal{L}_{\text{staggered-CS}} + \mathcal{L}_{\text{Maxwell}} + \mathcal{L}_{\text{tunnel}}, \\
\mathcal{L}_0 &= \sum_y \frac{i(-1)^y}{2\pi} \partial_x \tilde{\phi}_y \tilde{a}_{0,y} + \sum_y \frac{\tilde{v}_x}{4\pi} (\partial_x \tilde{\phi}_y - \tilde{a}_{1,y})^2, \\
\mathcal{L}_{\text{staggered-CS}} &= \sum_y \frac{i(-1)^y}{8\pi} (\Delta \tilde{a}_{0,y})(\tilde{a}_{1,y+1} + \tilde{a}_{1,y}), \\
\mathcal{L}_{\text{Maxwell}} &= \sum_y \frac{1}{16\pi} \left[\frac{1}{v_x} (\Delta \tilde{a}_{0,y})^2 + v_x (\Delta \tilde{a}_{1,y})^2 \right],
\end{aligned} \tag{3.55}$$

and $\Delta \tilde{a}_{i,y} \equiv \tilde{a}_{i,y+1} - \tilde{a}_{i,y}$. Now one can see that the dual Dirac theory is nothing but QED_3, where $\tilde{a}_{0,y}, \tilde{a}_{1,y}$ are now the emergent $U(1)$ gauge field under the gauge fixing $\tilde{a}_{2,y} = 0$. The theory is invariant under the gauge transformation

$$\begin{aligned}
\tilde{\phi}_y &\to \tilde{\phi}_y + f_y, \\
\tilde{a}_{0,y} &\to \tilde{a}_{0,y} + \partial_t f_y, \\
\tilde{a}_{1,y} &\to \tilde{a}_{1,y} + \partial_x f_y, \\
\tilde{a}_{2,y+1/2} &\to \tilde{a}_{2,y+1/2} + (f_{y+1} - f_y),
\end{aligned} \tag{3.56}$$

if we restore the $\tilde{a}_{2,y+1/2}$ component. Introducing these emergent gauge fields in the path integral only contributes an irrelevant overall multiplicative factor, which is unimportant. Thus the duality between a single Dirac fermion and QED_3 is established at the path integral level.

Let us now take a look at how symmetries transform under duality. If we define time reversal (TR) symmetry and particle-hole (PH) symmetry on the basis Ψ as

$$\mathcal{T} : \Psi \to i\sigma^y \Psi, \quad \mathcal{C} : \Psi \to i\sigma^y \Psi^\dagger, \tag{3.57}$$

then under the duality transformation (3.50) with some modifications to the transformation of ϕ variables, [20] we have

$$\tilde{\mathcal{T}} : \tilde{\Psi} \to i\sigma^y \tilde{\Psi}^\dagger, \quad \tilde{\mathcal{C}} : \tilde{\Psi} \to i\sigma^y \tilde{\Psi}. \tag{3.58}$$

We see that TR and PH symmetries are exchanged under duality. In the following discussion of the surface topological orders of ADE classifications, the generalization of the duality transformation for the single

Dirac fermion will be utilized.

3.4 D-series: SO(N) surface theory

3.4.1 Surface massless Majorana fermions in a coupled wire model

The coupled wire model for D-series has been discussed in Ref. [21] for the Majorana surfaces of topological superconductors. A particular case for $SO(6)$ was demonstrated in section 3.2. We here describe the general construction. The generic coupled wire Hamiltonian for N copies of surface massless Majorana fermions is the sum

$$\mathcal{H}_0 + \mathcal{H}_{\rm bc} = \sum_{y=-\infty}^{\infty} iv_x(-1)^j \boldsymbol{\psi}_y^T \partial_x \boldsymbol{\psi}_y + \sum_{y=-\infty}^{\infty} iv_y \boldsymbol{\psi}_y^T \boldsymbol{\psi}_{y+1}, \tag{3.59}$$

where the integer y labels the wire in the vertical direction (see figure 3.1), and $\boldsymbol{\psi} = (\psi^1, \ldots, \psi^N)$ is an N-component Majorana fermion. Majorana fermions on adjacent wires have opposite chiralities. The uniform non-dimerizing backscattering terms in $\mathcal{H}_{\rm bc}$ on the second line compete with neighboring ones, and the Hamiltonian describes N massless Majorana fermions with linear dispersion in both the x and y directions. In this chapter, we are interested in Abelian surface topological phases, and for this reason, we restrict $N = 2r > 4$. On each wire, Majorana fermion pairs form Dirac fermions, which can then be bosonized

$$c_y^a = \frac{1}{\sqrt{2}} \left(\psi_y^{2a-1} + i\psi_y^{2a} \right) \sim e^{i\phi_y^a}, \quad a = 1, \ldots, r. \tag{3.60}$$

The bosons satisfy the equal-time commutation relation

$$\begin{aligned} \left[\phi_y^a(x), \phi_{y'}^{a'}(x') \right] = i\pi(-1)^y \big[& \delta_{yy'} \delta^{aa'} \mathrm{sgn}(x - x') \\ & + \delta_{yy'} \mathrm{sgn}(a - a') \big] + i\pi \mathrm{sgn}(y' - y), \end{aligned} \tag{3.61}$$

where terms on the second line enforces mutual anticommutation product relations between Dirac fermions, and $\mathrm{sgn}(x) = x/|x| = \pm 1$ for $x \neq 0$ and $\mathrm{sgn}(0)$=0. The first line of Eq. (3.61) is equivalent to the commutator between conjugate fields

$$\left[\partial_x \phi_y^a(x), \phi_{y'}^{a'}(x') \right] = 2i\pi(-1)^y \delta_{yy'} \delta^{aa'} \delta(x - x'), \tag{3.62}$$

which is dictated by the "$p\dot{q}$" term of the Lagrangian density

$$\mathcal{L}_0 = \frac{1}{2\pi}\sum_y \sum_{a=1}^{r} (-1)^y \partial_x \phi_y^a \partial_t \phi_y^a. \tag{3.63}$$

The total Lagrangian density can be written in terms of boson fields as $\mathcal{L} = \mathcal{L}_0 - \mathcal{H}_0$, where

$$\mathcal{H}_0 = V_x \sum_y \sum_{a=1}^{r} \partial_x \phi_y^a \partial_x \phi_y^a \tag{3.64}$$

is the non-universal sliding Luttinger liquid (SLL) component along each wire. The non-dimerizing backscattering terms in (3.59) can also be bosonized, and take the form of $\mathcal{H}_{\rm bc} = V_y \sum_y \sum_{a=1}^{r} \cos\left(\phi_y^a - \phi_{y+1}^a\right)$. However, we suppress these single-body terms throughout this section for the following reason. The bosonized Hamiltonian density (3.64) has an additional local gauge symmetry

$$\phi_y^a \to \phi_y^a + 2\pi m_y^a \tag{3.65}$$

where $m_y^1, \ldots, m_y^r$ are either all integers or all half-integers. This represents a local $\mathbb{Z}_2$ gauge symmetry that transforms the Majorana fermions according to

$$\psi_y^j \to (-1)^{M_y} \psi_y^j, \tag{3.66}$$

where $M_y \equiv 2m_y^a$ modulo 2. Eq. (3.66) is violated by the fermionic Hamiltonian density (3.59). Instead, the fermionic $\mathcal{H}_0$ and $\mathcal{H}_{\rm bc}$ in (3.59) are only symmetric under a global $\mathbb{Z}_2$ symmetry where $m = m_y$ is uniform. Throughout this section, we focus on a *bosonic* coupled wire surface constructions that preserve the local $\mathbb{Z}_2$ symmetry (3.66). For example, the model mimics the surface of a bosonic topological superconductor that supports emergent Majorana fermion coupled with a $\mathbb{Z}_2$ gauge theory. The vectors $\mathbf{m}_y = (m_y^1, \ldots, m_y^r)^T$ that correspond to the gauge transformation (3.65) live in a lattice

$$\begin{aligned} \mathcal{L}^r_{\rm gauge} &= \left\{\mathbf{m} : 2m^a \in \mathbb{Z}, m^1 \equiv \ldots \equiv m^r \bmod 1\right\} \\ &= \mathrm{span}_{\mathbb{Z}} \left\{ \frac{1}{2}\boldsymbol{\varepsilon} = \frac{1}{2}(\varepsilon^1, \ldots, \varepsilon^r)^T : \varepsilon^a = \pm 1 \right\}. \end{aligned} \tag{3.67}$$

In this section, we focus on scenarios where $r = 2n$ is even. In this case, we further restricts the gauge vectors $\mathbf{m}_y$ in (3.65) to live in the *even* lattice

$$\mathcal{L}^{r,+}_{\text{gauge}} = \text{span}_{\mathbb{Z}} \left\{ \frac{1}{2}\boldsymbol{\varepsilon}_+ : \varepsilon^a_+ = \pm 1, \prod_{a=1}^{r} \varepsilon^a_+ = +1 \right\} \tag{3.68}$$

for $r = 2n \geq 4$. The $r = 2$ case is special and corresponds to the decomposable algebra $SO(4) = SU(2) \times SU(2)$, where the even gauge lattice is $\mathcal{L}^{2,+}_{\text{gauge}} = \text{span}_{\mathbb{Z}} \left\{ (1,-1)^T, (1/2,1/2)^T \right\}$.

Before moving on, we briefly comment on the symmetries of the model. If the surface state is supported by a bulk time-reversal symmetry-protected topology, then the coupled wire model exhibits an antiferromagnetic time-reversal (AFTR) symmetry, [21] which accompanies the time-reversal that flips the fermions' propagating direction with a half-translation that moves $y \to y+1$. In this case, the equal-time commutation relation (3.61) needs to be modified to

$$\begin{aligned} \left[\phi^a_y(x), \phi^{a'}_{y'}(x')\right] = i\pi(-1)^{\max\{y,y'\}} \big[& \delta_{yy'}\delta^{aa'}\text{sgn}(x'-x) \\ & + \delta_{yy'}\text{sgn}(a-a') + \text{sgn}(y-y')\big], \end{aligned} \tag{3.69}$$

to accommodate the antiferromagnetic symmetry

$$\mathcal{T} c^a_y \mathcal{T}^{-1} = (-1)^y c^{a\dagger}_{y+1}, \quad \mathcal{T}\phi^a_y\mathcal{T}^{-1} = \phi^a_{y+1} + \pi y. \tag{3.70}$$

The discretization of surface state by a coupled wire construction and its effect on symmetries was explained by the symmetry extension pattern discussed in Ref. [117, 118] when gapped symmetric boundary states are constructed. The AFTR symmetry protects an odd number of surface massless Majorana fermions from single-body backscattering. There can be additional global symmetries, such as mirror, that further protects an arbitrary number of surface Majorana's. In this work, we do not focus on a particular symmetry, but instead concentrate on the many-body gapping potential based on a fractionalization scheme (see figure 3.1(c)) that can preserve a range of symmetries. In this section, we also require the many-body gapping potential to respect the local $\mathbb{Z}_2$ gauge symmetry (3.66).

3.4.2 Gapping potentials for surface Majorana fermions

The simplest gapping terms are single-body backscattering ones, such as

$$\mathcal{H}_{\text{dimer}} = iu \sum_y \sum_{a=1}^{r} \psi_y^a \psi_{y+1}^{r+a} \tag{3.71}$$

that dimerize Majorana channels and introduce mass to all Majorana fermions. Unfortunately, these single-body dimerizations do not respect the local $\mathbb{Z}_2$ symmetry (3.66). Nevertheless, they illustrate the idea of decomposition of the degrees of freedom along each wire: $N = 2r = r + r$. In each pair, the two sets of Majorana fermions $\psi_y^1, \ldots, \psi_y^r$ and $\psi_y^{r+1}, \ldots, \psi_y^{2r}$ are backscattered independently to adjacent wires in the opposite directions. By introducing this single-body backscattering term, we explicitly break and split the $SO(2r)_1$ symmetry into $SO(r)_1 \times SO(r)_1$ along each wire.

With this idea in mind, we can introduce a second type of gapping terms, which preserve the local $\mathbb{Z}_2$ symmetry (3.66). From the decomposition of the $SO(2r)$ WZW Kac-Moody algebra (also known as conformal embedding)

$$SO(2r)_1 \supset SO(r)_1^A \times SO(r)_1^B, \tag{3.72}$$

we can introduce the two-body Kac-Moody current backscattering interactions

$$\mathcal{H}_{\text{dimer}} = u \sum_y \mathbf{J}_y^{SO(r)^B} \cdot \mathbf{J}_{y+1}^{SO(r)^A} \tag{3.73}$$

for positive u (see figure 3.1(c)). The A sector contains $\psi_y^1, \ldots, \psi_y^r$ and the B sector contains $\psi_y^{r+1}, \ldots, \psi_y^{2r}$. We will show that (3.73) introduces a non-vanishing excitation energy gap in the next subsection.

The $SO(2r)_1$ WZW theory along the y-th wire is generated by the chiral current operator

$$J_y^{(a,b)} = (-1)^y i \psi_y^a \psi_y^b. \tag{3.74}$$

Based on (3.72), we can decompose the current operators into two sets: $\text{SO}(r)_1^A$ contains $J^{(a,b)}$ for $1 \le a < b \le r$ and $\text{SO}(r)_1^B$ contains $J^{(a,b)}$ for $r+1 \le a < b \le 2r$. We can see that these two sets of operators decouple in the sense that their operator product expansions (OPE) are trivial up to non-singular terms. Moreover, the Sugawara energy-momentum tensor [54] of the total $\text{SO}(2r)_1$ algebra decomposes into two

decoupled parts,

$$T_{SO(2r)_1} = T_{SO(r)_1^A} + T_{SO(r)_1^B}, \tag{3.75}$$

$$T_{SO(r)_1^A} = \frac{1}{2(r-1)} \sum_{1\le a<b\le r} J^{(a,b)} J^{(a,b)}$$

$$= -\frac{1}{2}\sum_{a=1}^{r} \psi^a \partial \psi^a, \tag{3.76}$$

$$T_{SO(r)_1^B} = \frac{1}{2(r-1)} \sum_{r+1\le a<b\le 2r} J^{(a,b)} J^{(a,b)}$$

$$= -\frac{1}{2}\sum_{a=r+1}^{2r} \psi^a \partial \psi^a. \tag{3.77}$$

The interaction (3.73) can be expressed using the Majorana fermions

$$\mathcal{H}_{\text{dimer}} = u \sum_y \sum_{1\le a<b\le r} \psi_y^{r+a}\psi_y^{r+b}\psi_{y+1}^a\psi_{y+1}^b. \tag{3.78}$$

We notice in passing the following observations. First, it breaks $O(2r)$ symmetry into $O(r)^A \times O(r)^B$, which transforms

$$\psi_y^a \to (\mathcal{O}^{(-1)^y})_b^a \psi_y^b, \quad \psi_y^{r+a} \to (\mathcal{O}^{(-1)^y})_b^a \psi_y^{r+b}, \tag{3.79}$$

where $\mathcal{O}$ is an $r\times r$ orthogonal matrix. Second, there are alternative interaction terms, such as $\psi_y^a\psi_y^b\psi_{y+1}^{r+a}\psi_{y+1}^{r+b}$, that can compete with (3.78). However, as long as mirror symmetry is broken, one of these can be dominant and lead to a finite energy gap. Third, (3.78) is marginally relevant. The renormalization group (RG) equation for u is [119]

$$\frac{du}{dl} = +4\pi(r-2)u^2, \tag{3.80}$$

showing that the interaction strength is growing at low energy limit when $r > 2$, which is the case that we discuss.

Excitation energy gap

We now review that (3.78) introduces a non-vanishing excitation energy gap. A proof can also be found in Ref. [21]. We focus on a single coupled pair of counter-propagating $SO(r)_1$ channels (see figure 3.1(c)) at some even y. After relabeling $\psi_y^{r+a} = \psi_R^a$ and $\psi_{y+1}^a = \psi_L^a$ for $a = 1, \ldots, r$, the interaction term between the

y-th and $(y+1)$-th wires becomes the $O(r)$ Gross-Neveu (GN) model [120]

$$\mathcal{H}_{GN} = -\frac{u}{2}(\boldsymbol{\psi}_R \cdot \boldsymbol{\psi}_L)^2. \tag{3.81}$$

It is known that the GN model has an energy gap when $r > 2$. For even $r = 2n$, we can use (3.60) to pair Majorana fermions into Dirac fermions

$$c^a_{R/L} = \frac{1}{\sqrt{2}}(\psi^{2a-1}_{R/L} + i\psi^{2a}_{R/L}) \sim e^{i\phi^a_{R/L}}, \quad a = 1, \dots, n. \tag{3.82}$$

Eq. (3.81) bosonizes into

$$\begin{aligned}\mathcal{H}_{GN} &\sim u\sum_{a=1}^{n} \partial_x\phi^a_R \partial_x \phi^a_L - u\sum_{a_1\neq a_2}\sum_{\pm} \cos\left(2\theta^{a_1} \pm 2\theta^{a_2}\right) \\ &= u\sum_{a=1}^{n} \partial_x\phi^a_R \partial_x \phi^a_L - u\sum_{\boldsymbol{\alpha}\in\Delta} \cos\left(\boldsymbol{\alpha}\cdot\mathbf{2\Theta}\right),\end{aligned} \tag{3.83}$$

where $\mathbf{2\Theta} = (2\theta^1, \dots, 2\theta^n)$, $2\theta^a = \phi^a_R - \phi^a_L$, and $\boldsymbol{\alpha} = (\alpha_1, \dots, \alpha_n)^T$ are the $SO(2n)$ roots that lives in

$$\Delta = \left\{\boldsymbol{\alpha} \in \mathbb{Z}^n : |\boldsymbol{\alpha}|^2 = 2\right\}. \tag{3.84}$$

As a matter of fact, a subset of the sine-Gordon terms in (3.83) will be sufficient in introducing an energy gap. We take

$$\begin{aligned}-u\sum_{I=1}^{n} \cos\left(\boldsymbol{\alpha}^I \cdot \mathbf{2\Theta}\right) &= -u\sum_{I=1}^{n} \cos\left(\sum_{J=1}^{n} K_{IJ}(\phi'^J_R - \phi'^J_L)\right) \\ &= -u\sum_{I=1}^{n} \cos\left(\mathbf{n}^T_I \mathsf{K}\boldsymbol{\Phi}\right),\end{aligned} \tag{3.85}$$

where $\boldsymbol{\alpha}^I = (\alpha^I_1, \dots, \alpha^I_n)$ are the n linearly independent simple roots of $SO(2n)$ (c.f. (3.9) for $SO(6)$)

$$R_{SO(2n)} = \begin{pmatrix} -- & \boldsymbol{\alpha}^1 & -- \\ \vdots & \vdots & \vdots \\ -- & \boldsymbol{\alpha}^n & -- \end{pmatrix} = \begin{pmatrix} 1 & -1 & 0 & \dots & 0 & 0 \\ 0 & 1 & -1 & \dots & 0 & 0 \\ \vdots & \vdots & \vdots & \ddots & \vdots & \vdots \\ 0 & 0 & 0 & \dots & 1 & -1 \\ 0 & 0 & 0 & \dots & 1 & 1 \end{pmatrix}. \tag{3.86}$$

Here $K = (K_{IJ})_{n\times n} = R_{SO(2n)}R^T_{SO(2n)}$ is the Cartan matrix of $SO(2n)$, and $\mathsf{K} = K \oplus (-K) = \mathrm{diag}(K, -K)$ includes both the R and L movers. $\boldsymbol{\Phi} = (\boldsymbol{\phi}'_R, \boldsymbol{\phi}'_L)^T$, for $\boldsymbol{\phi}'_{R/L} = (\phi'^1_{R/L}, \ldots, \phi'^n_{R/L})$ and $\phi^a_{R/L} = (R^T_{SO(2n)})^a_J \phi'^J_{R/L} = (\alpha^J_a)\phi'^J_{R/L}$, are the bosonized variables in the Chevalley basis, and $\mathbf{n}_J = (\mathbf{e}_J, \mathbf{e}_J)^T$. The "$p\dot{q}$" component of the Lagrangian density expressed in terms of the Chevalley basis is

$$\mathcal{L}_0 = \frac{1}{2\pi}\sum_{a=1}^{n} \partial_x \phi^a_R \partial_t \phi^a_R - \partial_x \phi^a_L \partial_t \phi^a_L = \frac{1}{2\pi}\partial_x \boldsymbol{\Phi}^T \mathsf{K} \partial_t \boldsymbol{\Phi}. \tag{3.87}$$

The n vectors $\mathbf{n}_I$ are linearly independent and satisfy "Haldane's nullity gapping condition" [112]

$$\mathbf{n}_I^T \mathsf{K} \mathbf{n}_J = 0, \quad \text{for } I, J = 1, \ldots, n. \tag{3.88}$$

This shows (3.85) introduces a finite excitation energy gap.

The additional linearly dependent sine-Gordon terms in (3.83) are complementary when $u > 0$, and they collectively pin the non-competing ground state expectation values $\boldsymbol{\alpha} \cdot \langle 2\boldsymbol{\Theta}\rangle \in 2\pi\mathbb{Z}$. This defines the "Haldane's dual lattice" (c.f. (3.14) for $SO(6)$)

$$\begin{aligned} \mathcal{L}_{\boldsymbol{\Theta}} &\equiv \{2\boldsymbol{\Theta} : \boldsymbol{\alpha} \cdot 2\boldsymbol{\Theta} \in 2\pi\mathbb{Z} \text{ for all } \boldsymbol{\alpha} \in \Delta\} \\ &= 2\pi \mathrm{BCC}^n = \mathrm{span}_{\mathbb{Z}} \{2\pi\boldsymbol{\beta}_1, \ldots, 2\pi\boldsymbol{\beta}_n\}, \end{aligned} \tag{3.89}$$

where the simple dual roots $\boldsymbol{\beta}_I$ are

$$\begin{aligned} \boldsymbol{\beta}_I &= \frac{1}{n!\det(R_{SO(2n)})} \varepsilon_{IJ_1\ldots J_{n-1}} \boldsymbol{\alpha}^{J_1} \wedge \ldots \wedge \boldsymbol{\alpha}^{J_{n-1}} \\ R^{\vee}_{SO(2n)} &= \begin{pmatrix} -- & \boldsymbol{\beta}_1 & -- \\ \vdots & \vdots & \vdots \\ -- & \boldsymbol{\beta}_n & -- \end{pmatrix} \\ &= \begin{pmatrix} 1 & & & & & & \\ 1 & 1 & & & & & \\ 1 & 1 & 1 & & & & \\ \vdots & \vdots & \vdots & \ddots & & & \\ 1 & 1 & 1 & \ldots & 1 & & \\ 1/2 & 1/2 & 1/2 & \ldots & 1/2 & 1/2 & -1/2 \\ 1/2 & 1/2 & 1/2 & \ldots & 1/2 & 1/2 & 1/2 \end{pmatrix}. \end{aligned} \tag{3.90}$$

The dual lattice $\mathcal{L}_{\boldsymbol{\Theta}}$ (up to a factor of 2π) is the body-centered cubic lattice (BCC) in n dimensions, whose lattice vectors have either all integral or all half-integral entries. The mutual commutativity between the angle variables $2\theta^a$ ensures that (3.83) introduces a finite excitation energy gap. Details of the Haldane's nullity gapping condition for the K-matrix formalism is reviewed in Appendix B.1.

When $r = 2n + 1$ is odd, Eq. (3.73) can still be applied to introduce a finite energy gap. However, the gapping Hamiltonian here cannot be fully bosonized because of the extra odd Majorana fermion. Since this situation has been discussed in detail in Ref. [21], it will not be repeated here.

Quasiparticle excitations

The quasiparticle excitations of the sine-Gordon gapping potential (3.83) take a similar structure to that of the $SO(6)$ case described in section 3.2. Here, we only present the main results. A quasiparticle excitation at (x_0, y_0) can be created by a fractional vertex operator $V^{C,\boldsymbol{\gamma}}_{y_0}(x_0) = \exp\left[i\gamma_a \phi^{C,a}_{y_0}(x_0)\right]$, where $C = A, B$, $a = 1, \ldots, n$ and $\phi^{A,a} = \phi^a$, $\phi^{B,a} = \phi^{n+a}$ are the bosonized variables for the Dirac fermions $c^b = (\psi^{2b-1} + i\psi^{2b})/\sqrt{2} \sim e^{i\phi^b}$, for $b = 1, \ldots, r = 2n$. The vector $\boldsymbol{\gamma} = (\gamma_1, \ldots, \gamma_n)$ that corresponds to deconfined excitations can take all integral or all half-integral entries, and therefore it lives on the BCC dual lattice $\mathcal{L}_{\boldsymbol{\Theta}}$ defined in (3.89). There are four primary fields of the $SO(2n)_1$ WZW CFT that generate all deconfined excitations. Each primary field is a super-selection sector of vertex operators that form an irreducible representation of the $SO(2n)_1$ algebra (c.f. (3.22)). The first is the trivial vacuum excitation 1 that corresponds to the trivial representation of $SO(2n)$. The fermionic primary field ψ consists of the vertex operators $\{e^{i\phi^{C,1}_{y_0}(x_0)}, \ldots, e^{i\phi^{C,n}_{y_0}(x_0)}\}$. Each of the vertex operators has conformal scaling dimension $h_\psi = (-1)^{y_0}/2$, and creates a 2π kink to the ground state expectation value $\langle 2\boldsymbol{\Theta}_{y_0 \pm 1/2}\rangle$ at x_0 (c.f. 3.23), where the sign depends on $C = A, B$. Each of the two spinor primary fields $s_\pm$ consists of the set of fractional vertex operators $e^{i\boldsymbol{\varepsilon}\cdot\boldsymbol{\phi}^C_{y_0}(x_0)}/2$, where the vector $\boldsymbol{\varepsilon} = (\varepsilon_1, \ldots, \varepsilon_n)$ has unit entries and $\prod_a \varepsilon_a = 1$ for s_+ and -1 for s_-. The two super-sectors corresponds to the even and odd spinor representations of $SO(2n)$. Each of the vertex operators has a conformal scaling dimension $h_{s_\pm} = (-1)^{y_0} n/8$, and creates a π-kink of $\langle 2\boldsymbol{\Theta}_{y_0 \pm 1/2}\rangle$ at x_0 (c.f. 3.24).

The four primary fields $1, \psi, s_+, s_-$ in $SO(2n)_1$ follow a set of pair operator product expansion formulas. Consequently, the four types of quasiparticle excitations in the coupled wire model follow the corresponding

fusion rules

$$\psi \times \psi = 1, \quad \psi \times s_\pm = s_\mp,$$
$$s_\pm \times s_\pm = \begin{cases} 1, & \text{for even } n \\ \psi, & \text{for odd } n \end{cases}. \tag{3.91}$$

3.4.3 Duality transformation of the Hamiltonian and the symmetry

We now study the duality properties of the gapped surface. The duality transformation here generalizes that in Ref. [19].

$$\tilde{\phi}^a_y(x) = \sum_{y'} \mathrm{sgn}(y - y')(-1)^{y'} \phi^a_{y'}(x), \tag{3.92}$$

where the flavor index a is a spectator in the transformation. Physically it means that we bring two flux quanta from positive and negative infinities to each flavor of chiral fermions independently. Equivalently, we define the duality according to a particular $U(1)^r$subgroup of $SO(2r)$. We can check that the dual field $\tilde{\phi}^a_j$ preserves the commutation relation of the original boson field, up to a minus sign

$$\big[\tilde{\phi}^a_y(x), \tilde{\phi}^{a'}_{y'}(x')\big] = -\big[\phi^a_y(x), \phi^{a'}_{y'}(x')\big]. \tag{3.93}$$

Physically, the dual fermion defined by $\tilde{\psi}^a_y(x) = e^{i\tilde{\phi}^a_y(x)}$ still satisfies the correct fermion anticommutation relation, but it has the opposite chirality of the original fermion on each wire. After duality transformation, the kinetic energy term in Eq.(3.64) becomes highly nonlocal in terms of the dual bosons. This can be resolved by introducing emergent gauge fields $a^a_j(x)$ for each flavor of bosons (c.f. the review in Sec.3.3), and such description will not be repeated here. Instead, we focus on the gapping terms. Under Eq. (3.92), we have

$$\tilde{\phi}^a_{y+1} - \tilde{\phi}^a_y = (-1)^{y+1}(\phi^a_{y+1} - \phi^a_y). \tag{3.94}$$

Thus the sine-Gordon term in (3.83) keeps its original form, namely,

$$-u \sum_{\boldsymbol{\alpha}\in\Delta} \cos\big(\boldsymbol{\alpha}\cdot 2\tilde{\boldsymbol{\Theta}}\big) = -u \sum_{\boldsymbol{\alpha}\in\Delta} \cos\big(\boldsymbol{\alpha}\cdot 2\boldsymbol{\Theta}\big), \tag{3.95}$$

where $2\tilde{\Theta}^a \equiv \tilde{\phi}^a_j - \tilde{\phi}^a_{j+1}$. The sine-Gordon gapping potential is therefore self-dual.

There is a comment on this duality transformation. This self-dual interaction is a special case of the more general case, where the coefficient u of the current-current interaction is complex valued, as we discussed in Sec. 3.2. Without loss of generality, we assume that $|u| = 1$. Thus we can write $u = e^{i\theta}$. Eq. (3.95) corresponds to $\theta = 0$. As we vary θ, in addition to cosine terms, there are sine terms from current-current interaction, which flip sign under duality transformation, seen from Eq. (3.94). Thus the ground state structure would rotate in the Haldane lattice space correspondingly. Then the duality transformation is a reflection with respect to the real axis in the complex u plane. When $\delta = \pi$, the interaction becomes self-dual again. But now the system becomes gapless. Therefore, the phase diagram on the u plane is a unit circle centered at the origin, with self-dual points located at $\theta = 0, \pi$. All the points describe a gapped system except $\theta = \pi$.

We notice in passing the duality transformation of the antiferromagnetic time-reversal symmetry. Under the definition (3.70),

$$\mathcal{T}\tilde{\phi}^a_y\mathcal{T}^{-1} = -\tilde{\phi}^a_{y+1} - \frac{\pi}{2}(-1)^{y+1}. \tag{3.96}$$

The additional minus sign in front of $\tilde{\phi}^a_{y+1}$, when compared with (3.70), means $\mathcal{T} : \tilde{c} \to \tilde{c}$ now preserves dual Dirac fermion number, whereas $\mathcal{T} : c \to c^\dagger$ flips the original ones. The AFTR symmetry therefore carries an additional particle-hole component when transferred across the duality.

We conclude this section by making the following remarks. First, the duality transformation defined in Eq.(3.92) is not unique. There are alternative duality transformations that converge to the same equal-time commutation relation (3.93). Second, the duality transformation (3.92) does not work for the gapped phase of $SO(4)$. From Ref. [21], we see that $SO(4)$ requires special attention because the usual decomposition $SO(4) \sim SO(2) \times SO(2)$ leads to Gross-Neveu interactions that only renormalize the boson velocities without introducing an energy gap. For this purpose, an alternative decomposition is needed – $SO(4) \sim SU(2) \times SU(2)$, and it leads to a special gapping potential. The $SU(2)$ gapping potential is not self-dual under (3.92), and in fact, the dual theory is highly non-local. We suspect the $SO(4) \sim SU(2) \times SU(2)$ fractionalization is self-dual under some alternative duality transformation that is out of the scope of this work.

3.5 A-series: U(N) surface theory

3.5.1 Surface gapless Dirac Hamiltonian via coupled wire construction and decomposition

In this section, we discuss the $U(N)_1$ theories constructed from N Dirac fermions. The $U(4)_1$ prototype was discussed in section 3.2. Here we describe the general situations. The N surface Dirac fermions, with Hamiltonian

$$\mathcal{H}_0 = iv \sum_{a=1}^{N} \sum_{s,s'=\uparrow,\downarrow} c_s^{a\dagger} (\sigma_x \partial_x + \sigma_y \partial_y)_{ss'} c_{s'}^a, \tag{3.97}$$

can be supported by a topological bulk such as a reflection-symmetric topological crystalline insulator with mirror Chern number N [121, 122]. By introducing alternating symmetry breaking Dirac mass on the surface,

$$\delta V = \pm m \sum_{a=1}^{N} \sum_{s,s'=\uparrow,\downarrow} c_s^{a\dagger} (\sigma_z)_{ss'} c_{s'}^a, \tag{3.98}$$

the gapless electronic degrees of freedom are localized along an array of one-dimensional interfaces (see figure 3.1(a)). Each interface, that is sandwiched between adjacent stripes with opposite Dirac masses, hosts N chiral Dirac fermions that co-propagate in a single direction [102].

The Hamiltonian that describes the 1D arrays of low-energy Dirac channels is

$$\mathcal{H}_{D,0} = \sum_{y=-\infty}^{\infty} iv_x (-1)^y \mathbf{c}_y^\dagger \partial_x \mathbf{c}_y, \tag{3.99}$$

where $\mathbf{c}_y = (c_y^1, \ldots, c_y^N)$ is an N-component chiral Dirac fermion. After bosonizing these Dirac fermions via $c_y^a = e^{i\phi_y^a}$, we can write Eq. (3.99) in the same form as Eq. (3.64), namely,

$$\mathcal{H}_{D,0} = V_x \sum_y \sum_{a=1}^{N} \partial_x \phi_y^a \partial_x \phi_y^a, \tag{3.100}$$

where V_x is some non-universal velocity. We can decompose a $U(N)_1$ theory into a $U(1)$ charge sector and an $SU(N)$ spin sector. This decomposition makes the physics richer than that of the D-series, which we will

show later. The $U(1)$ charge sector is represented by the diagonal

$$\Phi_y^\rho = N\tilde{\phi}_y^\rho = \phi_y^1 + \ldots + \phi_y^N \tag{3.101}$$

and the neutral $SU(N)$ sector is represented by

$$\Phi_{y,I} = \sum_{J=1}^{N-1} K_{IJ}^{SU(N)} \tilde{\phi}_y^J = \sum_{a=1}^{N} \alpha_a^I \phi_y^a, \tag{3.102}$$

where $I = 1, \ldots, N-1$. Here $\boldsymbol{\alpha}^I = (\alpha_1^I, \ldots, \alpha_N^I)$, for $\alpha_I^a = \delta_I^a - \delta_{I+1}^a$, are the simple roots of $SU(N)$. The Cartan matrix of $SU(N)$ is the inner product $K_{IJ}^{SU(N)} = \boldsymbol{\alpha}^I \cdot \boldsymbol{\alpha}^J$. The roots of $SU(N)$ form the collection of integral vectors

$$\Delta_{SU(N)} = \left\{ \boldsymbol{\alpha} \in \mathbb{Z}^N : |\boldsymbol{\alpha}|^2 = 2, \sum_{a=1}^{N} \alpha_a = 0 \right\}. \tag{3.103}$$

Details can be found in Appendix B.2.

The "$p\dot{q}$" term of the Lagrangian density decomposes into

$$\begin{aligned} \mathcal{L}_0 &= \frac{1}{2\pi} \sum_y (-1)^y \sum_{a=1}^{N} \partial_x \phi_y^a \partial_t \phi_y^a \\ &= \frac{1}{2\pi} \sum_y (-1)^y N \partial_t \tilde{\phi}_y^\rho \partial_x \tilde{\phi}_y^\rho \\ &\quad + \frac{1}{2\pi} \sum_y (-1)^y \sum_{I,J=1}^{N-1} K_{IJ}^{SU(N)} \partial_t \tilde{\phi}_y^I \partial_x \tilde{\phi}_y^J. \end{aligned} \tag{3.104}$$

In this section, we focus on the partition $N = p + q$ that splits

$$\begin{aligned} U(N)_1 &\supset U(p)_1 \times U(q)_1 \\ &\supset \underbrace{(U(1)_p \times SU(p)_1)}_{A-\text{sector}} \times \underbrace{(U(1)_q \times SU(q)_1)}_{B-\text{sector}}. \end{aligned} \tag{3.105}$$

The partition separate the Dirac fermions into two groups. The A sector consists of $c^1, \ldots, c^p$, and the B sector consists of $c^{p+1}, \ldots, c^{p+q}$. We label the bosonized variables by $\phi^{A,a} = \phi^a$ for $a = 1, \ldots, p$ and

$\phi^{B,b} = \phi^{p+b}$ for $b = 1, \ldots, q$. The Lagrangian density (3.104) splits into

$$\begin{aligned} \mathcal{L}_0 &= \mathcal{L}_0^A + \mathcal{L}_0^B \\ \mathcal{L}_0^C &= \frac{1}{2\pi} \sum_y (-1)^y \sum_{c=1}^{r} \partial_x \phi_y^{C,c} \partial_t \phi_y^{C,c} \\ &= \frac{1}{2\pi} \sum_y (-1)^y r \partial_t \tilde{\phi}_y^{C,\rho} \partial_x \tilde{\phi}_y^{C,\rho} \\ &\quad + \frac{1}{2\pi} \sum_y (-1)^y \sum_{I,J=1}^{r-1} K_{IJ}^{SU(r)} \partial_t \tilde{\phi}_y^{C,I} \partial_x \tilde{\phi}_y^{C,J}. \end{aligned} \tag{3.106}$$

where the charged and neutral bosons $\tilde{\phi}^{C,\rho}$ and $\tilde{\phi}^{C,I}$ are defined similarly to (3.101) and (3.102), for $C = A, B$ and $r = p, q$ respectively. As there are no cross terms in the Lagrangian density, the A and B sectors are completely decoupled from one another.

If the surface Dirac fermions are supported from a mirror-symmetric topological bulk, the Dirac channels are related by reflection

$$M c_y^a M^{-1} = (-1)^y i c_{-y}^a, \quad M \phi_y^a M^{-1} = \phi_{-y}^a + (-1)^y \frac{\pi}{2}. \tag{3.107}$$

The surface array also admits an emergent anti-ferromagnetic time-reversal (AFTR) symmetry (c.f. (3.70) in section 3.4)

$$\mathcal{T} c_y^a \mathcal{T}^{-1} = (-1)^y c_{y+1}^a, \quad \mathcal{T} \phi_y^a \mathcal{T}^{-1} = -\phi_y^a + \frac{1-(-1)^y}{2}\pi. \tag{3.108}$$

The symmetries obey the algebraic relation $M^2 = (-1)^F$, $\mathcal{T}^2 = (-1)^F \text{translation}_{y \to y+2}$ and $TMT^{-1}M^{-1} = \text{translation}_{y \to y+2}$, where $(-1)^F$ is the fermion parity number operator. Mirror and AFTR symmetry preserving surface many-body gapping coupled wire models can be found in Ref. [23, 99]. Unlike the D-series discussion in section 3.4, in this section, we focus on symmetry breaking many-body gapping potentials that support to fractional quasiparticle excitations. For instance, the wire partition (3.105) respects neither one of the symmetries.

3.5.2 Gapping terms for surface Dirac fermions

We now discuss symmetry breaking gapping interactions to (3.99). The array of Dirac channels can acquire a finite excitation energy gap by backscattering dimerizations between adjacent wires. The simplest ones

are the single-body dimerizations

$$\mathcal{H}_{1-\text{body}} = m \sum_{y'} \left[\sum_{a=1}^{p} {c^a_{2y'-1}}^\dagger c^a_{2y'} + h.c. \right.$$
$$\left. + \sum_{b=1}^{q} {c^{p+b}_{2y'}}^\dagger c^{p+b}_{2y'+1} + h.c. \right]. \tag{3.109}$$

It partitions the N Dirac channels in a given wire into $p+q$, and backscatters the two sectors in opposite directions. The backscatterings are therefore non-competing and introduce a single-body mass gap. In this section, we focus on many-body backscattering dimerizations based on the decomposition (3.105). It partitions the N Dirac fermions in any given wire into the $U(1)_p$ and $U(1)_q$ charged sectors and the $SU(p)_1$ and $SU(q)_1$ neutral sectors. By backscattering these decoupled sectors independently, the potentials

$$\begin{aligned}
\mathcal{H} &= \mathcal{H}^A_\rho + \mathcal{H}^B_\rho + \mathcal{H}^A_{SU(p)_1} + \mathcal{H}^q_{SU(q)_1}, \\
\mathcal{H}^A_\rho &= -v_A \sum_{y'} \cos\left(\Phi^{A,\rho}_{2y'} - \Phi^{A,\rho}_{2y'+1}\right), \\
\mathcal{H}^B_\rho &= -v_B \sum_{y'} \cos\left(\Phi^{B,\rho}_{2y'-1} - \Phi^{B,\rho}_{2y'}\right), \\
\mathcal{H}^A_{SU(p)_1} &= u_A \sum_{y'} \mathbf{J}^{SU(p)}_{2y'} \cdot \mathbf{J}^{SU(p)}_{2y'+1}, \\
\mathcal{H}^B_{SU(q)_1} &= u_B \sum_{y'} \mathbf{J}^{SU(q)}_{2y'-1} \cdot \mathbf{J}^{SU(q)}_{2y'},
\end{aligned} \tag{3.110}$$

introduce a finite excitation energy gap to the coupled wire model. Here $\Phi^{A,\rho}_y = \phi^1_y + \ldots + \phi^p_y$ and $\Phi^{B,\rho}_y = \phi^{p+1}_y + \ldots + \phi^{p+q}_y$ are the bosonized variables that generate the charged $U(1)$ sectors, where $N = p+q$. The neutral sectors are generated by the $SU(r)_1$ Kac-Moody currents [54]

$$\begin{aligned}
J^{\boldsymbol{\alpha},SU(p)}_y &= \sum_{a,a'=1}^{p} {c^a_y}^\dagger t^{\boldsymbol{\alpha}}_{aa'} c^{a'}_y, \\
J^{\boldsymbol{\alpha},SU(q)}_y &= \sum_{b,b'=1}^{q} {c^{p+b}_y}^\dagger t^{\boldsymbol{\alpha}}_{bb'} c^{p+b'}_y,
\end{aligned} \tag{3.111}$$

where the fundamental matrix representations $t^{\boldsymbol{\alpha}}_{cc'}$ of $SU(r)$, for $r = p, q$, are listed in Appendix B.2.

The $SU(r)_1$ backscattering dimerizations can be expressed in terms of bosonized variables.

$$\mathcal{H}^A_{SU(p)_1} = u_A \sum_{y'} \left[\sum_{a,a'=1}^{p} V^A_{aa'} \partial_x \phi^a_{2y'} \partial_x \phi^{a'}_{2y'+1} - \sum_{\boldsymbol{\alpha}\in\Delta_{SU(p)}} \cos\left(\boldsymbol{\alpha}\cdot 2\boldsymbol{\Theta}^A_{2y'+1/2}\right) \right], \tag{3.112}$$

$$\mathcal{H}^B_{SU(q)_1} = u_B \sum_{y'} \left[\sum_{b,b'=1}^{q} V^B_{bb'} \partial_x \phi^{p+b}_{2y'-1} \partial_x \phi^{p+b'}_{2y'} - \sum_{\boldsymbol{\alpha}\in\Delta_{SU(q)}} \cos\left(\boldsymbol{\alpha}\cdot 2\boldsymbol{\Theta}^B_{2y'-1/2}\right) \right], \tag{3.113}$$

where $2\boldsymbol{\Theta}^A_{2y'+1/2} = (2\Theta^{A,1}_{2y'+1/2}, \ldots, 2\Theta^{A,p}_{2y'+1/2})$ has entries $2\Theta^{A,a}_{2y'+1/2} = \phi^a_{2y'} - \phi^a_{2y'+1}$, and $2\boldsymbol{\Theta}^B_{2y'-1/2} = (2\Theta^{B,1}_{2y'-1/2}, \ldots, 2\Theta^{B,q}_{2y'-1/2})$ has entries $2\Theta^{B,b}_{2y'-1/2} = \phi^{p+b}_{2y'} - \phi^{p+b}_{2y'}$. Here the velocity terms $V^C_{cc'}$ originate from the backscatterings of the Cartan generators $H^I \sim \boldsymbol{\alpha}^I \cdot \partial\boldsymbol{\phi}$ of $SU(r)_1$, where $\boldsymbol{\alpha}_I$ are the simple roots of $SU(r)$ presented below eq.(3.102). The sine-Gordon terms are responsible in introducing a finite excitation energy gaps in the neutral sectors, and they originate from the backscatterings of the raising and lowering operator $E^{\boldsymbol{\alpha}} \sim e^{i\boldsymbol{\alpha}\cdot\boldsymbol{\phi}}$, where $\boldsymbol{\alpha}$ are the root vectors in $\Delta_{SU(r)}$ defined in (3.103).

Similar to the D-series, the potentials (3.112) and (3.113) consists of more sine-Gordon terms than necessary in order to introduce a finite excitation gap. Instead of summing over all root vectors $\boldsymbol{\alpha}$ in $\Delta_{SU(r)}$, it suffices to include only a set of linearly independent simple roots $\boldsymbol{\alpha}^1, \ldots, \boldsymbol{\alpha}^{r-1}$, where we choose

$$\begin{aligned} R_{SU(r)} &= \begin{pmatrix} -- & \boldsymbol{\alpha}^1 & -- \\ \vdots & \vdots & \vdots \\ -- & \boldsymbol{\alpha}^{r-1} & -- \end{pmatrix}_{(r-1)\times r} \\ &= \begin{pmatrix} 1 & -1 & 0 & \ldots & 0 & 0 \\ 0 & 1 & -1 & \ldots & 0 & 0 \\ \vdots & \vdots & \vdots & \ddots & \vdots & \vdots \\ 0 & 0 & 0 & \ldots & 1 & -1 \end{pmatrix} \end{aligned} \tag{3.114}$$

so that $K = (K_{IJ})_{n\times n} = R_{SU(r)} R^T_{SU(r)}$ is the Cartan matrix of $SU(r)$. All roots $\boldsymbol{\alpha}$ are integer combinations of the simple ones, and given u_A, u_B are positive, the redundant sine-Gordon gapping terms are non-competing. Together with the gapping Hamiltonians $\mathcal{H}_\rho$ in (3.110) for the charged sectors, they collec-

tively pin the ground state expectation values of the angle variables to live in the dual lattice

$$\mathcal{L}_{\boldsymbol{\Theta}} \equiv \left\{ 2\boldsymbol{\Theta} \in \mathbb{R}^r : \begin{array}{c} \boldsymbol{\alpha} \cdot 2\boldsymbol{\Theta}, \boldsymbol{\alpha}^0 \cdot 2\boldsymbol{\Theta} \in 2\pi\mathbb{Z} \\ \boldsymbol{\alpha} \in \Delta_{SU(r)}, \boldsymbol{\alpha}^0 = (1, \ldots, 1) \end{array} \right\} \tag{3.115}$$

so that all sine-Gordon terms in (3.110), (3.112) and (3.113) are simultaneously minimized (c.f. the discussion on $U(4)$ in section 3.2).

The dual lattice decomposes into the orthogonal $U(1)$ and $SU(r)$ sectors

$$\begin{aligned} \mathcal{L}_{\boldsymbol{\Theta}} &= \mathcal{L}_{\boldsymbol{\Theta}}^{U(1)} \oplus \mathcal{L}_{\boldsymbol{\Theta}}^{SU(r)}, \\ \mathcal{L}_{\boldsymbol{\Theta}}^{U(1)} &= \mathrm{span}_{\mathbb{Z}}\{2\pi\boldsymbol{\beta}_0\}, \\ \mathcal{L}_{\boldsymbol{\Theta}}^{SU(r)} &= \mathrm{span}_{\mathbb{Z}}\{2\pi\boldsymbol{\beta}_1, \ldots, 2\pi\boldsymbol{\beta}_{r-1}\}, \end{aligned} \tag{3.116}$$

where the primitive reciprocal vectors of $\mathcal{L}_{\boldsymbol{\Theta}}^{U(1)}$ and $\mathcal{L}_{\boldsymbol{\Theta}}^{SU(r)}$ are

$$\begin{aligned} \boldsymbol{\beta}_I &= \frac{1}{(r-1)!} \varepsilon_{IJ\ldots K} \frac{\boldsymbol{\alpha}^J \wedge \ldots \wedge \boldsymbol{\alpha}^K}{\boldsymbol{\alpha}^0 \cdot (\boldsymbol{\alpha}^1 \wedge \ldots \wedge \boldsymbol{\alpha}^{r-1})}, \\ \boldsymbol{\beta}_0 &= \frac{1}{r}(1, \ldots, 1) \end{aligned} \tag{3.117}$$

so that $\boldsymbol{\alpha}^\mu \cdot \boldsymbol{\beta}_\nu = \delta^\mu_\nu$, for $\mu, \nu = 0, 1, \ldots, r-1$. Here, the entries of the reciprocal vectors $\boldsymbol{\beta}_I = (\beta_I^1, \ldots, \beta_I^r)$ of $SU(r)$ take the explicit form

$$\beta_I^a = \begin{cases} (r-I)/r, & \text{if } a \leq I \\ -I/r, & \text{if } a > I \end{cases} \tag{3.118}$$

for $I = 1, \ldots, r-1$.

A $\mathbb{Z}_2$ twist

Contrary to the D-series, here there is an alternative choice of gapping potentials, which involves the product of the neutral and charged sectors

$$\begin{aligned}
\mathcal{H}_{\mathbb{Z}_2} &= \mathcal{H}^A_{\mathbb{Z}_2} + \mathcal{H}^B_{\mathbb{Z}_2}, \\
\mathcal{H}^A_{\mathbb{Z}_2} &= -u_A \sum_{y'} \cos\left(\Phi^{A,\rho}_{2y'} - \Phi^{A,\rho}_{2y'+1}\right) \\
&\qquad \times \sum_{I=1}^{p-1} \cos\left(\boldsymbol{\alpha}^I_{SU(p)} \cdot 2\boldsymbol{\Theta}^A_{2y'+1/2}\right), \\
\mathcal{H}^B_{\mathbb{Z}_2} &= -u_B \sum_{y'} \cos\left(\Phi^{B,\rho}_{2y'-1} - \Phi^{B,\rho}_{2y'}\right) \\
&\qquad \times \sum_{I=1}^{q-1} \cos\left(\boldsymbol{\alpha}^I_{SU(q)} \cdot 2\boldsymbol{\Theta}^B_{2y'-1/2}\right),
\end{aligned} \tag{3.119}$$

where $2\boldsymbol{\Theta}^A_{2y'+1/2} = (2\Theta^{A,1}_{2y'+1/2}, \ldots, 2\Theta^{A,p}_{2y'+1/2})$ has entries $2\Theta^{A,a}_{2y'+1/2} = \phi^a_{2y'} - \phi^a_{2y'+1}$, and $2\boldsymbol{\Theta}^B_{2y'-1/2} = (2\Theta^{B,1}_{2y'-1/2}, \ldots, 2\Theta^{B,q}_{2y'-1/2})$ has entries $2\Theta^{B,b}_{2y'-1/2} = \phi^{p+b}_{2y'} - \phi^{p+b}_{2y'}$. Here, unlike the previous sine-Gordon terms in $\mathcal{H}^C_{SU(r)_1}$ in (3.112) and (3.113), the $\mathbb{Z}_2$ terms $\mathcal{H}^C_{\mathbb{Z}_2}$ in (3.119) consist of sums of only the simple roots $\boldsymbol{\alpha}^I_{SU(r)}$ of $SU(r)$ (see (3.114)).

Eq.(3.119) introduces a finite excitation energy gap. To see this, we notice each product of cosine terms generates two sine-Gordon terms using the combine angle formula

$$\begin{aligned}
&\cos\left(\Phi^{C,\rho}_y - \Phi^{C,\rho}_{y+1}\right) \cos\left(\boldsymbol{\alpha}^I_{SU(r)} \cdot 2\boldsymbol{\Theta}^C_{y+1/2}\right) \\
&= \cos\left(\boldsymbol{\alpha}^0_{U(1)_r} \cdot 2\boldsymbol{\Theta}^C_{y+1/2}\right) \cos\left(\boldsymbol{\alpha}^I_{SU(r)} \cdot 2\boldsymbol{\Theta}^C_{y+1/2}\right) \\
&= \frac{1}{2} \cos\left[\left(\boldsymbol{\alpha}^0_{U(1)_r} + \boldsymbol{\alpha}^I_{SU(r)}\right) \cdot 2\boldsymbol{\Theta}^C_{y+1/2}\right] \\
&\quad + \frac{1}{2} \cos\left[\left(\boldsymbol{\alpha}^0_{U(1)_r} - \boldsymbol{\alpha}^I_{SU(r)}\right) \cdot 2\boldsymbol{\Theta}^C_{y+1/2}\right],
\end{aligned} \tag{3.120}$$

where $\boldsymbol{\alpha}^0_{U(1)_r} = (1, \ldots, 1)$ is the r-dimensional charge vector and $\boldsymbol{\alpha}^I_{SU(r)}$, for $I = 1, \ldots, r$ are the simple roots of $SU(r)$. The combined angle variables satisfy the "Haldane nullity" gapping condition [112]

$$\left[\left(\boldsymbol{\alpha}^0_{U(1)_r} + s\boldsymbol{\alpha}^I_{SU(r)}\right) \cdot 2\boldsymbol{\Theta}^C_{y+1/2}, \left(\boldsymbol{\alpha}^0_{U(1)_{r'}} + s'\boldsymbol{\alpha}^{I'}_{SU(r')}\right) \cdot 2\boldsymbol{\Theta}^{C'}_{y'+1/2}\right] = 0 \tag{3.121}$$

where $C, C' = A$ (B) and $r, r' = p$ (q) for even (odd) y, y' respectively, and $s, s' = \pm$. There are $2r - 2$ sine-Gordon terms between adjacent wires at each $y + 1/2$. This provides more than enough sine-Gordon terms,

when $r \geq 2$, to introduce an energy gap for the r pairs of counter-propagating channels. The redundant terms are non-competing and they collectively pin the bosonized angle variables $2\boldsymbol{\Theta}^C_{y+1/2}$ to the energy-minimizing ground state expectation values in the dual lattice

$$\mathcal{L}^{\mathbb{Z}_2}_{\boldsymbol{\Theta}} \equiv \left\{ 2\boldsymbol{\Theta} \in \mathbb{R}^r : \left(\boldsymbol{\alpha}^0_{U(1)_r} \pm \boldsymbol{\alpha}^I_{SU(r)} \right) \cdot 2\boldsymbol{\Theta} \in 2\pi\mathbb{Z} \right\}. \tag{3.122}$$

$\mathcal{L}^{\mathbb{Z}_2}_{\boldsymbol{\Theta}}$ contains twice as many lattice points as the original dual lattice $\mathcal{L}_{\boldsymbol{\Theta}}$ in (3.115) for the previous coupled wire model (3.110), and consequently, there are twice as many ground states between each adjacent wires. The scalar products $\boldsymbol{\alpha}^\mu \cdot 2\boldsymbol{\Theta}$ can now either be all even or all odd multiples of 2π, for $\mu = 0, 1, \ldots, r-1$. Therefore, the dual lattice admits a $\mathbb{Z}_2$ grading

$$\mathcal{L}^{\mathbb{Z}_2}_{\boldsymbol{\Theta}} = \mathcal{L}^0_{\boldsymbol{\Theta}} + \mathcal{L}^1_{\boldsymbol{\Theta}}. \tag{3.123}$$

The even lattice $\mathcal{L}^0_{\boldsymbol{\Theta}} = \mathcal{L}_{\boldsymbol{\Theta}}$ is identical to the dual lattice defined in (3.115). The odd lattice $\mathcal{L}^1_{\boldsymbol{\Theta}}$ displaces from the even one by half a lattice spacing

$$\mathcal{L}^1_{\boldsymbol{\Theta}} = 2\pi\boldsymbol{\beta}_{1/2} + \mathcal{L}^0_{\boldsymbol{\Theta}}. \tag{3.124}$$

Here $\boldsymbol{\beta}_{1/2}$ can be chosen to be any vector so that $\boldsymbol{\alpha}^0 \cdot \boldsymbol{\beta}_{1/2}$ and $\boldsymbol{\alpha}^I \cdot \boldsymbol{\beta}_{1/2}$ are all half integers. For example, one can take the entries of $\boldsymbol{\beta}_{1/2} = (\beta^1_{1/2}, \ldots, \beta^r_{1/2})$ to be $\beta^a_{1/2} = (2+r-2ar+r^2)/(4r)$ so that $\boldsymbol{\alpha}^\mu \cdot \boldsymbol{\beta}_{1/2} = 1/2$ for $\mu = 0, 1, \ldots, r-1$. The Hamiltonian $\mathcal{H}_{\mathbb{Z}_2}$ in (3.119), the half dual vector $\boldsymbol{\beta}_{1/2}$ as well as the odd lattice $\mathcal{L}^1_{\boldsymbol{\Theta}}$ all depend explicitly on the choice of simple roots $\boldsymbol{\alpha}^I_{SU(r)}$. They therefore explicitly breaks the $SU(r)$ symmetry. Distinct choices of simple roots correspond to inequivalent ground states with distinct odd angle expectation values $\mathcal{L}^1_{\boldsymbol{\Theta}}$.

At this point, one can also consider gapping potentials that sum over all roots of $SU(r)$.

$$\begin{aligned}
\mathcal{H}_{\text{even}} &= \mathcal{H}^A_{\text{even}} + \mathcal{H}^B_{\text{even}}, \\
\mathcal{H}^A_{\text{even}} &= -u_A \sum_{y'} \cos\left(\Phi^{A,\rho}_{2y'} - \Phi^{A,\rho}_{2y'+1}\right) \\
&\qquad \times \sum_{\boldsymbol{\alpha}\in\Delta_{SU(p)}} \cos\left(\boldsymbol{\alpha}\cdot 2\boldsymbol{\Theta}^A_{2y'+1/2}\right), \\
\mathcal{H}^B_{\text{even}} &= -u_B \sum_{y'} \cos\left(\Phi^{B,\rho}_{2y'-1} - \Phi^{B,\rho}_{2y'}\right) \\
&\qquad \times \sum_{\boldsymbol{\alpha}\in\Delta_{SU(q)}} \cos\left(\boldsymbol{\alpha}\cdot 2\boldsymbol{\Theta}^B_{2y'-1/2}\right).
\end{aligned} \tag{3.125}$$

In this case, the Hamiltonian still introduces a finite excitation energy gap. However, the additional non-simple root terms put extra restrictions to the ground state expectation values of $2\boldsymbol{\Theta}^C_{y+1/2}$. The angle values minimize energy only when $\left(\boldsymbol{\alpha}^0_{U(1)_r} \pm \boldsymbol{\alpha}_{SU(r)}\right)\cdot 2\boldsymbol{\Theta}$ are all integer multiples of 2π, for *all* roots $\boldsymbol{\alpha}_{SU(r)}$. This rules out the odd solutions in $\mathcal{L}^1_{\boldsymbol{\Theta}}$ for $r \geq 3$. For instance, $\boldsymbol{\alpha}^1 + \boldsymbol{\alpha}^2$ is also a root vector, and the above restriction implies $\boldsymbol{\alpha}^0_{U(1)_r}\cdot 2\boldsymbol{\Theta}$ as well as $\boldsymbol{\alpha}_{SU(r)}\cdot 2\boldsymbol{\Theta}$ to be full integer multiples of 2π. The energy-minimizing angle variables to Hamiltonian (3.125) therefore must be even and live exclusively in $\mathcal{L}^0_{\boldsymbol{\Theta}}$. This is not unexpected since the exactly solvable Hamiltonian (3.125) preserves the $SU(r)$ symmetry and so must its ground state. For instance, the angle values that belong to the $SU(r)$-breaking odd lattice $\mathcal{L}^1_{\boldsymbol{\Theta}}$ in (3.124) correspond to confined excitations that cost linearly diverging energy.

On the other hand, one can also consider another set of gapping potentials

$$\begin{aligned}
\mathcal{H}_{\text{odd}} &= \mathcal{H}^A_{\text{odd}} + \mathcal{H}^B_{\text{odd}}, \\
\mathcal{H}^A_{\text{odd}} &= u_A \sum_{y'} \cos\left(\Phi^{A,\rho}_{2y'} - \Phi^{A,\rho}_{2y'+1}\right) \\
&\qquad \times \sum_{\boldsymbol{\alpha}\in\Delta_{SU(p)}} (-1)^{\text{Tr}(\boldsymbol{\alpha})} \cos\left(\boldsymbol{\alpha}\cdot 2\boldsymbol{\Theta}^A_{2y'+1/2}\right), \\
\mathcal{H}^B_{\text{odd}} &= u_B \sum_{y'} \cos\left(\Phi^{B,\rho}_{2y'-1} - \Phi^{B,\rho}_{2y'}\right) \\
&\qquad \times \sum_{\boldsymbol{\alpha}\in\Delta_{SU(q)}} (-1)^{\text{Tr}(\boldsymbol{\alpha})} \cos\left(\boldsymbol{\alpha}\cdot 2\boldsymbol{\Theta}^B_{2y'-1/2}\right),
\end{aligned} \tag{3.126}$$

where $(-1)^{\text{Tr}(\boldsymbol{\alpha})}$ is even (odd) if $\boldsymbol{\alpha} = a_1\boldsymbol{\alpha}^1 + \ldots + a_{r-1}\boldsymbol{\alpha}^{r-1}$ is an even (resp. odd) combination of the simple roots, for $\text{Tr}(\boldsymbol{\alpha}) = a_1 + \ldots + a_{r-1}$. Contrary to the even Hamiltonian (3.125), the odd Hamiltonian (3.126) here has minimum energy when the angle variables live inside the odd lattice $\mathcal{L}^1_{\boldsymbol{\Theta}}$ in (3.124) that breaks

$SU(r)$.

These gapping potentials can be continuously deformed into one another, for example, via linear interpolation

$$\mathcal{H}_t = (1-t)\mathcal{H}_{\text{even}} + t\mathcal{H}_{\text{odd}}. \tag{3.127}$$

The ground states between an adjacent pair of wires are specified by the even (odd) dual lattice $\mathcal{L}^0_{\boldsymbol{\Theta}}$ ($\mathcal{L}^1_{\boldsymbol{\Theta}}$) when $t < 1/2$ ($t > 1/2$) respectively. At the transition at $t = 1/2$, the Hamiltonian only carries sine-Gordon terms from roots that are odd combinations of the simple ones. Consequently, the ground states are identical to that of $\mathcal{H}_{\mathbb{Z}_2}$ and corresponds to the same $\mathbb{Z}_2$ graded angle expectation value structure $\mathcal{L}^{\mathbb{Z}_2}_{\boldsymbol{\Theta}}$ in (3.122) and (3.123). This transition is analogous to Zeeman transition across the ordered phase of the Ising model

$$H_{\text{Ising}} = -J\sum_i \sigma^z_i\sigma^z_{i+1} - h\sum_i \sigma^x_i - B\sum_i \sigma^z_i, \tag{3.128}$$

where B is the magnetic field for the Zeeman coupling. When $J > h$ and $B = 0$, the ordered phase has two degenerate ground states specified by $\langle\sigma^z_i\rangle = \pm 1$. The Zeeman coupling B introduces a preference of up spins versus down ones, and breaks the degeneracy. Here, the parameter $t - 1/2$ in (3.127) takes a similar role as the Zeeman field B.

In general, there is an intricate phase diagram when the strengths and signs of the sine-Gordon terms $\cos(\boldsymbol{\alpha}\cdot 2\boldsymbol{\Theta})$ can vary from one to another. There are multiple distinct $\mathbb{Z}_2$ critical phases, where the ground states between an adjacent pair of wires take a $\mathbb{Z}_2$ graded structure. In the thermodynamic limit with an infinite number of wires, this introduces a diverging ground state degeneracy. This signifies a gap-closing critical transition between distinct 2D gapped phases. On the other hand, the diverging degeneracy could also be lifted if the theory is coupled with a $\mathbb{Z}_2$ gauge theory (similar to the one studied for the D-series in section 3.4). These discussions are out of the scope of this article and we refer them to future works.

Quasiparticle excitations

The deconfined quasiparticle excitations of the coupled wire model (3.110) are kinks of the angle variables $\langle 2\boldsymbol{\Theta}^C_{y+1/2}\rangle$. Similar discussions were provided for $U(4)$ in section 3.2. Here, we summarized the results for the general $U(N)$. The ground state expectation values $\langle 2\boldsymbol{\Theta}^C_{y+1/2}\rangle$ belong in the dual lattice $\mathcal{L}_{\boldsymbol{\Theta}}$ defined in (3.115). A quasiparticle excitation at (x_0, y_0) is a kink where the angle variable $\langle 2\boldsymbol{\Theta}^C_{y_0+1/2}(x)\rangle$ jumps discontinuously from one value to another in $\mathcal{L}_{\boldsymbol{\Theta}}$ when x passes across x_0. A quasiparticle excitation can be created by acting a vertex operator $V^{C,\boldsymbol{\gamma}}_{y_0}(x_0) = \exp\left[i\boldsymbol{\gamma}_a\phi^{C,a}_{y_0}(x_0)\right]$ on a ground state, where $C = A$ (B)

and $a = 1, \ldots, r$ for $r = p$ (q). These vertex operators are classified according to the primary fields of the $U(1)_r \times SU(r)_1$ Kac-Moody algebra. Each primary field is a super-selection sector of vertex operators that form an irreducible representation of the $U(1) \times SU(r)$ (c.f. (3.22) for $SO(6)_1$). For example, the smallest primary field $[1]_\rho$ for the $U(1)_r$ charge sector is the single vertex operator $e^{i\tilde{\phi}^{C,\rho}_{y_0}(x_0)}$, where $\tilde{\phi}^{C,\rho} = \Phi^{C,\rho}/r = (\phi^{C,1} + \ldots + \phi^{C,r})/r$. It creates a fractional excitation with spin (equivalently, conformal scaling dimension) $1/2r$. General primay field excitations $[m]_\rho$ in the $U(1)_r$ sector are generated by higher order copies $e^{im\tilde{\phi}^{C,\rho}_{y_0}(x_0)}$. They carry spin $m^2/2r$ and follow the fusion rule $[m]_\rho \times [m']_\rho = [m+m']_\rho$.

There are r primary fields in the $SU(r)_1$ sector. Examples were presented for the $SU(4)_1$ case in section 3.2. Here, we demonstrate the general case. We begin with the smallest non-trivial primary field, denoted by E^1, that corresponds to the fundamental representation of $SU(r)$. The super-selection sector E^1 consists of the collection of vertex operators

$$E^{C,1}_{y_0}(x_0) \sim \text{span}_{\mathbb{C}} \left\{ e^{i\boldsymbol{\gamma}\cdot\boldsymbol{\phi}^C_{y_0}(x_0)} : \boldsymbol{\gamma} = \sigma(\boldsymbol{\beta}_1), \sigma \in S_r \right\} \tag{3.129}$$

where $\boldsymbol{\beta}_1$ is the primitive dual root $(r-1, -1, \ldots, -1)/r$ (see (3.117) and (3.118)), and σ permutes the entries of the r-dimensional vector. The super-selection sector irreducibly represents $SU(r)_1$ in the sense that it is closed under operator products with the $SU(r)_1$ currents (c.f. (3.22)). Since all entries of $\boldsymbol{\beta}_1$ is identical except one, there are exactly r permutations $\sigma(\boldsymbol{\beta})$. Therefore E^1 are generated by r vertex operators, which form the fundamental representation of $SU(r)$.

In general, the primary field E^c, for $c = 1, \ldots, r-1$, is the super-selection sector

$$E^{C,c}_{y_0}(x_0) \sim \text{span}_{\mathbb{C}} \left\{ e^{i\boldsymbol{\gamma}\cdot\boldsymbol{\phi}^C_{y_0}(x_0)} : \boldsymbol{\gamma} = \sigma(\boldsymbol{\beta}_c), \sigma \in S_r \right\}, \tag{3.130}$$

where the simple dual root $\boldsymbol{\beta}_c$ was defined in (3.117) and (3.118). There are exactly $C^r_c = r!/[c!(r-c)!]$ entry permutations and therefore E^c forms a C^r_c dimensional irreducible representation of $SU(r)_1$. Since $\sigma(\boldsymbol{\beta}_c)$ has c entries being $(r-c)/r$ and $r-c$ entries being $-c/r$, the primary field has spin (equivalently, conformal scaling dimension)

$$h_{E^c} = \frac{c(r-c)^2 + (r-c)c^2}{2r^2} = \frac{(r-c)c}{2r}. \tag{3.131}$$

Lastly, the trivial primary field is $E^0 = 1$. The primary fields obey the fusion rules

$$E^c \times E^{c'} = E^{[c+c']_{\text{mod } r}}. \tag{3.132}$$

3.5.3 Duality transformation

We generalize the duality properties of the coupled wire model from that of the free Dirac fermion reviewed in section 3.3. Under the duality transformation

$$\tilde{\phi}^a_y = \sum_{y'} \mathrm{sgn}(y-y')(-1)^{y'} \phi^a_{y'}, \tag{3.133}$$

the angle variables in the sine-Gordon terms in (3.110), (3.112) and (3.113) are self-dual up to a sign

$$2\tilde{\Theta}^{A,a}_{2y'+1/2} \equiv \tilde{\phi}^a_{2y'} - \tilde{\phi}^a_{2y'+1} = -2\theta^{A,a}_{2y'+1/2}. \tag{3.134}$$

Therefore, the sine-Gordon terms in (3.110), (3.112) and (3.113) are also self-dual

$$\begin{aligned}
\tilde{\mathcal{H}}^A_\rho &= -v_A \sum_{y'} \cos\left(\boldsymbol{\alpha}^0_{U(1)_p} \cdot 2\tilde{\boldsymbol{\Theta}}_{2y'+1}\right) \\
&= -v_A \sum_{y'} \cos\left(\boldsymbol{\alpha}^0_{U(1)_p} \cdot 2\boldsymbol{\Theta}_{2y'+1}\right) = \mathcal{H}^A_\rho
\end{aligned} \tag{3.135}$$

$$\begin{aligned}
\tilde{\mathcal{H}}^A_{SU(p)_1} &= -u_A \sum_{y'} \sum_{\boldsymbol{\alpha}\in\Delta_{SU(p)}} \cos\left(\boldsymbol{\alpha} \cdot 2\tilde{\boldsymbol{\Theta}}^A_{2y'+1/2}\right) \\
&= -u_A \sum_{y'} \sum_{\boldsymbol{\alpha}\in\Delta_{SU(p)}} \cos\left(\boldsymbol{\alpha} \cdot 2\boldsymbol{\Theta}^A_{2y'+1/2}\right) \\
&= \mathcal{H}^A_{SU(p)_1}
\end{aligned} \tag{3.136}$$

Similarly, the sine-Gordon terms for the B sector are also self-dual.

Lastly, we consider vertex operators that correspond to primary fields and create quasiparticle excitations. The duality transformation (3.133) can be re-expressed in terms of the angle variables $2\theta^a_y(x)$ as

$$\begin{aligned}
\tilde{\phi}^a_{2y}(x) &= \phi^a_{2y+1}(x) + \sum_{y'} \mathrm{sgn}(y-y') 2\theta^{A,a}_{2y'+1/2}(x) \\
\tilde{\phi}^a_{2y+1}(x) &= \phi^a_{2y}(x) + \sum_{y'} \mathrm{sgn}(y-y') 2\theta^{A,a}_{2y'+1/2}(x)
\end{aligned}, \tag{3.137}$$

and similarly for the B sector. We see that the dual vertex operators are dressed with non-local strings, similar to (3.51) in section 3.3. When acting on a ground state, the angle variables $2\theta^{A,a}_{2y'+1/2}$ are pinned and can be replaced by their ground state expectation values. The non-local string therefore condenses into the ground state leaving only complex phases behind.

Like D-series, if we extend the coupling constants of the sine-Gordon terms $u_{A/B}$ to be complex valued, then the ground state manifold change continuously as we vary the phases $\theta_{A/B}$ of $u_{A/B}$. The self-dual points are $\theta_{A/B} = 0, \pi$ and duality transformation (3.133) on the complex u plane is a reflection with respect to the real axis. The ground state manifold can be visualized for SU(3) or SU(4) cases and it should be true for the general SU(N) theories.

3.6 E-series surface theory

The exceptional Lie algebra E_6, E_7 and E_8 are the remaining simply-laced Lie algebra in the ADE classification. We first discuss the E_8 algebra. In addition to the conventional topological insulators that host protected Dirac surface states, topological paramagnets [63, 64] are alternative time reversal and charge $U(1)$ symmetry preserving topological states enabled by interactions. These are short-ranged entangled SPT states in three dimensions that do not exhibit bulk quasiparticle fractionalization or topological order. However, they do carry anomalous surface states that cannot be supported in a pure two dimensional system. We are interested in the *efmf* topological paramagnetic state. Like a conventional topological insulator, its surface state is unstable against time reversal breaking perturbations. A finite excitation energy gap can be introduced on the surface by a magnetic order without requiring surface topological order or fractionalization. The *efmf* topological paramagnet is distinct from a conventional topological insulator in that a magnetic surface domain wall – a line interface that separates two time reversal breaking gapped surface domains with opposite magnetic orientations – hosts quasi-one-dimensional low-energy electronic degrees of freedom that are chiral only in energy but has no electric charge transport. Electronic quasiparticles are chiral in the sense that they propagate in a single forward direction along the line interface. They collectively account for a chiral heat current $I_{\text{eng}} = I^R_{\text{eng}} - I^L_{\text{eng}}$ that obey the differential thermal conductance $\kappa = dI_{\text{eng}}/dT = c(\pi^2 k_B^2/3h)T$ in low temperature T, where the central charge is $c = 8$. However, electric charge transport is non-chiral in that the chiral electric current $I = I^R - I^L$ does not response to change of electric potential, $\sigma = dI/dV = 0$. These low-energy degrees of freedom can be effectively described by a $1+1$D E_8 Kac-Moody CFT at level 1. They can be described by the bosonized Lagrangian density

$$\begin{aligned}\mathcal{L}_0 &= \frac{1}{2\pi}\sum_{a=1}^{8}\partial_t\phi^a\partial_x\phi^a - \sum_{a,b=1}^{8}V_{ab}\partial_x\phi^a\partial_x\phi^b \\ &= \frac{1}{2\pi}\sum_{I,J=1}^{8}(K_{E_8})_{IJ}\partial_t\phi'^I\partial_x\phi'^J - \sum_{I,J=1}^{8}V'_{IJ}\partial_x\phi'^I\partial_x\phi'^J,\end{aligned} \tag{3.137}$$

where the "Cartan-Weyl" and "Chevalley" bosonized variables ϕ and ϕ' are related by the basis transformation

$$\begin{aligned}
\phi'^I &= (K_{E_8}^{-1})^{IJ}\Phi_J = \sum_{a=1}^{8}(R_{E_8}^{-1})_a^I\phi^a, \\
R_{E_8} &= \begin{pmatrix} -- & \boldsymbol{\alpha}^1 & -- \\ \vdots & \vdots & \vdots \\ -- & \boldsymbol{\alpha}^8 & -- \end{pmatrix} \\
&= \begin{pmatrix} 1 & -1 & 0 & 0 & 0 & 0 & 0 & 0 \\ 0 & 1 & -1 & 0 & 0 & 0 & 0 & 0 \\ 0 & 0 & 1 & -1 & 0 & 0 & 0 & 0 \\ 0 & 0 & 0 & 1 & -1 & 0 & 0 & 0 \\ 0 & 0 & 0 & 0 & 1 & -1 & 0 & 0 \\ 0 & 0 & 0 & 0 & 0 & 1 & -1 & 0 \\ 0 & 0 & 0 & 0 & 0 & 0 & 1 & -1 \\ -\frac{1}{2} & -\frac{1}{2} & -\frac{1}{2} & -\frac{1}{2} & -\frac{1}{2} & \frac{1}{2} & \frac{1}{2} & \frac{1}{2} \end{pmatrix},
\end{aligned} \tag{3.138}$$

and the Cartan matrix of E_8

$$K_{E_8} = R_{E_8}R_{E_8}^T \tag{3.139}$$

(see Eq. (B.19) in Appendix B.2 for an explicit expression) has determinant 1 and is invertible.

Here, it is important to realize that the neutral fermionic vertex operators $e^{i\phi^a}$ are non-local and fractional. They are not the primary field excitations of the E_8 CFT, which only supports local integral excitations. Instead, the low-energy physical excitations are generated by the local bosonic vertex operators $e^{i\Phi_I} = e^{iK_{IJ}\phi'^J} = e^{iR_a^I\phi^a}$. Since K_{E_8} has integral inverse, $e^{i\phi'^I} = e^{i(K^{-1})^{IJ}\Phi_J}$ are also local and bosonic. These are even integral combinations of electrons/holes, each of which is assumed to carry net zero electric charge. All odd combinations of electrons/holes correspond to gapped fermionic excitations. They do not contribute to the low-temperature chiral energy transport and are not described by the low-energy effective E_8 CFT.

The E_8 Kac-Moody currents consist of the 8 Cartan generators $\partial\Phi_I$ and the 240 roots $E^{\boldsymbol{\alpha}} = e^{i\boldsymbol{\alpha}\cdot\boldsymbol{\phi}}$. The

240 roots can be decomposed into the 112 $SO(16)$ roots and 128 spinor representations of $SO(16)$.

$$\Delta_{E_8} = \Delta_{SO(16)} \cup \Delta_{s_-} \tag{3.140}$$

The 112 root vectors in $\Delta_{SO(16)}$ were defined in (3.86) in section 3.4, and they take the form $\boldsymbol{\alpha} = \pm\mathbf{e}_a \pm \mathbf{e}_b$, where $a \neq b$. In this chapter, we adopt the convention where the E_8 roots extends from that of $SO(16)$ by its *odd* spinors s_-. The 128 odd spinor vectors in Δ_{s_-} take the form $\boldsymbol{\alpha} = (\varepsilon_1, \ldots, \varepsilon_8)/2$ where $\varepsilon_a = \pm 1$ and $\varepsilon_1 \ldots \varepsilon_8 = -1$. All 240 roots of E_8 are integral combinations of the simple ones defined by the row vectors of R_{E_8} in (3.138). Since $e^{iR^I_a\phi^a}$ are bosonic integral combinations of local electrons, so are all the E_8 current operators.

We consider time reversal breaking stripes with alternating magnetic orientation on the surface of the *efmf* topological paramagnet (c.f. figure 3.1). This reduces the low-energy electronic degrees of freedom to an array of E_8 wires with alternating propagating directions. Similar to the D-series coupled wire model discussed in section 3.4, the E_8 array exhibits an emergent antiferromagnetic time reversal symmetry, which composes of a time reversal and a half-translation $y \to y+1$. AFTR preserving fractionalization $E_8 \sim SO(8) \times SO(8)$ and gapping interactions were studied in ref. [21]. Instead, in this section, we focus on AFTR symmetry breaking gapping interactions based on asymmetric partitions of the E_8 current algebra. In particular, we concentrate on the conformal embeddings

$$E_8 \supseteq E_7 \times SU(2), \quad E_8 \supseteq E_6 \times SU(3) \tag{3.141}$$

that involve the other two exceptional simply-laced Lie algebras. The coupled wire model is constructed by backscattering the two decoupled components E_7 and $SU(2)$ (or E_6 and $SU(3)$) on each wire to adjacent wires in opposite directions.

Before discussing these surface models, we first consider a set of simple gapping potentials that fully dimerizes the E_8 wires.

$$\begin{aligned}
\mathcal{H}_{\text{dimer}} &= u \sum_{y'} \mathbf{J}^{E_8}_{2y'-1} \cdot \mathbf{J}^{E_8}_{2y'} \\
&= u \sum_{y'} \sum_{a=1}^{8} \partial_x \phi^a_{2y'-1} \partial_x \phi^a_{2y'} \\
&\quad - u \sum_{y'} \sum_{\boldsymbol{\alpha} \in \Delta_{E_8}} \cos\left(\boldsymbol{\alpha} \cdot 2\boldsymbol{\Theta}_{2y'-1/2}\right),
\end{aligned} \tag{3.142}$$

where the sine-Gordon angle parameter is $\Theta^a_{2y'-1/2} = \phi^a_{2y'-1} - \phi^a_{2y'}$. Similar to the coupled wire models in

the previous sections, to simultaneously minimize the sine-Gordon terms in (3.142), the angle parameters take ground state expectation values inside the dual lattice (c.f. (3.89))

$$\begin{aligned}\mathcal{L}^{E_8}_{\boldsymbol{\Theta}} &\equiv \{2\boldsymbol{\Theta} : \boldsymbol{\alpha}\cdot 2\boldsymbol{\Theta} \in 2\pi\mathbb{Z}, \quad \boldsymbol{\alpha}\in\Delta_{E_8}\},\\ &= \mathrm{span}_{\mathbb{Z}}\{2\pi\boldsymbol{\beta_1},\ldots,2\pi\boldsymbol{\beta_8}\},\\ \boldsymbol{\beta}_I &= \frac{1}{8!}\varepsilon_{IJ_1\ldots J_7}\frac{\boldsymbol{\alpha}^{J_1}\wedge\ldots\wedge\boldsymbol{\alpha}^{J_7}}{\boldsymbol{\alpha}^1\cdot(\boldsymbol{\alpha}^2\wedge\ldots\wedge\boldsymbol{\alpha}^8)},\end{aligned} \tag{3.143}$$

where $\boldsymbol{\alpha}^1,\ldots,\boldsymbol{\alpha}^8$ are the simple roots in (3.138). The primitive dual root vectors satisfy $\boldsymbol{\beta}_I\cdot\boldsymbol{\alpha}^J=\delta_I^J$, i.e. $R^{\vee}_{E_8}R^T_{E_8}=\mathbf{I}_{8\times 8}$, and they take the explicit form

$$\begin{aligned}R^{\vee}_{E_8} &= \begin{pmatrix} -- & \boldsymbol{\beta}_1 & -- \\ \vdots & \vdots & \vdots \\ -- & \boldsymbol{\beta}_8 & -- \end{pmatrix}\\ &= -\frac{1}{2}\begin{pmatrix} -1 & 1 & 1 & 1 & 1 & 1 & 1 & 1\\ 0 & 0 & 2 & 2 & 2 & 2 & 2 & 2\\ 1 & 1 & 1 & 3 & 3 & 3 & 3 & 3\\ 2 & 2 & 2 & 2 & 4 & 4 & 4 & 4\\ 3 & 3 & 3 & 3 & 3 & 5 & 5 & 5\\ 2 & 2 & 2 & 2 & 2 & 2 & 4 & 4\\ 1 & 1 & 1 & 1 & 1 & 1 & 1 & 3\\ 2 & 2 & 2 & 2 & 2 & 2 & 2 & 2\end{pmatrix}.\end{aligned} \tag{3.144}$$

The dual lattice is self-dual up to a 2π multiplicative factor in the sense that $\mathrm{span}_{\mathbb{Z}}\{\boldsymbol{\alpha}^1,\ldots,\boldsymbol{\alpha}^8\} = \mathrm{span}_{\mathbb{Z}}\{\boldsymbol{\beta}_1,\ldots,\boldsymbol{\beta}_8\}$ because

$$R^{\vee}_{E_8} = {R^T_{E_8}}^{-1} = K^{-1}_{E_8}R_{E_8} \tag{3.145}$$

and K_{E_8} has integral inverse. This is consistent with the fact that the root lattice of E_8 is unimodular. Consequently, all deconfined excitations of the coupled wire model (3.142) that correspond to kinks of $\langle 2\boldsymbol{\Theta}_{2y'-1/2}\rangle \in \mathcal{L}^{E_8}_{\boldsymbol{\Theta}}$ are local and can be created by integral combination of electron/hole operators.

3.6.1 $E_7 \times SU(2)$

We now construct the coupled wire model that utilizes the partition $E_8 \supset E_7 \times SU(2)$ and describes a gapped symmetry breaking surface of a topological paramagnet. Each E_8 wire on the 2D surface array (c.f. figure 3.1(c)) is decomposed into a E_7 and a $SU(2)$ Kac-Moody CFT at level 1. These two sectors decouple from each other and act on orthogonal Hilbert spaces. This motivates the gapping Hamiltonian

$$\mathcal{H} = u \sum_{y'} \mathbf{J}^{E_7}_{2y'-1} \cdot \mathbf{J}^{E_7}_{2y'} + \mathbf{J}^{SU(2)}_{2y'} \cdot \mathbf{J}^{SU(2)}_{2y'+1} \tag{3.146}$$

that backscatters the two decoupled currents from a wire into adjacent wires in opposite directions. In the following, we define the current embeddings of $\mathbf{J}^{E_7}$ and $\mathbf{J}^{SU(2)}$ into E_8.

We begin with the new set of simple root vectors of $E_7 \times SU(2)$

$$\begin{aligned} \boldsymbol{\alpha}^I &= \mathbf{e}_{I+1} - \mathbf{e}_{I+2}, \quad i = 1, \ldots, 6, \\ \boldsymbol{\alpha}^7 &= \frac{1}{2}(-1,-1,-1,-1,-1,1,1,1), \\ \boldsymbol{\alpha}^8 &= \frac{1}{2}(-1,1,1,1,1,1,1,1), \end{aligned} \tag{3.147}$$

where $\boldsymbol{\alpha}^1, \ldots, \boldsymbol{\alpha}^7$ are the simple root vectors of E_7 and $\boldsymbol{\alpha}^8$ generates $SU(2)$. It is easy to see that the Cartan K-matrix splits

$$K_{E_7 \times SU(2)} = \left(\boldsymbol{\alpha}^I \cdot \boldsymbol{\alpha}^J\right)_{8\times 8} = \begin{pmatrix} K_{E_7} & 0 \\ 0 & K_{SU(2)} \end{pmatrix}, \tag{3.148}$$

where the explicit form of K_{E_7} can be found in Eq. (B.19) in Appendix B.2 and $K_{SU(2)} = 2$. The E_7 root system can be embedded in E_8 by taking the subset

$$\Delta_{E_7} = \left\{\boldsymbol{\alpha} \in \Delta_{E_8} : \boldsymbol{\alpha} \cdot \boldsymbol{\alpha}^8 = 0\right\} \subseteq \Delta_{E_8}. \tag{3.149}$$

The 126 roots in Δ_{E_7} is an extension of the 42 roots of $SU(7)$ – a subgroup of E_7 – by the weight vectors of the irreducible representations $\mathbf{7}$, $\overline{\mathbf{7}}$, $\mathbf{35}$, and $\overline{\mathbf{35}}$.

$$\Delta_{E_7} = \iota\Delta_{SU(7)} + \mathbf{7} + \overline{\mathbf{7}} + \mathbf{35} + \overline{\mathbf{35}}. \tag{3.150}$$

To illustrate this, we embed the root system of $SU(7)$ (see (3.103)) in that of $SO(16) \subseteq E_8$ by putting the

7 dimensional root vectors $\boldsymbol{\alpha} \in \Delta_{SU(7)}$ in the 8 dimensional space,

$$\begin{aligned} \iota : \boldsymbol{\alpha} = (\alpha_1, \ldots, \alpha_7) \mapsto \iota\boldsymbol{\alpha} = (0, \alpha_1, \ldots, \alpha_7), \\ \iota\Delta_{SU(7)} = \left\{ \iota\boldsymbol{\alpha} : \boldsymbol{\alpha} \in \Delta_{SU(7)} \right\}. \end{aligned} \tag{3.151}$$

Next, we observe that certain sub-collections of the E_8 roots form the weight vectors of the representations $\mathbf{7}$, $\overline{\mathbf{7}}$, $\mathbf{35}$, and $\overline{\mathbf{35}}$. They are given by

$$\begin{aligned} \mathbf{7} &= \{\mathbf{e}_1 + \mathbf{e}_j : j = 2, \ldots, 8\}, \\ \overline{\mathbf{7}} &= \{-\mathbf{e}_1 - \mathbf{e}_j : j = 2, \ldots, 8\}, \\ \mathbf{35} &= \left\{ \frac{1}{2}(1, s_2, \ldots, s_8) : s_2, \ldots, s_8 = \pm 1, \sum_{j=2}^{8} s_j = 1 \right\}, \\ \overline{\mathbf{35}} &= \left\{ \frac{1}{2}(-1, s_2, \ldots, s_8) : s_2, \ldots, s_8 = \pm 1, \sum_{j=2}^{8} s_j = -1 \right\}. \end{aligned}$$

Each of these weight vectors is orthogonal to $\boldsymbol{\alpha}^8$ and therefore decouples from the $SU(2)$. While $\mathbf{7}$ and $\overline{\mathbf{7}}$ can be embedded in the root system of $SO(16)$, $\mathbf{35}$ and $\overline{\mathbf{35}}$ can only be embedded in E_8 as they consists of half-integral vectors. Each of these collections of weight vectors $\boldsymbol{\gamma}^a$ corresponds to a super-selection sector of vertex operators $\mathrm{span}\{e^{i\boldsymbol{\gamma}^a \cdot \boldsymbol{\phi}}\}$ that transforms closely and irreducibly under the $SU(7)_1$ Kac-Moody algebra (c.f. (3.22)). Each sector splits into $\eta \otimes E^c$, where E^c is a primary field of $SU(7)_1$ and η is a primary field of the coset $(E_7)_1/SU(7)_1$, so that the combined spin (conformal scaling dimension) is 1.

The coupled wire model (3.146) can be expressed as a sum of sine-Gordon gapping interactions

$$\mathcal{H} = -u \sum_{y'} \sum_{\boldsymbol{\alpha} \in \Delta_{E_7}} \cos\left(\boldsymbol{\alpha} \cdot 2\boldsymbol{\Theta}_{2y'-1/2}\right) - u \sum_{y'} \cos\left(\boldsymbol{\alpha}^8 \cdot 2\boldsymbol{\Theta}_{2y'+1/2}\right), \tag{3.152}$$

where $\boldsymbol{\alpha}^8$ is the root vector of $SU(2)$ when embedded in E_8 and we have suppressed the non-gapping Cartan generator terms that renormalize velocities. Here, $2\boldsymbol{\Theta} = (2\theta^1, \ldots, 2\theta^8)$ and $2\theta^a_{y+1/2} = \phi^a_y - \phi^a_{y+1}$. The sine-Gordon terms in the first line in (3.152) dimerize the E_7 currents between wire $2y'-1$ and $2y'$ while terms in the second line dimerize the remaining $SU(2)$ currents between wire $2y'$ and $2y'+1$. Together, they introduce a finite excitation energy gap.

Quasiparticle excitation can be created by primary fields of the E_7 or the $SU(2)$ sector. The semionic primary field of $SU(2)$ at wire y is the super-selection sector of vertex operators $s \sim \mathrm{span}\{e^{i\boldsymbol{\beta}_8 \cdot \boldsymbol{\phi}_y}, e^{-i\boldsymbol{\beta}_8 \cdot \boldsymbol{\phi}_y}\}$. Here, the weight vector $\boldsymbol{\beta}_8 = (-1, 1, \ldots, 1)/4 = \boldsymbol{\alpha}^8/2$ is orthogonal to all E_7 roots and has length square

$|\boldsymbol{\beta}_8|^2 = 1/2$. Consequently, the primary field decouples from the E_7 sector and carries conformal scaling dimension $h_s = |\boldsymbol{\beta}_8|^2/2 = 1/4$. Each of the vertex operators creates a bulk quasiparticle excitation in the form of a kink of the sine-Gordon angle parameter between wire y and $y+1$ $(y-1)$ if y is even (resp. odd). The anti-semionic primary field of E_7 at wire y is the super-selection sector of vertex operators

$$\bar{s} \sim \text{span}\{e^{i\boldsymbol{\beta}\cdot\boldsymbol{\phi}_y} : \boldsymbol{\beta} \in \mathcal{S}_{E_7}\}, \tag{3.153}$$

where $\mathcal{S}_{E_7}$ is the collection of dual vectors

$$\begin{aligned}\mathcal{S}_{E_7} = &\{\boldsymbol{\beta}_8 - \mathbf{e}_I - \mathbf{e}_J : 2 \le I < J \le 8\} \\ &\cup \{-\boldsymbol{\beta}_8 + \mathbf{e}_I + \mathbf{e}_J : 2 \le I < J \le 8\} \\ &\cup \{\boldsymbol{\beta}_8 + \mathbf{e}_1 - \mathbf{e}_I : 2 \le I \le 8\} \\ &\cup \{-\boldsymbol{\beta}_8 - \mathbf{e}_1 + \mathbf{e}_I : 2 \le I \le 8\}.\end{aligned} \tag{3.154}$$

This collection of 56 vertex operators form the 56 dimensional irreducible representation of E_7 and corresponds to the only non-trivial primary field of E_7 at level 1. All weight vectors in $\mathcal{S}_{E_7}$ are orthogonal to $\boldsymbol{\alpha}^8$ and they all have length square $|\boldsymbol{\beta}|^2 = 3/2$. Therefore the primary field $\bar{s}$ decouples from $SU(2)$ and carries conformal scaling dimension $h_{\bar{s}} = 3/4$. It creates a kink of the sine-Gordon angle parameter between wire y and $y-1$ $(y+1)$ if y is even (resp. odd).

3.6.2 $E_6 \times SU(3)$

The discussion of $E_6 \times SU(3)$ resembles that of $E_7 \times SU(2)$. The gapping Hamiltonian takes the current backscattering form

$$\mathcal{H} = u \sum_{y'} \mathbf{J}^{E_6}_{2y'-1} \cdot \mathbf{J}^{E_6}_{2y'} + \mathbf{J}^{SU(3)}_{2y'} \cdot \mathbf{J}^{SU(3)}_{2y'+1}. \tag{3.155}$$

E_6 and $SU(3)$ are embedded in the E_8 by setting the simple roots

$$\begin{aligned}\boldsymbol{\alpha}^I &= \mathbf{e}_{I+2} - \mathbf{e}_{I+3}, \quad I = 1, \ldots, 5, \\ \boldsymbol{\alpha}^6 &= \frac{1}{2}(-1,-1,-1,-1,-1,1,1,1), \\ \boldsymbol{\alpha}^7 &= (1,-1,0,0,0,0,0,0), \\ \boldsymbol{\alpha}^8 &= \frac{1}{2}(-1,1,1,1,1,1,1,1).\end{aligned} \tag{3.156}$$

The Cartan K-matrix

$$K_{E_6\times SU(3)} = \left(\boldsymbol{\alpha}^I \cdot \boldsymbol{\alpha}^J\right)_{8\times 8} = \begin{pmatrix} K_{E_6} & 0 \\ 0 & K_{SU(3)} \end{pmatrix} \tag{3.157}$$

splits, and therefore the E_7 and $SU(2)$ sectors decouple. The explicit form of the Cartan matrices of E_6 and $A_2 = SU(3)$ can be found in Eq. (B.19) Appendix B.2. The $SU(3)$ root system, as embedded in E_8, consists of vectors in

$$\Delta_{SU(3)} = \{\pm\boldsymbol{\alpha}^7, \pm\boldsymbol{\alpha}^8, \pm(\boldsymbol{\alpha}^7 + \boldsymbol{\alpha}^8)\} \subseteq \Delta_{E_8}. \tag{3.158}$$

Like the roots of E_7, the roots of E_6 are the orthogonal complement of $SU(3)$ in E_8,

$$\Delta_{E_6} = \{\boldsymbol{\alpha} \in \Delta_{E_8} : \boldsymbol{\alpha} \cdot \boldsymbol{\alpha}^7 = \boldsymbol{\alpha} \cdot \boldsymbol{\alpha}^8 = 0\} \subseteq \Delta_{E_8}. \tag{3.159}$$

The 72 roots of E_6 extend the 30 roots of $SU(6)$ by including weight vectors of the irreducible representations $\mathbf{1}$, $\overline{\mathbf{1}}$, $\mathbf{20}$, and $\overline{\mathbf{20}}$.

$$\Delta_{E_6} = \iota\Delta_{SU(6)} + \mathbf{1} + \overline{\mathbf{1}} + \mathbf{20} + \overline{\mathbf{20}}. \tag{3.160}$$

Here, ι embeds the $SU(6)$ roots into E_8 (c.f. (3.151) for the E_7 case) so that the embedded simple $SU(6)$ roots are $\boldsymbol{\alpha}^1, \ldots, \boldsymbol{\alpha}^5$. The four irreducible representations of $SU(6)$ involved in the extension have weight vectors

$$\begin{aligned}
\mathbf{1} &= \{\mathbf{e}_1 + \mathbf{e}_2\}, \quad \overline{\mathbf{1}} = \{-\mathbf{e}_1 - \mathbf{e}_2\}, \\
\mathbf{20} &= \left\{ \frac{1}{2}(1, 1, s_3, \ldots, s_8) : s_3, \ldots, s_8 = \pm 1, \sum_{j=3}^{8} s_j = 0 \right\}, \\
\overline{\mathbf{20}} &= \left\{ \frac{-1}{2}(1, 1, s_3, \ldots, s_8) : s_3, \ldots, s_8 = \pm 1, \sum_{j=3}^{8} s_j = 0 \right\}.
\end{aligned}$$

Up to non-gapping boson velocity terms, the coupled wire model (3.155) can be expressed as a sum of sine-Gordon potentials

$$\mathcal{H} = -u \sum_{y'} \sum_{\boldsymbol{\alpha}\in\Delta_{E_6}} \cos\left(\boldsymbol{\alpha} \cdot 2\boldsymbol{\Theta}_{2y'-1/2}\right) - u \sum_{y'} \sum_{\boldsymbol{\alpha}\in\Delta_{SU(3)}} \cos\left(\boldsymbol{\alpha} \cdot 2\boldsymbol{\Theta}_{2y'+1/2}\right), \tag{3.161}$$

where $2\boldsymbol{\Theta} = (2\theta^1, \ldots, 2\theta^8)$ and $2\theta^a_{y+1/2} = \phi^a_y - \phi^a_{y+1}$. The sine-Gordon terms in the first line in (3.161) dimerize the E_6 currents between wire $2y'-1$ and $2y'$ while terms in the second line dimerize the remaining $SU(3)$ currents between wire $2y'$ and $2y'+1$. They can be shown to introduce a finite excitation energy gap. The proof is similar to the previous cases for the A and D-series and will be omitted.

Quasiparticle excitations, in the form of kinks of angle parameters in (3.161), can be created by primary fields $e^{i\boldsymbol{\beta}\cdot\boldsymbol{\phi}}$ in the E_6 and $SU(3)$ Kac-Moody CFT at level 1. We begin with the $SU(3)$ sector. The fundamental representation corresponds to the primary field $e^+ \sim \text{span}\{e^{i\boldsymbol{\beta}\cdot\boldsymbol{\phi}} : \boldsymbol{\beta} \in \mathcal{S}_{SU(3)}\}$, where the weight vectors are

$$\begin{aligned} \mathcal{S}_{SU(3)} &= \{-\boldsymbol{\beta}_7, \boldsymbol{\beta}_8, \boldsymbol{\beta}_7 - \boldsymbol{\beta}_8\}, \\ \boldsymbol{\beta}_8 &= \frac{1}{3}(0,0,1,\ldots,1), \quad \boldsymbol{\beta}_7 = \boldsymbol{\alpha}_7 + \boldsymbol{\alpha}_8 - \boldsymbol{\beta}_8. \end{aligned} \tag{3.162}$$

The anti-fundamental representation corresponds to the hermitian conjugation $e^- = (e^+)^\dagger$. Both primary fields carry conformal scaling dimension $h_{e^\pm} = 1/3$.

The fundamental 27-dimensional representation of E_6 corresponds to the primary field $\overline{e^+} \sim \text{span}\{e^{i\boldsymbol{\beta}\cdot\boldsymbol{\phi}} : \boldsymbol{\beta} \in \mathcal{S}_{E_6}\}$, where the weight vectors are

$$\begin{aligned} \mathcal{S}_{E_6} &= \{-\boldsymbol{\beta}_8 + \mathbf{e}_I + \mathbf{e}_J : 3 \le I < J \le 8\} \\ &\quad \cup \{\boldsymbol{\beta}_6 - \mathbf{e}_I + \mathbf{e}_8 : I = 3, \ldots, 8\} \\ &\quad \cup \{-\boldsymbol{\beta}_1 - \mathbf{e}_I + \mathbf{e}_8 : I = 3, \ldots, 8\}, \\ \boldsymbol{\beta}_6 &= \frac{1}{6}(-3,-3,1,1,1,1,1,-5), \\ \boldsymbol{\beta}_1 &= \frac{1}{6}(-3,-3,5,-1,-1,-1,-1,-1). \end{aligned} \tag{3.163}$$

The anti-fundamental representation corresponds to the primary field $\overline{e^-} \sim \text{span}\{e^{-i\boldsymbol{\beta}\cdot\boldsymbol{\phi}} : \boldsymbol{\beta} \in \mathcal{S}_{E_6}\} = (\overline{e^+})^\dagger$. The two primary fields both share the same conformal scaling dimension $h_{\overline{e^\pm}} = 2/3$.

Duality properties for E-series

The ground state structure of E-series has similar behaviors like A- and D-series, namely, if we extend the coupling constant of the sine-Gordon terms to complex regime, duality transformation acts as a reflection with respect to the real axis of the complex plane of the coupling constant. Although we can't visualize it due to the high dimensionality of the root systems, it is reasonable to conclude that all the points on the

complex plane describe a gapped surface except those points on the negative real axis.

Chapter 4

Boundary conformal field theories and symmetry protected topological phases

This chapter is larged based on Ref. [123].

4.1 Introduction

4.1.1 SPT phases and quantum anomalies

Symmetry-protected topological (SPT) phases are quantum states of matter with a global symmetry G, which can be either an internal or a space-time symmetry [38, 39, 124, 6, 5, 122, 125, 33]. This symmetry prevents one from adiabatically connecting an SPT state to a topologically trivial state, namely, a product state. More precisely, this means that one cannot find a symmetry-preserving quasilocal unitary transformation that maps an SPT state to a product state [38]. In fact, as long as the symmetry is unbroken (either explicitly or spontaneously), the phase space of gapped systems is partitioned into topologically distinct sectors that cannot be adiabatically connected to each other. The trivial state lies in the trivial (in the topological sense) sector of this classification. We will henceforth refer to it as the trivial SPT phase.

The existence of SPT phases has a close connection with quantum anomalies which are purely quantum phenomena without any classical analog. Crudely speaking, it is expected that on the d-dimensional boundary of an SPT phase in $d+1$-dimensional space-time lives an interesting phase of matter which is anomalous in the sense that it cannot exist on a pure d-dimensional spacetime manifold, but must always be realized on the boundary of a $d+1$ manifold under the condition that the symmetry is realized in the same way as in the bulk [41, 39, 126, 127, 128] .

Put differently, consistency conditions of a conformal field theory (CFT) at the boundary and topological properties of a bulk phase are closely related. Basically, a consistent CFT, when realized at the edge of a bulk system, implies that the bulk is trivial, namely, continuously deformable to a trivial state. On the other hand, if a bulk supports a CFT that is inconsistent as its boundary theory, the bulk cannot be deformed into a trivial state. This leads us to the question: *What are the criteria for a CFT to be consistent?*

For a (2+1)d SPT phase, modular (non)invariance of its (1+1)d edge theory has been used as a diagnostic for the (non)trivial bulk [129, 130]. For a nontrivial SPT phase protected by symmetry G, there is a conflict between G and modular invariance of the edge CFT; more precisely, the edge theory orbifolded by G is not modular invariant[129, 130]. A similar argument can be applied to boundary theories of SPT phases in space dimensions higher than 2 [131, 132].

4.1.2 Edgeability

In this chapter, we will give further thought on consistency conditions of CFTs. We will rely on the simple geometrical identity, $\partial^2 = 0$, which essentially says there is no boundary to a boundary of a bulk system. This would mean, in the context of SPT phases and their boundaries, that boundary theories of SPT phases are not allowed to have boundaries. Conversely, it is likely that any "healthy" (conformal) field theories should be possible to have boundaries − this may be a consistency condition of the (conformal) field theories.

In studies of surface topological orders of $(3 + 1)d$ SPT phases, such a consistency condition was called "edgeability" [63, 133]. $(2 + 1)$-dimensional surface theories are said to be "nonedgeable", meaning that it is not possible to create an edge between the theory in question and the vacuum. The only boundary that one can possibly create is a domain wall. In contrast, any consistent $(2 + 1)d$ theory should be "edgeable" to the trivial vacuum. Here "edgeability" may be also called "cuttability", meaning that the original theory defined on a closed spacetime can be cut open.

We will follow this idea but focus on one lower dimension. In $(1 + 1)d$ CFTs, in addition to modular invariance, it is often claimed that a consistent conformal field theory with boundaries must have a complete set of boundary states. (See, for example, Refs. [134, 135].) This reminds us of edgeability. In fact, the construction of modular invariant partition functions are closely related to boundary conformal field theories (BCFTs). The perspective from SPT phases gives us some insight about why BCFT is crucial for consistency, which may look a little puzzling from other viewpoints. In order for a CFT to exist as a pure $(1 + 1)d$ system, both edgeability and modular invariance must be satisfied. (Once again, here edgeability may be also called cuttability, meaning that the original closed $(1 + 1)d$ CFT can be cut open into a well-defined BCFT.) In many known cases, these two conditions are actually equivalent.

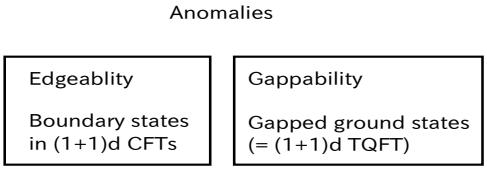

Figure 4.1: Edgeability and gappability of conformal field theories are closely related – they both diagnose if they must be realized as a boundary of (topological) systems in one higher dimensions. Hence, edgeability and gappability are both related to quantum anomalies.

The simplest examples of (non)edgeability can be provided by chiral edge theories of topologically ordered phases, in which the chiral central charge is nonzero. In these edge theories, it is not possible to find conformally invariant boundary conditions or boundary states. These conformal field theories are hence non-edgeable and must be realized at the boundary of a (topological) phase in one higher dimensions.

In the context of SPT phases, Ref. [136], gives an explicit lattice construction of an $(1+1)d$ CFT, which is the edge theory of $(2+1)d$ bosonic SPT phases protected by $\mathbb{Z}_N$ on-site unitary symmetry. In this construction, while the CFT is successfully put on a one-dimensional lattice, the $\mathbb{Z}_N$ symmetry is not realized in a purely local way – the action of the $\mathbb{Z}_N$ transformation is non-on-site, and it involves links of the lattice. It was claimed that its non-on-site symmetry has been gauged, which is equivalent to orbifolding $\mathbb{Z}_N$ symmetry. As we will clarify, within this CFT with the non-onsite action of the $\mathbb{Z}_N$ symmetry (and its lattice realization), it is not possible to make a boundary which is consistent with the $\mathbb{Z}_N$ symmetry. Hence, this theory is nonedgeable.

4.1.3 Gappability

Let us now also give a slightly different perspective from the correspondence between $(1+1)d$ gapped states and boundary states in CFTs. In Refs. [137, 138], $(1+1)d$ conformal field theories perturbed by some operators are considered. If the perturbation is such that it fully gaps out the theory, we flow from the CFT to a massive phase. It was claimed that the ground state of the massive phase is described, with the Hilbert space of the CFT, by a boundary state. In particular, in Ref. [137] this claim is explicitly verified for various symmetry-protected topological phases in $(1+1)d$, which are obtained by perturbing CFTs. These phases are fully gapped $(1+1)d$ phases protected by a certain set of symmetries. In particular, topological invariants, for instance, the group cocycle $\varepsilon \in H^2(G, \mathrm{U}(1))$ of the group cohomology classification of $(1+1)d$ SPT phases [39, 126], can be fully extracted from boundary states that describe SPT phases.

In this chapter, instead of $(1+1)d$ SPT phases, we are concerned with $(2+1)d$ SPT phases, and in

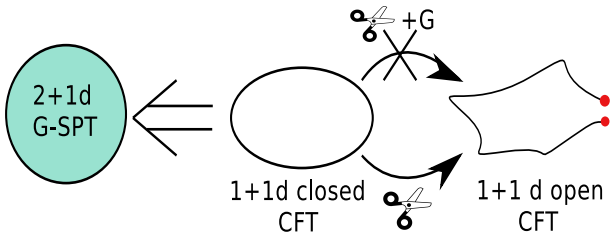

Figure 4.2: We claim that one cannot "cut" or "make a boundary" while preserving G symmetry for certain CFTs and certain symmetry implementations. These symmetry implementations correspond precisely to $(2+1)$d G-symmetric SPT phases and the corresponding CFTs are their edge theories.

particular their edge theories. In various examples, we establish a claim similar to the above claim for the bulk $(1+1)$ dimensions; we again establish a connection between gapped ground states in the edge theories and conformal boundary states. The relation between edgeability and gappability is schematically illustrated in Fig. 4.1. In particular, for the edge theories described by the K-matrix theory, we establish the connection between Haldane's null vector criterion for gapping potentials [112] and the boundary states.

More precisely, the main question we ask is which boundary conditions (including symmetry projections) can be imposed on conformal field theories that are defined on the edge of $(2+1)d$ systems with boundaries. We show the equivalence between our BCFT formalism and the K-matrix formalism used in Ref. [41] and show that those CFTs that admit a consistent boundary state correspond to edge theories of trivial SPTs and those that do not admit a consistent boundary state correspond to edges of nontrivial SPTs.

This criterion is very similar to that imposed by the modular invariance of CFTs field theories on the torus. Putting a theory on a torus in this context implies that it can be realized on a strictly $(1+1)d$ manifold and need not be realized on the boundary of an SPT phase[129, 130, 139, 140].

4.1.4 Working Principles

Following these motivations, let us now describe our strategy to detect and diagnose non-trivial SPT phases. We claim that one cannot construct a symmetry invariant Cardy state (conformal boundary state) for a CFT corresponding to the edge of a non-trivial SPT. As mentioned in the above example, this is due to the fact that although one may be able to put the edge theory of an SPT on a lattice, G symmetry cannot be implemented in an on-site way – this shows up as nonedgeablity.

A Cardy state in conformal field theory is a coherent state in the Hilbert space of the closed sector of the CFT which satisfies an open-closed consistency relation, namely the Cardy condition [141, 142]. We show that in the case of nontrivial SPT phases, it is not possible to implement the symmetry and simultaneously satisfy the Cardy condition.

We list our procedure for diagnosis of SPT phases as follows (see Fig. 4.2 for an illustration).

1. First, cut the $1d$ circle and impose appropriate boundary conditions on the two ends.

2. Second, solve for Ishibashi states [143] of this open system, which correspond to solutions to the boundary conditions imposed.

3. Third, try to construct a boundary state that is a linear combination of Ishibashi states, which satisfies the Cardy condition and is also symmetry invariant. If such a state exists, then there is no nontrivial SPT phase in a $(2+1)d$ bulk system; if such a state does not exist, then the corresponding $(2+1)d$ bulk is a nontrivial SPT phase.

4. Fourth, once we have detected nontrivial SPT phases, we can obtain its classification from the transformation of the Cardy state under symmetry operation, which will be explained in detail in later sections.

Using this technique, we can study SPT phases protected by space-time and/or some internal symmetries. Examples include the time-reversal symmetric topological insulators, bosonic SPT phases with $\mathbb{Z}_N$ symmetry, and topological superconductors protected by $\mathbb{Z}_2 \times \mathbb{Z}_2$ symmetries. These examples have been also analyzed in the literature by different methods [144, 145, 124, 146, 147].

The organization of the rest of the chapter is as follows. In Sec. 4.2, a brief introduction to BCFT is provided. In Sec. 4.3, we study $(2+1)d$ time-reversal symmetric topological insulators from the edge theories and the corresponding symmetric Cardy boundary states. Edge theories of more general $(2+1)d$ SPT phases described by the K-matrix theories are considered in Sec. 4.4, where a connection between the Cardy states and gapped phases in $(1+1)$ dimensions is shown explicitly. Then we apply our approach to topological superconductors in Sec. 4.5.

4.2 An introduction to BCFT

A boundary condition in a CFT defines a relation between the holomorphic and antiholomorphic sectors. In other words, the two sectors are related to one another on the boundary via an automorphism of the form

$$S(z) = \rho_\beta\left(\bar{S}(\bar{z})\right), \tag{4.1}$$

where S belongs to some symmetry algebra, ρ_β denotes an automorphism of the algebra of fields, and β is a constant that parametrizes the boundary condition. $S(z)$ and $\bar{S}(\bar{z})$ are fields which have the following

expansion in terms of modes:

$$S(z) = \sum_{n\in\mathbb{Z}} S_n z^{-n-h}, \quad \bar{S}(\bar{z}) = \sum_{n\in\mathbb{Z}} \bar{S}_n \bar{z}^{-n-\bar{h}}, \tag{4.2}$$

where h and $\bar{h}$ are the conformal weights of S and $\bar{S}$ respectively. In most general situations, S and $\bar{S}$ are the holomorphic and antiholomorphic components of the stress-energy tensor with $h = 2$. For CFTs with current algebra symmetries, S and $\bar{S}$ are taken to be the currents with $h = 1$.

In the closed picture, a boundary condition is represented by a state in the Hilbert space of a CFT defined on a circle. According to Cardy, such a boundary state must transform consistently under the S-modular transformation, namely, a $\pi/2$ rotation of the space-time manifold (worldsheet) illustrated in Fig. 4.3. To construct physical boundary states obeying this consistency condition (the Cardy condition), one first constructs a set of states, the so-called Ishibashi states, $|i,\beta\rangle\!\rangle$, which are annihilated by the boundary conditions (known as gluing conditions) in the operator form after the $\pi/2$ rotation, $\left[S_n - \rho_\beta\left(\bar{S}_n\right)\right] \xrightarrow{\text{worldsheet rotation}} \left[S_n - (-1)^h \rho_\beta\left(\bar{S}_n\right)\right]$, namely,

$$\left[S_n - (-1)^h \rho\left(\bar{S}_n\right)\right] |i,\beta\rangle\!\rangle = 0. \tag{4.3}$$

A Cardy state is a suitable superposition of the Ishibashi states that satisfy the Cardy condition, which is an implementation of open-closed channel consistency:

$$Z_{\alpha\beta}(-1/\tau) = \langle B_\alpha | e^{2\pi i \tau H_{\text{closed}}} | B_\beta \rangle, \tag{4.4}$$

where $Z_{\alpha\beta}$ is the partition function computed in the open-channel picture, and given as a trace over the open Hilbert space with boundary conditions α, β on the two ends, and τ is parameterized by the size of the system [148]. The states $|B_\alpha\rangle$ and $|B_\beta\rangle$ which satisfy the above condition are the bona fide boundary states, the Cardy states. For a more detailed introduction to boundary conformal field theory, see, for example, Refs. [141, 142, 54, 148, 149, 150].

Symmetry invariant Cardy states and the obstruction A generic Cardy boundary state $|B\rangle$ (here we are suppressing the label α, β specifying boundary conditions) lies in the subspace of the closed Hilbert space and satisfies

$$(T - \bar{T})|B\rangle = 0 \quad \text{(on a boundary)}, \tag{4.5}$$

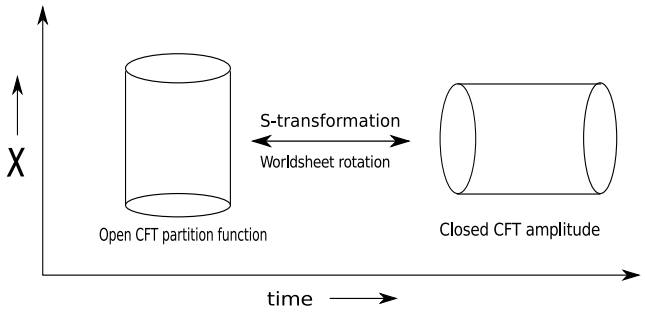

Figure 4.3: An illustration of the Cardy condition; a consistency condition for conformal boundary states. For boundary states that preserve conformal symmetry, the open channel partition function $Z_{\text{open}} := \text{Tr}_{\mathcal{H}_{\text{open}}}\left[e^{-(2\pi i/\tau)H_{\text{open}}}\right]$ must equal the amplitude for a "Cardy" state $\mathcal{A} = \langle B|e^{2\pi i\tau H_{\text{closed}}}|B\rangle$.

where T and $\bar{T}$ are the holomorphic and anti-holomorphic parts of the energy density operator, respectively. In terms of the Virasoro generators, this condition can be written as

$$(L_n - \bar{L}_{-n})|B\rangle = 0. \tag{4.6}$$

Equation (4.6) implies $(c - \bar{c})|B\rangle = 0$, where c and $\bar{c}$ represent the central charges for the holomorphic and antiholomorphic sectors, respectively. Thus, as expected, one cannot construct (conformally invariant) boundary states when $c \neq \bar{c}$ since in this case, the $(1+1)$d CFT suffers from the (infinitesimal) gravitational anomaly, and hence it must be realized as the boundary theory of an appropriate bulk system living in one higher dimension.

For the rest of the chapter, we will deal with systems with the vanishing chiral central charge, $c - \bar{c} = 0$, and hence there is no infinitesimal gravitational anomaly. We will also focus on $(1+1)d$ CFTs for which one can construct a modular invariant, if one is willing not to impose any additional symmetry. Hence, in the absence of symmetries, the $(1+1)d$ CFT can be safely gapped by adding a suitable perturbation. However, if we impose some symmetry, e.g., if we consider $(1+1)d$ CFTs realized potentially on the boundary of $(2+1)d$ SPT phases, there may be a conflict between the symmetry and modular invariance. Once symmetry is gauged (orbifold), the modular invariance may be spoiled. Conversely, if the modular invariance is enforced, the symmetry must be broken.

At the level of BCFT, this would mean that one may not be able to construct boundary states which are invariant under the symmetry. More precisely, we consider a symmetry that preserves T and $\bar{T}$, respectively, or exchanges them. Classically, such a symmetry preserves the conformally invariant boundary condition

$T = \bar{T}$ along the boundary. However, once the theory is quantized, there may be an obstruction to construct the corresponding a boundary state. A symmetry of a CFT (on a closed space-time manifold) is anomalous if one cannot make a boundary that preserves this symmetry both classically and quantum mechanically. Typically, this happens when there is a conflict between the Cardy condition (4.4) and the symmetry, so a symmetric Cardy state does not exist. In this situation, the theory itself, together with the symmetry, cannot be consistently defined and must appear as a boundary theory of a SPT phase with the same symmetry in one higher dimensions. Nevertheless, by "stacking" copies of such SPT phases, the number of degrees of freedom at boundaries increase, and the solution space of Eq. (4.5) is enlarged – it may be possible to find a symmetric Cardy state if the number of the copies is large enough. When this occurs, the corresponding CFT is anomaly free with respect to such a symmetry and can exist alone in its own dimension.

4.3 Edge theories of (2 + 1)d time-reversal symmetric topological insulators

Let us begin with a simple example. Consider the edge theory of a $(2+1)d$ time-reversal symmetric topological insulator, which is described by $(1+1)d$ massless Dirac fermions on a closed two-manifold Σ:

$$S = \frac{1}{2\pi}\int_{\Sigma} dtdx \left(i\bar{\psi}_R\partial_+\psi_R + i\bar{\psi}_L\partial_-\psi_L\right), \tag{4.7}$$

where $\partial_\pm = \partial_t \pm \partial_x$. The system is invariant under both charge $\mathrm{U}(1)_C$ and time-reversal symmetries, which are defined as

$$\begin{aligned} \mathrm{U}(1)_C &: \psi_R \to e^{-i\theta}\psi_R, \quad \psi_L \to e^{-i\theta}\psi_L \\ \mathcal{T}_\eta &: \psi_R \to \psi_L, \quad \psi_L \to \eta\psi_R, \quad \eta = \pm 1. \end{aligned} \tag{4.8}$$

Here in principle we have two choices for time-reversal symmetry (characterized by η): $\mathcal{T}_1^2 = 1$ and $\mathcal{T}_{-1}^2 = (-1)^F$, where F is the total fermion number operator. By analyzing the stability (gappability) of the theory (4.7), at least at the quadratic level (namely, by considering adding symmetry-respecting fermion mass bilinears to the action), we know that $\eta = 1$ ($\eta = -1$) corresponds to the edge of the topologically trivial (nontrivial) phase. It can also be shown the nontrivial topological phases form a $\mathbb{Z}_2$ class.

Now let us study the same problem (classification of topological insulators) by the BCFT approach. Consider putting the theory (4.7) on a cylinder Σ with boundary at $x = 0, \pi$. Then we would like to know,

based on the discussion in the previous sections, if there exists a Cardy boundary state, which satisfies the conditions (4.4) and (4.5), invariant under $\mathrm{U}(1)_C$ and $\mathcal{T}_\eta$. If such a Cardy state does not exist, the corresponding theory must be the edge of a $(2+1)d$ topological insulator.

One obtains the boundary conditions by varying the action (4.7) on the cylinder Σ,

$$\left[\bar{\psi}_R\delta\psi_R+\psi_R\delta\bar{\psi}_R-\bar{\psi}_L\delta\psi_L-\psi_L\delta\bar{\psi}_L\right]\big|_{\partial\Sigma}=0. \tag{4.9}$$

This boundary condition can be solved by the following set of gluing conditions [151]:

$$\begin{aligned} B_\beta \text{ type}: &\quad \psi_L=e^{-i\beta}\psi_R, \quad \bar{\psi}_L=e^{i\beta}\bar{\psi}_R,\\ A_\alpha \text{ type}: &\quad \psi_L=e^{-i\alpha}\bar{\psi}_R, \quad \bar{\psi}_L=e^{i\alpha}\psi_R. \end{aligned} \tag{4.10}$$

The two kinds of boundary conditions have been labeled B_β and A_α, respectively. Note that, as the bulk theory respects all symmetries, the presence of boundary might in general break (some of) the symmetries. To be specific, the B_β boundary condition (with arbitrary β) preserves both $\mathrm{U}(1)_C$ and $\mathcal{T}_1$, while either the B_β or the A_α boundary condition cannot preserve both $\mathrm{U}(1)_C$ and $\mathcal{T}_{-1}$. Therefore, it is impossible to, at least for a single copy of the theory (4.7), find a symmetric Cardy state with respect to both $\mathrm{U}(1)_C$ and $\mathcal{T}_{-1}$, because there is no such symmetry invariant boundary condition.

Let us first focus on the case of the symmetry group $\mathrm{U}(1)_C\rtimes\mathbb{Z}_2^{\mathcal{T}_1}$, where $\mathbb{Z}_2^{\mathcal{T}_1}$ is generated by $\mathcal{T}_1$. Although the B_β boundary condition preserves $\mathrm{U}(1)_C\rtimes\mathbb{Z}_2^{\mathcal{T}_1}$, we still have to check that the corresponding Cardy state is also symmetry invariant.

We impose boundary conditions B_0, B_β at $x=0,\pi$, respectively. In order to satisfy the boundary conditions, we define a mode expansion

$$\begin{aligned} \psi_L&=\sum_{r\in\mathbb{Z}+\beta/2\pi}\psi_r(t)e^{irx}, \quad \bar{\psi}_L=\sum_{r''\in\mathbb{Z}-\beta/2\pi}\bar{\psi}_{r'}(t)e^{ir'x},\\ \psi_R&=\sum_{r\in\mathbb{Z}+\beta/2\pi}\psi_r(t)e^{-irx}, \quad \bar{\psi}_R=\sum_{r'\in\mathbb{Z}-\beta/2\pi}\bar{\psi}_{r'}(t)e^{-ir'x}. \end{aligned} \tag{4.11}$$

The mode operators satisfy the following algebra:

$$\begin{aligned} &\{\psi_r(t),\psi^\dagger_{r'}(t)\}=2\pi\delta_{r+r',0},\\ &\{\psi_r(t),\psi_{r'}(t)\}=\{\psi^\dagger_r(t),\psi^\dagger_{r'}(t)\}=0. \end{aligned} \tag{4.12}$$

We define the normal ordering with respect to a vacuum $|0,\beta\rangle$ which is annihilated by ψ_r (≥ 0) and $\bar{\psi}_{r'}$ (≥ 0):

$$: \bar{\psi}_{-r}\psi_r := \begin{cases} \bar{\psi}_{-r}\psi_r & \text{if } r \geq 0, \\ -\psi_r\bar{\psi}_{-r} & \text{if } r < 0. \end{cases} \tag{4.13}$$

The Hamiltonian and $\mathrm{U}(1)_C$ charge operator F take the form

$$\begin{aligned} H_o &= \sum_{r\in\mathbb{Z}+\frac{\beta}{2\pi}} r : \bar{\psi}_{-r}\psi_r : + \frac{1}{2}\left(\frac{\beta}{2\pi} - \left[\frac{\beta}{2\pi}\right] - \frac{1}{2}\right)^2 - \frac{1}{24}, \\ F &= \sum_{r\in\mathbb{Z}+\frac{\beta}{2\pi}} : \bar{\psi}_{-r}\psi_r : + \frac{\beta}{2\pi} - \left[\frac{\beta}{2\pi}\right] - \frac{1}{2}. \end{aligned} \tag{4.14}$$

The open-channel partition function with insertion of symmetry flux $e^{-2\pi i(a-1/2)F}$ on the cylinder with $(\ell_{\text{space}}, \beta_{\text{time}}) = (\pi, 2\pi T)$ is

$$\begin{aligned} Z^a_{0\beta}(T) &= \mathrm{Tr}_{\mathcal{H}_o}\left[e^{-2\pi i(a-1/2)F} e^{-2\pi T H_o}\right] \\ &= \frac{\vartheta\left[\begin{smallmatrix}\beta/2\pi - 1/2 \\ -(a-1/2)\end{smallmatrix}\right](0, iT)}{\eta(iT)}. \end{aligned} \tag{4.15}$$

To construct the Cardy states, we work in Euclidean signature, by performing the Wick rotation $t = -i\tau$, and consider boundary conditions in the closed channel [after the space-time cylinder has been rotated by $\pi/2$, namely, $(x', \tau') = (\tau, -x)$]:

$$\psi'_L = e^{-i\beta} e^{-i\pi/2}\psi'_R, \quad \bar{\psi}'_L = e^{i\beta} e^{-i\pi/2}\bar{\psi}'_R, \tag{4.16}$$

where we have introduced the notation

$$\begin{aligned} \psi'_R &= e^{i\pi/4}\psi_R, \quad \bar{\psi}'_R = e^{i\pi/4}\bar{\psi}_R, \\ \psi'_L &= e^{-i\pi/4}\psi_L, \quad \bar{\psi}'_L = e^{-i\pi/4}\bar{\psi}_L, \end{aligned} \tag{4.17}$$

for the fields with respect to the coordinate system after the $\pi/2$ space-time rotation.

In Euclidean signature, the original time-reversal symmetry $\mathcal{T}_\eta$, which is an anti-unitary operator in the Lorentz signature, becomes the unitary $(\mathcal{CP})_\eta$ symmetry, the product of charge conjugation and spatial reflection that flips τ to $-\tau$. From the relation (4.17), this $(\mathcal{CP})_\eta$ is further translated to $(\mathcal{CP})'_{-\eta}$, which acts

on the fermions as

$$(\mathcal{CP})'_{-\eta}: \psi'_R(x',\tau') \to e^{i\pi/2}\bar{\psi}'_L(-x',\tau'),$$
$$\psi'_L(x',\tau') \to \eta e^{-i\pi/2}\bar{\psi}'_R(-x',\tau'). \tag{4.18}$$

Therefore, under the $\pi/2$ space-time rotation (together with an analytic continuation from the Lorentz to Euclidean signature), we have the following correspondence:

$$\mathcal{T}_\eta^2 = \eta^F \longleftrightarrow (\mathcal{CP})'^2_{-\eta} = (-\eta)^F, \quad \eta = \pm 1. \tag{4.19}$$

One can check that $(\mathcal{CP})'_{-1}$ preserves the boundary condition (4.16) as $\mathcal{T}_1$ preserves the B_β-type boundary condition in (4.10).

Now, since we inserted a $\mathrm{U}(1)_C$ charge operator in the trace when evaluating the open-channel partition function, the corresponding boundary states in the closed channel must lie in the subspace of the Hilbert space of the twisted fields that satisfy

$$\psi'_R(x'+2\pi,\tau') = e^{2\pi i a}\psi'_R(x',\tau'),$$
$$\psi'_L(x'+2\pi,\tau') = e^{2\pi i a}\psi'_L(x',\tau'). \tag{4.20}$$

(Here we compactify the space direction as $x' \equiv x'+2\pi$.) Hence, we get the following mode expansions:

$$\psi'_R = \sum_{r\in\mathbb{Z}+a} \psi'_r e^{irw'}, \quad \bar{\psi}'_R = \sum_{r'\in\mathbb{Z}-a} \bar{\psi}'_{r'} e^{ir'w'},$$
$$\psi'_L = \sum_{\tilde{r}\in\mathbb{Z}-a} \tilde{\psi}'_{\tilde{r}} e^{-i\tilde{r}w'}, \quad \bar{\psi}'_L = \sum_{\tilde{r}'\in\mathbb{Z}+a} \bar{\tilde{\psi}}'_{\tilde{r}'} e^{-i\tilde{r}'w'}, \tag{4.21}$$

where $\omega' = x' + i\tau'$. The Hamiltonian is

$$H_c = \sum_{r\in\mathbb{Z}+a} r : \bar{\psi}'_{-r}\psi'_r : + \sum_{\tilde{r}\in\mathbb{Z}-a} \tilde{r} : \bar{\psi}'_{-\tilde{r}}\psi'_{\tilde{r}} :$$
$$+ \frac{1}{2}\left(a - [a] - \frac{1}{2}\right)^2 + \frac{1}{2}\left(a + [-a] + \frac{1}{2}\right)^2 - \frac{1}{12}. \tag{4.22}$$

The ground state $|0\rangle_{a,-a}$ is defined to be the state annihilated by ψ'_r $(r \geq 0)$, $\bar{\psi}'_{r'}$ $(r' > 0)$, $\tilde{\psi}'_{\tilde{r}}$ $(\tilde{r} \geq 0)$, $\bar{\tilde{\psi}}'_{\tilde{r}'}$ $(\tilde{r}' > 0)$.

The gluing condition (4.16) for the mode operators takes the form

$$\begin{aligned}\psi'_r &= ie^{i\beta}\tilde{\psi}'_{-r} \quad \forall r \in \mathbb{Z}+a,\\ \bar{\psi}'_{r'} &= ie^{-i\beta}\bar{\tilde{\psi}}'_{-r'} \quad \forall r' \in \mathbb{Z}-a.\end{aligned} \tag{4.23}$$

An incoming boundary state that solves the above gluing condition is

$$|B_\beta\rangle_a = \exp\left(ie^{-i\beta}\sum_{r'\geq 0}\psi'_{-r'}\bar{\tilde{\psi}}'_{-r'} + ie^{i\beta}\sum_{r>0}\bar{\psi}'_{-r}\tilde{\psi}'_{-r}\right)|0\rangle_{a,-a}, \tag{4.24}$$

while the outgoing boundary state is

$${}_a\langle B_\beta| = {}_{a,-a}\langle 0|\exp\left(ie^{i\beta}\sum_{r'\geq 0}\tilde{\psi}'_{r'}\bar{\psi}'_{r'} + ie^{-i\beta}\sum_{r>0}\bar{\tilde{\psi}}'_{r}\psi'_{r}\right). \tag{4.25}$$

Then the closed-channel partition function on the cylinder with $(\beta_{\text{space}}, \ell_{\text{time}}) = (2\pi, \pi L)$ is given by

$${}_a\langle B_0|e^{-\pi L H_c}|B_\beta\rangle_a = \frac{\vartheta\left[\begin{smallmatrix}\beta/2\pi-1/2\\ -(a-1/2)\end{smallmatrix}\right](0, iL^{-1})}{\eta(iL^{-1})}. \tag{4.26}$$

Identifying $T = L^{-1}$, we find that $|B_\beta\rangle_a$ is indeed a Cardy state that satisfies the Cardy condition

$$Z^a_{0\beta}(T) = {}_a\langle B_0|e^{-\pi L H_c}|B_\beta\rangle_a. \tag{4.27}$$

It is clear that the state $|B_\beta\rangle_a$ is invariant under both $\mathrm{U}(1)_C$ and $(\mathcal{CP})'_{-1}$ (corresponding to $\mathcal{T}_1$). This is verified by looking at the symmetry action on the modes (deduced from (4.18) and (4.21) at $\tau' = 0$):

$$\begin{aligned}&U(1)_C : \psi'_r \to e^{-i\theta}\psi'_r, \quad \tilde{\psi}'_r \to e^{-i\theta}\tilde{\psi}'_r\\ &(\mathcal{CP})'_{-\eta} : \psi'_r \to e^{i\pi/2}\bar{\tilde{\psi}}'_r, \quad \tilde{\psi}'_r \to -\eta e^{i\pi/2}\bar{\psi}'_r, \quad \eta = \pm 1.\end{aligned} \tag{4.28}$$

Note that we have assumed the ground state $|0\rangle_{a,-a}$ is also invariant under all symmetries. On the other hand, the state $|B_\beta\rangle_a$ is only invariant under $\mathrm{U}(1)_C$; it is not invariant under $(\mathcal{CP})'_{+1}$ (corresponding to $\mathcal{T}_{-1}$).

Let us now consider two copies of complex fermions $\{\psi_{1,R}, \psi_{1,L}, \psi_{2,R}, \psi_{2,L}\}$. One can show that it is now possible to construct a $\mathrm{U}(1)_C \rtimes \mathbb{Z}_2^{\mathcal{T}_{-1}}$ symmetric Cardy state. One considers the following boundary

conditions (before $\pi/2$ space-time rotation):

$$\psi_{1,L} = e^{-i\beta_1}\psi_{2,R}, \quad \bar{\psi}_{1,L} = e^{i\beta_1}\bar{\psi}_{2,R},$$
$$\psi_{2,L} = e^{-i\beta_2}\psi_{1,R}, \quad \bar{\psi}_{2,L} = e^{i\beta_2}\bar{\psi}_{1,R}, \tag{4.29}$$

which preserve $\mathrm{U}(1)_C \rtimes \mathbb{Z}_2^{\mathcal{T}_{-1}}$ if $\beta_1 = \beta_2 \pm \pi$. The corresponding (total) Cardy state is the tensor product of the outgoing boundary states associated with these two boundary conditions,

$$|B_{\beta_1,\beta_2}\rangle_a = |B_{\beta_1}\rangle_a \otimes |B_{\beta_2}\rangle_a, \tag{4.30}$$

which is invariant under both $\mathrm{U}(1)_C$ and $(\mathcal{CP})'_1$ (corresponding to $\mathcal{T}_{-1}$).

In summary, a single copy (two copies), or in general, any number of copies (an even number of copies) of the theory (4.7) can be consistently formulated, in the presence of $\mathrm{U}(1)_C$ and $\mathcal{T}_1$ ($\mathcal{T}_{-1}$) symmetries, on a cylinder Σ. Therefore, the BCFT approach agrees with the classification of $(2+1)d$ fermionic SPT phases with $\mathrm{U}(1)_C$ and time-reversal symmetries given by the gappability argument. In fact, there is a correspondence between the form of Cardy boundary states and gapped phases in $(1+1)$ dimensions. In the following section, we study theories of multicomponent bosons, which describe (the edges of) more general SPT phases in $(2+1)$ dimensions, and will see such correspondence explicitly.

4.4 More general SPT phases in (2 + 1)d

4.4.1 Canonical quantization

Let us consider the edge of a $(2+1)d$ Abelian SPT phase (either fermionic or bosonic ones) described by the K-matrix theory of multicomponent compactified boson fields [41],

$$S = \frac{1}{4\pi}\int d^2x \left[K_{IJ}\partial_t\phi^I\partial_x\phi^J - V_{IJ}\partial_x\phi^I\partial_x\phi^J\right], \tag{4.31}$$

where K is a $2N\times 2N$ integer-valued symmetric matrix and $I, J = 1, \ldots, 2N$. We are interested in studying SPT phases, namely, those that have no topological order, hence we will restrict ourselves to theories with $\det K = 1$. Moreover, since SPT phases can be adiabatically connected to trivial phases in the absence of symmetry, their edge theories are always non-chiral. V_{IJ} in Eq. (4.31) is a non-universal positive definite matrix, which does not affect the topological properties of the theory; ϕ^I are compact U(1) bosons that satisfy the compactification condition $\phi^I \equiv \phi^I + 2\pi n^I, n^I \in \mathbb{Z}$. When put on a cylinder of circumference 2π,

they satisfy the commutation relations

$$\left[\partial_x \phi^I(x), \partial_x \phi^J(x')\right] = \sum_{m\in\mathbb{Z}} 2\pi i (K^{-1})^{IJ} \partial_x \delta(x - x' + 2\pi m).$$

It is more convenient to carry out the quantization in the redefined basis φ^I which we define by diagonalizing the K matrix as [140]

$$\mathbf{A}\phi = \varphi, \quad \mathbf{A}^T \eta \mathbf{A} = K, \tag{4.32}$$

where $\mathbf{A} \in O(2N)$ and η is a diagonal matrix with ± 1 on the diagonal. To have a non-chiral theory, we assume η has equal number of $+1$ and -1 in its diagonal. Without loss of generality we assume $\eta = \text{diag}(1, \ldots, 1, -1, \ldots, -1)$. The theory has N copies of nonchiral bosons. The action in the φ basis takes the form

$$S = \frac{1}{4\pi} \int d^2x \left[(\partial_t \varphi)^T \eta (\partial_x \varphi) - (\partial_x \varphi)^T (\partial_x \varphi)\right], \tag{4.33}$$

where we have chosen V such that $\mathbf{A} V \mathbf{A}^T = \mathbb{I}_{2N}$. The Hamiltonian and momentum operators are obtained from the action (4.33) as

$$\begin{aligned} H &= \frac{1}{4\pi} \int dx \left[(\partial_x \varphi)^T (\partial_x \varphi)\right], \\ P &= \frac{1}{4\pi} \int dx \left[(\partial_x \varphi)^T \eta (\partial_x \varphi)\right]. \end{aligned} \tag{4.34}$$

After basis transformation, the redefined bosons satisfy the compactification condition

$$\varphi^I \sim \varphi^I + 2\pi \left(\mathbf{A} n\right)^I, \quad n^I \in \mathbb{Z}, \tag{4.35}$$

and the canonical commutation relation

$$\left[\partial_x \varphi^I(x), \partial_x \varphi^J(x')\right] = 2\pi i (\eta^{-1})^{IJ} \partial_x \sum_{m\in\mathbb{Z}} \delta(x - x' + 2\pi m).$$

The mode expansion compatible with the equations of motion, $\partial_t \varphi^I \eta_{II} - \partial_x \varphi_I = 0$, and the compactification conditions takes the form

$$\varphi^I = \varphi_0^I + \frac{2\pi}{L}[t + \mathrm{sgn}(\eta^{II})x]a_0^I + \frac{1}{\sqrt{2}}\sum_{r\neq 0} a_r^I e^{-\frac{2\pi r i}{L}[t+\mathrm{sgn}(\eta^{II})x]}. \tag{4.36}$$

Since $\left[\varphi_0^I, a_0^J\right] = 2\pi i \eta^{IJ}$ and $\varphi_0^I \sim \varphi_0^I + 2\pi(\mathbf{A}n)^I$,

$$v^I \in (\mathbf{A}m)^I \mathbb{Z}, \quad m^I \in \mathbb{Z}, \tag{4.37}$$

where v^I is the eigenvalue of a_0^I. The mode operators obey the following canonical commutation relation:

$$\left[a_n^I, a_m^J\right] = n\delta^{IJ}\delta_{n+m,0}, \quad n, m \neq 0. \tag{4.38}$$

4.4.2 Ishibashi states

States that represent a conformal invariant boundary condition are called Ishibashi states. They satisfy

$$[L_r - \bar{L}_{-r}]|I\rangle\rangle = 0, \tag{4.39}$$

where L_r and $\bar{L}_r$ are the holomorphic and antiholomorphic Virasoro generators, respectively. For the K-matrix theory defined in Eq. (4.33), they are given by

$$\begin{aligned} L_r &= \frac{1}{2}\sum_{n\in\mathbb{Z}} :(a_{r-n,L})^T a_{n,L}:, \\ \bar{L}_r &= \frac{1}{2}\sum_{n\in\mathbb{Z}} :(a_{r-n,R})^T a_{n,R}:, \end{aligned} \tag{4.40}$$

where

$$a_r^T = (a_{r,L}, a_{r,R})^T := (a_r^1, \ldots, a_r^N, a_r^{N+1}, \ldots, a_r^{2N})^T \tag{4.41}$$

are operators that appear in the mode expansion (4.36). While the general solution of (4.39) is not known, a sufficient condition for it is given by [152]

$$(a_{r,L} - Ra_{-r,R})|\mathbf{v}\rangle\rangle = 0, \quad \forall r \in \mathbb{Z}, \tag{4.42}$$

where the matrix $R \in O(N)$ does not depend on r. Solutions to Eq. (4.42) have the form

$$|\mathbf{v}\rangle\!\rangle := \exp\left(\sum_{r=1}^{\infty} \frac{1}{r} (a_{-r,L})^T R a_{-r,R}\right) |\mathbf{v}\rangle, \tag{4.43}$$

where $|\mathbf{v}\rangle$ are eigenstates of a_0^I with eigenvalues v^I that are characterized by Eq. (4.37). The Ishibashi condition in Eq. (4.42) can be further simplified by a basis transformation, after which R is rotated to be $\pm\mathbf{1}$. Let us clarify this point. The Ishibashi condition in Eq. (4.42) is equivalent to

$$\varphi_L = R\varphi_R. \tag{4.44}$$

Now we can choose a $\mathbf{B} \in O(2N)$ to be

$$\mathbf{B} = \begin{pmatrix} 1 & 0 \\ 0 & R \end{pmatrix}. \tag{4.45}$$

If we redefine the boson fields

$$\begin{pmatrix} \varphi'_L \\ \varphi'_R \end{pmatrix} = \pm\, \mathbf{B} \begin{pmatrix} \varphi_L \\ \varphi_R \end{pmatrix}, \tag{4.46}$$

then Eq. (4.44) becomes

$$\varphi'_{L/R} = \pm\varphi'_{L/R}. \tag{4.47}$$

In terms of the mode operators, we have the Ishibashi condition

$$(a'_{r,L} \mp a'_{-r,R})|\mathbf{v}\rangle\!\rangle = 0, \quad \forall r \in \mathbb{Z}. \tag{4.48}$$

This basis rotation and Eq. (4.32) can be simultaneously done if we define $\mathbf{A}' = \mathbf{B}\mathbf{A}$. In the following discussion, we assume this has been done. To lighten the notation, we drop the prime on the field and mode operators.

4.4.3 Equivalence between the Ishibashi condition and Haldane's null vector condition

Haldane's null vector condition of N copies of nonchiral compactified massless bosons states: if there is a set of N linearly independent integer vectors $\{\mathbf{l}_i\}$ satisfying the condition

$$\mathbf{l}_i^T K^{-1} \mathbf{l}_j = 0, \quad \forall i, j = 1, \cdots, N, \tag{4.49}$$

then we can find a potential which can gap out the N-component boson theory completely. [41] This condition comes from the locality requirement such that all the bosons can be pinned at the minimum values in the gapping potentials simultaneously. When Haldane's null vector condition is met, one can find the gapping potential

$$S_{gapping} = \sum_{\{\mathbf{l}\}} c_{\mathbf{l}} \int dt\, dx \cos\left(\mathbf{l} \cdot \phi + \alpha_{\mathbf{l}}\right), \tag{4.50}$$

where $\{\mathbf{l}\}$ is a set of independent gapping vectors.

In this section, we discuss the equivalence between the Ishibashi condition and Haldane's null condition. We will establish their equivalence at the level of Cardy states, from which the correspondence between Cardy states and gapped phases (from condensation of independent elementary bosons in the language of Ref. [41]) is manifest.

We start from the total Cardy state for the N-copy boson system

$$|B, \{\alpha_i\}\rangle = \otimes_{i=1}^{N} |B, \alpha_i\rangle, \tag{4.51}$$

where [148]

$$|B, \alpha_i\rangle = \frac{1}{2^{1/4}} \sum_{n_i \in \mathbb{Z}} e^{i n_i \alpha_i} |\mathbf{v}_i\rangle\!\rangle_{n_i} \tag{4.52}$$

(the repeated indices i are not summed over) is the Cardy state for the ith copy of the system and

$$|\mathbf{v}_i\rangle\!\rangle_{n_i} = e^{-\sum_{r>0} (1/r)(\mathbf{v}_{i,L} \cdot a_{-r,L})(\mathbf{v}_{i,R} \cdot a_{-r,R})} |n_i \mathbf{v}_i\rangle, \quad n_i \in \mathbb{Z}, \tag{4.53}$$

is an Ishibashi state satisfying the Ishibashi condition (4.48). Here $\{\mathbf{v}_i = (\mathbf{v}_{i,L}, \mathbf{v}_{i,R}) \mid i = 1, ..., N \text{ and } \mathbf{v}_{i,L} = -\mathbf{v}_{i,R}\}$ is a set of linearly independent $2N$-component vectors that generates, with integer coefficients, all

the solutions satisfying both Eqs. (4.37) and (4.48).

Note that the Cardy state (4.51) satisfies the Cardy condition automatically, since it is the direct product of decoupled Cardy states, each one satisfying Cardy condition separately. Now we want to rewrite Eq. (4.51) in another form in which the connection to the gapping potentials satisfying Haldane's null condition is manifest. First, let us write the ground state in a coherent state, namely,

$$|n_i \mathbf{v}_i\rangle = e^{in_i \mathbf{v}_i \cdot \varphi_0} |0\rangle_i = e^{in_i \mathbf{e}_i \cdot \phi_0} |0\rangle_i, \tag{4.54}$$

where $|0\rangle_i = |0\rangle_{i,L} \otimes |0\rangle_{i,R}$ is the true vacuum associated with the new zero modes $\mathbf{v}_{i,L/R} \cdot a_{0,L/R}$ and $\{\mathbf{e}_i := \mathbf{A}^{-1}\mathbf{v}_i\}$ is a set of linearly independent integer vectors [by the definition of $\{\mathbf{v}_i\}$ defined in Eq. (4.37)]. Plugging Eqs. (4.52)- (4.54) into Eq. (4.51), we obtain

$$\begin{aligned} |B, \{\alpha_i\}\rangle &= \otimes_{i=1}^{N} \left(\frac{1}{2^{1/4}} \sum_{n_i \in \mathbb{Z}} e^{in_i\alpha_i} e^{-\sum_{r>0}(1/r)(\mathbf{v}_{i,L}\cdot a_{-r,L})(\mathbf{v}_{i,R}\cdot a_{-r,R})} e^{in_i \mathbf{e}_i \cdot \phi_0} |0\rangle_i \right) \\ &= \frac{1}{2^{N/4-1}} e^{-\sum_{i=1}^{N}\sum_{r>0}(1/r)(\mathbf{v}_{i,L}\cdot a_{-r,L})(\mathbf{v}_{i,R}\cdot a_{-r,R})} \sum_{\{n_i \in \mathbb{Z}\}} \cos\left[n_i(\mathbf{e}_i \cdot \phi_0 + \alpha_i)\right] |0\rangle_1 \otimes \cdots \otimes |0\rangle_N. \end{aligned} \tag{4.55}$$

Note that the cosine term in the last line of Eq. (4.55) is nothing but a gapping potential, and the summation is over all the lattice constructed from the elementary or primitive lattice vectors introduced in Ref. [41]. Then we conclude that in the N-boson system, once we have a Cardy state satisfying the Ishibashi condition, Haldane's null vector condition is also implied, since gapping vectors satisfy Haldane's null condition.

Conversely, given a set of N vectors satisfying Haldane's null vector condition, we can always find the set of primitive lattice vectors. Let us assume this is done. Then we can construct the Cardy state by following Eq. (4.55) backward, from the bottom to the top line. This state satisfies the Ishibashi condition and Cardy condition manifestly.

4.4.4 Symmetry analysis

In the following subsections, in order to facilitate the discussion, we use different bases interchangeably. One can easily see their relations from Eqs. (4.32) and (4.46).

We consider an on-site discrete Abelian symmetry group G with the group action of the form

$$\hat{g} : \phi \to \phi + \delta\phi^g, \quad \forall g \in G, \tag{4.56}$$

where we assume that $\delta\phi^g$ is constant. From the mode expansion of ϕ, we can read off that $\hat{g}$ only acts on the zero mode $\phi_{\mathbf{0}}$,

$$\hat{g} : \phi_0 \to \phi_0 + \delta\phi^g, \quad \forall g \in G, \tag{4.57}$$

Hence a complete set of symmetry invariant gapping potentials, related by boundary conditions, is described by

$$\hat{g} : (\mathbf{l}^T\phi_0 + \alpha) \to (\mathbf{l}^T\phi_0 + \alpha) \bmod 2\pi\mathbb{Z}. \tag{4.58}$$

From the discussion in Sec. 4.4.3, if we have a set of symmetry invariant Haldane vectors, we can find a set of decoupled symmetry invariant Ishibashi states, with which we can construct a symmetry invariant Cardy state. We will show it in the following discussion with two examples.

4.4.5 Example: $\mathbb{Z}_2$ symmetric bosonic SPT

Let us consider the simple case of $\mathbb{Z}_2$ symmetric bosonic SPT phases. The edge theory is described by

$$\mathcal{L} = \frac{1}{4\pi}\left[(\partial_x\phi)^T K(\partial_t\phi) - v(\partial_x\phi)^T(\partial_x\phi)\right], \tag{4.59}$$

where $K = \sigma^x$. The $\mathbb{Z}_2$ symmetry, $\mathbb{Z}_2 = \{e, g\}$, acts on the ϕ fields as

$$\hat{g} : \begin{pmatrix} \phi_1 \\ \phi_2 \end{pmatrix} \to \begin{pmatrix} \phi_1 \\ \phi_2 \end{pmatrix} + \pi \begin{pmatrix} 1 \\ q \end{pmatrix}. \tag{4.60}$$

The theory describes a trivial and a nontrivial SPT phases for $q = 0, 1$ respectively.

As claimed above, for a trivial SPT phase, that is, for which one can find a symmetric gapping potential, there exists a symmetry invariant boundary state. The conditions to be satisfied by a set of symmetric gapping vectors $\{\mathbf{l}_i\}$ are

$$\begin{aligned} \mathbf{l}_i^T K^{-1}\mathbf{l}_j &= 0, \\ \hat{g}(\mathbf{l}_i^T\phi + \alpha)\hat{g}^{-1} &= (\mathbf{l}_i^T\phi + \alpha) \bmod 2\pi \quad \forall i, j. \end{aligned} \tag{4.61}$$

Since for the present case we only consider a single nonchiral boson, we need to find a single gapping vector $\mathbf{l}$. In the case for $q = 0$ the above conditions are satisfied by $\mathbf{l} = (0, 1)^T$. Hence the symmetric gapping term

is $\cos(\phi_2+\alpha)$. In the chiral basis, this corresponds to $\cos\left((\varphi_L-\varphi_R)/\sqrt{2}\right)$.

On the other hand, this gapping potential corresponds to the Dirichlet boundary state that has the gluing condition $a_{0,L}-a_{0,R}=0$. The Ishibashi state takes the form

$$|\mathbf{v}\rangle\!\rangle = e^{\sum_{r>0}^{\infty}(1/r)a_{-r}\bar{a}_{-r}}|a_{0,L}=a_{0,R}\rangle, \tag{4.62}$$

and the Cardy state is

$$|B,\phi_0\rangle = \frac{1}{\mathcal{N}_D}\sum_{n\in\mathbb{Z}} e^{in\phi_0}e^{\sum_{r>0}^{\infty}(1/r)a_{-r}\bar{a}_{-r}}|a_{0,L}=a_{0,R}=n\rangle, \tag{4.63}$$

where ϕ_0 specifies the position of the Cardy state with the Dirichlet boundary condition.

On the other hand, in the nontrivial case, namely, for $q=1$, one cannot find a nontrivial symmetric gapping vector as the conditions (4.61) imply that $l^1l^2=0$ and $l^1+l^2=0 \bmod 2$. These cannot be satisfied simultaneously for any nontrivial $\mathbf{l}$.

However, we expect [41, 39, 126] a $\mathbb{Z}_2$ classification so that two copies of the above theory must be trivial. This double copy is described by $\phi:=(\phi^1,\phi^2,\phi^3,\phi^4)^T$ and $K=\sigma^x\oplus\sigma^x$. The symmetry action on the two copies is taken to be identical. In order to be $\mathbb{Z}_2$ symmetric the two gapping vectors must satisfy

$$\begin{aligned} &l_i^1l_j^2+l_i^2l_j^1+l_i^3l_j^4+l_i^4l_j^3=0,\\ &\sum_{n=1}^{2}l_i^n=0 \bmod 2, \end{aligned} \tag{4.64}$$

which comes from Eq. (4.61). These conditions can be satisfied simultaneously by the following two gapping vectors:

$$\mathbf{l}_1=\begin{pmatrix}1\\0\\0\\1\end{pmatrix},\quad \mathbf{l}_2=\begin{pmatrix}0\\1\\-1\\0\end{pmatrix}. \tag{4.65}$$

This choice is not unique, for example an alternate choice of gapping vectors could be

$$\tilde{\mathbf{l}}_1 = \begin{pmatrix} 0 \\ 1 \\ 1 \\ 0 \end{pmatrix}, \quad \tilde{\mathbf{l}}_2 = \begin{pmatrix} 1 \\ 0 \\ 0 \\ -1 \end{pmatrix}. \tag{4.66}$$

For the set $\{\mathbf{l}\}$, the gapping terms are

$$\begin{aligned} \mathcal{L}_{\text{gapping}} &= \lambda \cos\left(\phi^1 + \phi^4 + \alpha\right) + \lambda' \cos\left(\phi^2 - \phi^3 + \alpha'\right) \\ &= \lambda \cos\left(\frac{1}{\sqrt{2}}(\varphi_{1,L} + \varphi_{1,R} + \varphi_{2,L} - \varphi_{2,R}) + \alpha\right) \\ &\quad + \lambda' \cos\left(\frac{1}{\sqrt{2}}(\varphi_{1,L} - \varphi_{1,R} - \varphi_{2,L} - \varphi_{2,R}) + \alpha'\right) \\ &= \lambda \cos\left(\Phi_{1,L} + \Phi_{1,R} + \alpha\right) + \lambda' \cos\left(\Phi_{2,L} + \Phi_{2,R} + \alpha'\right), \end{aligned} \tag{4.67}$$

where we define basis transformed bosons

$$\begin{aligned} \Phi_{1,L} &:= \frac{1}{\sqrt{2}}\big(\varphi_{1,L} + \varphi_{2,L}\big), \\ \Phi_{1,R} &:= \frac{1}{\sqrt{2}}\big(\varphi_{1,R} - \varphi_{2,R}\big), \\ \Phi_{2,L} &:= \frac{1}{\sqrt{2}}\big(\varphi_{1,L} - \varphi_{2,L}\big), \\ \Phi_{2,R} &:= -\frac{1}{\sqrt{2}}\big(\varphi_{1,R} + \varphi_{2,R}\big). \end{aligned} \tag{4.68}$$

The mode expansion of Φ_i is

$$\begin{aligned} \Phi_{i,L} &= \Phi_{i,0,L} + \frac{2\pi}{L}(t+x)b_{i,0} + \frac{1}{\sqrt{2}}\sum_{r\neq 0} b_{i,r} e^{-(2\pi i r/L)(t+x)}, \\ \Phi_{i,R} &= \Phi_{i,0,R} + \frac{2\pi}{L}(t-x)\bar{b}_{i,0} + \frac{1}{\sqrt{2}}\sum_{r\neq 0} \bar{b}_{i,r} e^{-(2\pi i r/L)(t-x)}, \end{aligned} \tag{4.69}$$

where $b_{1,0} = \frac{1}{\sqrt{2}}(a_{1,0,L} + a_{2,0,L})$, $\bar{b}_{1,0} = \frac{1}{\sqrt{2}}(a_{1,0,R} - a_{2,0,R})$, $b_{2,0} = \frac{1}{\sqrt{2}}(a_{1,0,L} - a_{2,0,L})$ and $\bar{b}_{2,0} = -\frac{1}{\sqrt{2}}(a_{1,0,R} + a_{2,0,R})$. The oscillator modes $b_{i,r}$ for the redefined bosons can be written in terms of mode operators in the original basis based on Eq. (4.68).

The redefined mode operators satisfy the following commutation relation:

$$[b_{i,m}, b_{j,n}] = m\delta_{m+n,0}\delta_{ij}, \tag{4.70}$$

and there is a similar relation for the right-moving mode operators.

Hence the symmetry invariant Ishibashi states corresponding to gapping vectors $\mathbf{l}_1$ and $\mathbf{l}_2$ can now be written in terms of symmetric bosons $\Phi_{i,L} + \Phi_{i,R}$,

$$|\mathbf{v}_i\rangle\!\rangle_n = e^{-\sum_{r>0}(1/r)b_{i,-r}\bar{b}_{i,-r}}|b_{i,0} = -\bar{b}_{i,0} = n\rangle. \tag{4.71}$$

We note that these Ishibashi states which are essentially Neumann states for Φ_i are manifestly symmetric as the bosons $\Phi_{i,L} + \Phi_{i,R}$ are symmetric. The Cardy state constructed from the Ishibashi states is

$$|B, \{\alpha_i\}\rangle = \left(\frac{1}{2^{1/4}}\sum_{n_1\in\mathbb{Z}} e^{in_1\alpha_1}|\mathbf{v}_1\rangle\!\rangle_{n_1}\right) \otimes \left(\frac{1}{2^{1/4}}\sum_{n_2\in\mathbb{Z}} e^{in_2\alpha_2}|\mathbf{v}_2\rangle\!\rangle_{n_2}\right). \tag{4.72}$$

To show that this satisfies the Cardy condition, we first compute the amplitude. The closed sector Hamiltonian factorizes in b^i basis as

$$H_{\rm c} = \sum_{i=1,2}\left[\frac{1}{2}(b^i_0)^2 + \sum_{r>0} b^i_{-r}b^i_r + \sum_{r>0}\bar{b}^i_{-r}\bar{b}^i_r - \frac{c+\bar{c}}{24}\right]. \tag{4.73}$$

Note that this Hamiltonian is not the physical Hamiltonian that we started with for the boson system with boundaries, but the Hamiltonian obtained after we perform the S-transformation between space and time. The amplitude decomposes as

$$\mathcal{A} = \langle B, \{\alpha_i\}|q^{H_{\rm c}}|B, \{\alpha_i\}\rangle = \otimes_{i=1,2}\left[\langle B, \alpha_i|q^{H^i}|B, \alpha_i\rangle\right], \tag{4.74}$$

where $q = \exp(-2\pi L)$ and we have used the decomposition of the Hamiltonian. Both the decomposed parts give rise to the following modular function [149]:

$$\langle B, \alpha_i|q^{H^i}|B, \alpha_i\rangle = \frac{1}{\mathcal{N}_N^2}\frac{1}{\eta(2iL)}, \tag{4.75}$$

which transforms to the open channel partition function under modular S transformation and hence satisfies the Cardy condition. The subscript "N" stands for Neumann boundary conditions.

4.4.6 Generalization to $\mathbb{Z}_N$ cases

The discussion on $\mathbb{Z}_2$ symmetric bosonic SPT phases can be generalized to case of $\mathbb{Z}_N$ symmetry. As before [41] the edge of a $\mathbb{Z}_N$ symmetric SPT is described by a K-matrix Luttinger liquid with $K = \sigma^x$ in Eq. (4.31). The symmetry acts as

$$\hat{g} : \begin{pmatrix} \phi_1 \\ \phi_2 \end{pmatrix} \to \begin{pmatrix} \phi_1 \\ \phi_2 \end{pmatrix} + \frac{2\pi}{N} \begin{pmatrix} 1 \\ q \end{pmatrix}, \tag{4.76}$$

where $\hat{g}$ is the generator of $\mathbb{Z}_N$ group. When $q = 0$, this corresponds to a trivial SPT phase and $q = 1, \ldots, N-1$ corresponds to nontrivial SPT phases. In analogy to the analysis for the $\mathbb{Z}_2$ case, one cannot find a symmetric gapping vector when $q \neq 0$. This further implies the inability to find a symmetry invariant Cardy state. However, N copies of a nontrivial $\mathbb{Z}_N$ SPT phase can be deformed to a trivial phase, hence we expect to construct a symmetric boundary state for this enlarged theory.

We consider $K = \oplus_{i=1}^{N} \sigma^x$, namely, N copies of non-chiral bosons. In this case, the $\mathbb{Z}_N$ symmetry transformation is simply copies of the above transformation, namely

$$\hat{g} : \begin{pmatrix} \phi_i^1 \\ \phi_i^2 \end{pmatrix} \to \begin{pmatrix} \phi_i^1 \\ \phi_i^2 \end{pmatrix} + \frac{2\pi}{N} \begin{pmatrix} 1 \\ q \end{pmatrix}, \quad i = 1, \ldots, N. \tag{4.77}$$

To completely gap out the system, we need N $\mathbf{l}$ vectors that satisfy

$$\begin{aligned} &\mathbf{l}_i^T K^{-1} \mathbf{l}_j = 0, \\ &\hat{g}\, \mathbf{l}_i^T \phi\, \hat{g}^{-1} = \mathbf{l}_i^T \phi \bmod 2\pi \quad \forall i, j. \end{aligned} \tag{4.78}$$

Equation (4.78) is equivalent to

$$\begin{aligned} &\sum_{\alpha=1}^{N} \left(l_i^{2\alpha} l_j^{2\alpha-1} + l_i^{2\alpha-1} l_j^{2\alpha} \right) = 0, \\ &\sum_{\alpha=1}^{N} l_i^{2\alpha-1} + q l_i^{2\alpha} = 0 \bmod N \quad \forall i, j. \end{aligned} \tag{4.79}$$

Here we choose a simple set of $\mathbf{l}$ vectors,

$$\begin{aligned}\{\mathbf{l}\} : \mathbf{l}_1 &= (1,0,1,0,\cdots,1,0)^T \\ \mathbf{l}_2 &= (0,1,0,-1,0,0,\cdots,0,0)^T \\ \mathbf{l}_3 &= (0,0,0,1,0,-1,0,0,\cdots,0,0)^T \\ &\vdots \\ \mathbf{l}_N &= (0,0,\cdots,0,1,0,-1)^T. \end{aligned} \tag{4.80}$$

We can check that in this set, the $\mathbf{l}$ vectors are linearly independent. Then following what is done from Eq. (4.67), we can write down the gapping potential term

$$\begin{aligned}\mathcal{L}^{\{\mathbf{l}\}}_{gapping} &= \lambda_1 \cos\left(\phi^1_1 + \phi^1_3 + \cdots + \phi^1_N + \alpha_1\right) + \cdots \\ &= \lambda_1 \cos\left(\Phi_1 + \alpha_1\right) + \cdots,\end{aligned}$$

where the redefinitions are

$$\begin{aligned}\Phi_1 &= \frac{1}{\sqrt{N}}\left(\phi^1_1 + \phi^1_3 + \cdots + \phi^1_N\right) \\ \Phi_2 &= \frac{1}{\sqrt{2}}\left(\phi^2_1 - \phi^2_2\right) \\ &\vdots \\ \Phi_N &= \frac{1}{\sqrt{2}}\left(\phi^2_{N-1} - \phi^2_N\right),\end{aligned} \tag{4.81}$$

based on the gapping vectors in Eq. (4.80). Then the Φ_i fields can be expanded in terms of b fields like those in Eq. (4.69). Then the analysis of Cardy states and the amplitude between boundary states follow that of the $\mathbb{Z}_2$ case.

We work in the "Φ_i-bosonic" basis. In this basis, the Ishibashi states are taken as Neumann free boson states and are manifestly $\mathbb{Z}_N$ symmetric. They take the form

$$|\mathbf{v}_i\rangle\rangle_n = \frac{1}{\mathcal{N}^i_N} \exp\left\{-\sum_{r>0}\frac{1}{r} b_{i,-r}\bar{b}_{i,-r}\right\} |b_{i,0} = -\bar{b}_{i,0} = n\rangle, \tag{4.82}$$

where $b_{i,r}$ and $\bar{b}_{i,r}$ are left and right mode operators corresponding to the boson Φ_i and $b_{i,0}$,$\bar{b}_{i,0}$ are defined

similarly as those in Eq. (4.71). The Cardy state for Φ_i takes the form

$$|B,\alpha_i\rangle = \frac{1}{2^{1/4}}\sum_{n\in\mathbb{Z}} e^{in\alpha_i}|\mathbf{v}_i\rangle\!\rangle_n. \tag{4.83}$$

The complete boundary state is a tensor product of individual boundary states corresponding to vectors in $\{\mathbb{1}\}$,

$$|B,\{\alpha_i\}\rangle = \otimes_{i=1}^{N}|B,\alpha_i\rangle. \tag{4.84}$$

4.4.7 General symmetry groups

Finally, let us consider a more generic symmetry group G acting on the boson fields:

$$\hat{g}:\varphi\to U_g\varphi+\delta\varphi^g,\quad \forall g\in G. \tag{4.85}$$

The mode operators transform under $g\in G$ as

$$\hat{g}: a_r\to U_g a_r,\quad \varphi_0\to U_g\varphi_0+\delta\varphi^g. \tag{4.86}$$

In this case, we need to consider both the zero mode part and the oscillator part in Eq. (4.55). In the previous discussion, we had $U_g=\mathbb{I}$. Thus we could focus on the zero mode part, namely, the gapping potential of Eq. (4.55). To simplify the discussion, we take one copy of compactified boson fields. In this case, $\eta=\sigma^z$ and the mass matrix coupling the left and right moving mode operators can be taken as $M=\sigma^x$ from Eq. (4.48). Then the invariance of the Hamiltonian or the action of the theory gives the constraints

$$U_g^TU_g=\mathbb{I}_2,\quad U_g^T\sigma^zU_g=\pm\sigma^z. \tag{4.87}$$

Then we have the following general solutions $U_g=\sigma^x,i\sigma^y,\sigma^z$. When $U_g=\sigma^x$, we have $U_g^TMU_g=M$, which means that the oscillator part in Eq. (4.55) is invariant. However, when $U_g=i\sigma^y$ or σ^z, we have $U_g^TMU_g=-M$, meaning that the oscillator part would flip sign. Physically, it means that the boundary state changes into a Dirichlet boundary state from the Neumann boundary state. It is reminiscent of T duality in string theory. In this case, the zero mode part is usually not invariant. Therefore, for general symmetry groups, we can focus on the zero mode part, which is equivalent to the gapping potential analysis in Ref. [41]. We will have more discussions on duality in Sec. 5.

4.5 (2+1)D topological superconductors

In this section, we study the (2+1)d topological superconductors protected by $\mathbb{Z}_2 \times \mathbb{Z}_2$ symmetry.

From the discussion in the last section, we have seen that the construction of a symmetric boundary state is closely related to finding a gapping potential to gap a given (edge) CFT without spontaneous symmetry breaking. In this section, we show that there is another way to construct a symmetric Cardy boundary state by considering only the fundamental boundary conditions of the free fermions.

An example is the class of $(2+1)d$ topological superconductors protected by a $\mathbb{Z}_2 \times \mathbb{Z}_2$ unitary on-site symmetry. The classification of these topological superconductors is $\mathbb{Z}_8$ [129, 153]. Again, we consider the edge theories, which can be described by the N_f copies of real fermion fields in $1+1$ dimensions. For $N_f = 1$, they are described by the action

$$S = \frac{1}{2\pi} \int d^2x i\bar{\Psi}\gamma^\mu \partial_\mu \Psi \tag{4.88}$$

Upon picking a Clifford basis where $\gamma^0 = \sigma^x$ and $\gamma^1 = i\sigma^y$ and writing $\Psi = (\psi_L, \psi_R)$, one can decompose a Majorana fermion into two Majorana-Weyl fermions. This action is invariant under a $\mathbb{Z}_2 \times \mathbb{Z}_2$ symmetry group that is generated by the fermion number parity for each chirality.

4.5.1 Quantization and boundary states

Due to the fermionic nature of the fields, there are two sectors depending on the periodicity of the fields under rotations by 2π. The real fermion could have Ramond sector (R) or antiperiodic, Neveu-Schwarz (NS) sector, boundary conditions along the spatial direction. For the closed system, the left and right moving fermion fields are decoupled. We can choose boundary conditions independently for them. Therefore, there are four sectors corresponding to the boundary conditions:

$$(L, R) = \text{(R,R),(R,NS),(NS,R),(NS,NS)}. \tag{4.89}$$

The fermionic mode expansion takes the form

$$\begin{aligned} \psi_L(x,t) &= \sqrt{\frac{2\pi}{L}} \sum_r \psi_r e^{-(2\pi i r(t+x)/L)}, \\ \psi_R(x,t) &= \sqrt{\frac{2\pi}{L}} \sum_r \tilde{\psi}_r e^{-(2\pi i r(t-x)/L)}, \end{aligned} \tag{4.90}$$

where the mode operators satisfy $\{\psi_r, \psi_{r'}\} = \delta_{r+r',0}$, $\{\tilde{\psi}_r, \tilde{\psi}_{r'}\} = \delta_{r+r',0}$ and $\{\psi_r, \tilde{\psi}_{r'}\} = 0$ and $r \in \mathbb{Z}(+1/2)$ for the Ramond and Neveu-Schwarz sectors respectively.

Boundary state: By varying the action (4.88) and requiring the boundary variation to vanish, one can read off the suitable boundary conditions to be $\{\psi_L \pm \psi_R\}|_{x=0} = 0$. In order to construct the Cardy state, we rotate the space-time cylinder by $\pi/2$ such that the manifold has a temporal boundary. Upon space-time rotation the boundary conditions transform to $\{\psi_L \pm i\psi_R\}|_{t=0} = 0$ These are the relevant boundary conditions for constructing the Ishibashi and Cardy states. The Ishibashi states satisfy the following gluing conditions:

$$\left(\psi_k + i\eta\tilde{\psi}_{-k}\right)|\eta\rangle\!\rangle = 0, \tag{4.91}$$

where $\eta = \pm 1$. Since this is a free theory, the solutions to the above gluing condition are known. There are two solutions for each η corresponding to the NS-NS and R-R sectors. These Ishibashi states are [148]

$$\begin{aligned}
|\eta\rangle\!\rangle_{NS\text{-}NS} &= e^{-i\eta\sum_{r>0}\psi_{-r}\tilde{\psi}_{-r}}|0\rangle_{NS\text{-}NS}, \\
|\eta\rangle\!\rangle_{R\text{-}R} &= e^{-i\eta\sum_{r>0}\psi_{-r}\tilde{\psi}_{-r}}|\eta\rangle_{R\text{-}R},
\end{aligned} \tag{4.92}$$

where $|0\rangle_{NS-NS}$ and $|\eta\rangle_{R-R}$ denote the nondegenerate vacuum in the NS-NS sector and the degenerate ground state associated with the η boundary condition in the R-R sector, respectively.

Before moving onto the discussion of topological superconductors we note the crucial fact that unless we can construct a Cardy state with only a single boundary condition (namely, $\eta = +1$ or -1) in the NS sector, it is impossible to satisfy the Cardy condition without including both sectors. This can be seen by considering the overlap of real-fermion Ishibashi states [154],

$$\begin{aligned}
{}_{NS}\langle\!\langle\eta|e^{-2\pi L H_c}|\eta\rangle\!\rangle_{NS} &= \frac{\vartheta_3(2iL)}{\eta(2iL)}, \\
{}_{NS}\langle\!\langle\eta|e^{-2\pi L H_c}|-\eta\rangle\!\rangle_{NS} &= \frac{\vartheta_4(2iL)}{\eta(2iL)}, \\
{}_{R}\langle\!\langle\eta|e^{-2\pi L H_c}|\eta\rangle\!\rangle_{R} &= \frac{\vartheta_2(2iL)}{\eta(2iL)}, \\
{}_{R}\langle\!\langle\eta|e^{-2\pi L H_c}|-\eta\rangle\!\rangle_{R} &= 0,
\end{aligned} \tag{4.93}$$

where $\vartheta_{2,3,4}$ are the Jacobi θ functions. Under modular S transformation, these modular functions transform

as

$$\begin{aligned}
\frac{\vartheta_3}{\eta(2iL)} &\xrightarrow{L=1/2t} \frac{\vartheta_3(it)}{\eta(it)}, \\
\frac{\vartheta_4}{\eta(2iL)} &\xrightarrow{L=1/2t} \frac{\vartheta_2(it)}{\eta(it)}, \\
\frac{\vartheta_2}{\eta(2iL)} &\xrightarrow{L=1/2t} \frac{\vartheta_4(it)}{\eta(it)}.
\end{aligned} \tag{4.94}$$

One can see that unless one can construct a Cardy state with a single Ishibashi state (either $\eta = +1$ or -1), the S-transformation mixes the R-R and NS-NS sectors.

We define the fermion number parity operators, $(-1)^F$ and $(-1)^{\tilde{F}}$, for the left and right moving fermions, respectively, which generate $\mathbb{Z}_2 \times \mathbb{Z}_2$ symmetry. By construction, these satisfy the following (anti)commutation relations: $\{(-1)^F, \psi_r\} = \{(-1)^{\tilde{F}}, \tilde{\psi}_r\} = 0$, and $[(-1)^F, \tilde{\psi}_r] = [(-1)^{\tilde{F}}, \psi_r] = 0$.

the NS-NS sector: It is straightforward to check that the $\mathbb{Z}_2 \times \mathbb{Z}_2$ invariant boundary state in the NS-NS sector is

$$|B\rangle_{NS\text{-}NS} = \frac{1}{\sqrt{2}}\big[|+\rangle\!\rangle_{NS\text{-}NS} - |-\rangle\!\rangle_{NS\text{-}NS}\big], \tag{4.95}$$

since we have

$$(-1)^F|\eta\rangle\!\rangle_{NS\text{-}NS} = (-1)^{\tilde{F}}|\eta\rangle\!\rangle_{NS\text{-}NS} = -|-\eta\rangle\!\rangle_{NS\text{-}NS}, \tag{4.96}$$

as the vacuum $|0\rangle_{NS\text{-}NS}$ is the eigenstate of both $(-1)^F$ and $(-1)^{\tilde{F}}$ with the eigenvalue -1. It can be seen that both $\eta = \pm 1$ Ishibashi states are needed to construct a fermion parity invariant boundary state in the NS-NS sector. We need to include the R-R sector in order to construct a symmetric Cardy state.

the R-R sector: The R-R sector is a bit more subtle because of the presence of zero modes. Let us define

$$\Gamma_\pm := \frac{1}{\sqrt{2}}(\psi_0 \pm i\tilde{\psi}_0), \tag{4.97}$$

which satisfies the anticommutation relations $\{\Gamma_+, \Gamma_-\} = 1$ and $\{\Gamma_+, \Gamma_+\} = \{\Gamma_-, \Gamma_-\} = 0$. In terms of the zero mode operators, the fermion parity operators take the following form

$$\begin{aligned}(-1)^F &= \sqrt{2}\psi_0 = \Gamma_+ + \Gamma_-, \\ (-1)^{\tilde{F}} &= i\sqrt{2}\tilde{\psi}_0 = \Gamma_+ - \Gamma_-.\end{aligned} \tag{4.98}$$

The vacuum in the two sectors $\eta = \pm$ can be defined as

$$\begin{aligned}|\eta = +\rangle &= e^{i\Phi_+}|0\rangle, \\ |\eta = -\rangle &= e^{i\Phi_-}\Gamma_-|0\rangle,\end{aligned} \tag{4.99}$$

where $\Phi_\pm$ are arbitrary phase factors.

It can be shown that a fermion parity invariant Ishibashi state does not exist for a single fermion flavor in the R-R sector and consequently we cannot construct a fermion parity invariant boundary state.

4.5.2 Boundary states and the $\mathbb{Z}_8$ classification

Having found out that, for a single copy of fermions, it is not possible to construct a Cardy state that preserves the fermion number parity, we now proceed to analyze multiple copies of real fermions. We will show that for $8n$ copies of fermions, there exists a fermion number parity conserving Cardy state. This implies a $\mathbb{Z}_8$ classification of topological superconductors. This agrees with results in Refs. [153, 129].

The boundary condition for N_f copies of fermions is

$$\psi^M + i\eta\tilde{\psi}^M = 0, \quad M = 1, \ldots, N_f. \tag{4.100}$$

More generally, we may take η^M to be different for different copies. But since later we will take direct a product of Ishibashi states with the same η value, it is always possible to transform such boundary conditions to the identical η case. There could be mixing between different copies, which is the most general case. We do not discuss it here. Since one can already construct an NS-NS Ishibashi state for a single flavor of real fermions, we will focus our discussion on the R-R sector. We follow the convention in Ref. [155].

We first assume that N_f is even, namely, $N_f = 2n, n \in \mathbb{Z}$. It is convenient to define

$$\Gamma^{a\pm} := \frac{1}{\sqrt{2}}(\psi_0^{2a-1} \pm i\psi_0^{2a}), \quad a = 1, \ldots, n, \tag{4.101}$$

which satisfy the algebra $\{\Gamma^{a+}, \Gamma^{b-}\} = \delta^{ab}$, $\{\Gamma^{a+}, \Gamma^{b+}\} = \{\Gamma^{a-}, \Gamma^{b-}\} = 0$. Then the Ishibashi vacua $|\eta\rangle\!\rangle^0_{RR}$ must satisfy

$$(\Gamma^{b-} + i\eta\tilde{\Gamma}^{b-})|\eta\rangle\!\rangle^0_{RR} = 0. \tag{4.102}$$

The solution to this constraint is given by

$$|\eta\rangle\!\rangle^0_{RR} = e^{-i\eta\sum_b \Gamma^{b+}\tilde{\Gamma}^{b-}}|0\rangle_{RR}, \tag{4.103}$$

where the Fock vacuum is defined as $\Gamma^{a-}|0\rangle_{RR} = \tilde{\Gamma}^{a+}|0\rangle_{RR} = 0$. Finally, the Ishibashi state in the R-R sector can be written as

$$|\eta\rangle\!\rangle_{RR} = e^{-i\eta\sum_{r>0}\sum_{M=1}^{N_f}\psi^M_{-r}\tilde{\psi}^M_{-r}}|\eta\rangle\!\rangle^0_{RR}. \tag{4.104}$$

By construction, $(-1)^F$ anticommutes with left-moving fermionic modes, but commutes with all other modes, while $(-1)^{\tilde{F}}$ anticommutes with all right-moving fermionic modes, but commutes with all other modes. From the expressions (4.103) and (4.104), we thus have

$$(-1)^{F(\tilde{F})}|\eta\rangle\!\rangle_{RR} = |-\eta\rangle\!\rangle_{RR}, \tag{4.105}$$

provided $(-1)^F|0\rangle_{RR} = (-1)^{\tilde{F}}|0\rangle_{RR} = |0\rangle_{RR}$. On the other hand, the fermion number parity operators can also be represented, in the space of the ground states in the R-R sector, in terms of the zero mode operators as

$$\begin{aligned}(-1)^F &= \left(\frac{1}{i}\right)^n \prod_{a=1}^{n}\left(1 - 2\Gamma^{a+}\Gamma^{a-}\right), \\ (-1)^{\tilde{F}} &= \left(\frac{1}{i}\right)^n \prod_{a=1}^{n}\left(1 - 2\tilde{\Gamma}^{a+}\tilde{\Gamma}^{a-}\right).\end{aligned} \tag{4.106}$$

Using the above relations, one can show

$$(-1)^F|\eta\rangle\!\rangle^0_{RR} = (-i)^n\,|-\eta\rangle\!\rangle^0_{RR},\ (-1)^{\tilde{F}}|\eta\rangle\!\rangle^0_{RR} = i^n|-\eta\rangle\!\rangle^0_{RR}, \tag{4.107}$$

which implies, as the action of $(-1)^{F(\tilde{F})}$ on the non-zero modes is as before,

$$(-1)^F|\eta\rangle\!\rangle_{RR} = (-i)^n\,|-\eta\rangle\!\rangle_{RR},\ (-1)^{\tilde{F}}|\eta\rangle\!\rangle_{RR} = i^n|-\eta\rangle\!\rangle_{RR}. \tag{4.108}$$

Now, it seems there are two different ways of how $(-1)^{F(\tilde{F})}$ acts on the Ishibashi states, namely, Eqs (4.105) and (4.108). To avoid this ambiguity, we must require $n = 0 \mod 4$ or $N_f = 0 \mod 8$ to have a well-defined fermion number parity for each chirality.

Therefore, the symmetry invariant boundary state in the R-R sector takes the form

$$|B\rangle_{RR} = \frac{1}{\sqrt{2}}\left\{|+\rangle\!\rangle_{RR} + |-\rangle\!\rangle_{RR}\right\}, \quad N_f = 0 \mod 8. \tag{4.109}$$

The total Cardy states are now the combination of both the NS-NS and R-R parts

$$|B\rangle_{\pm} = \frac{1}{\mathcal{N}}\left(|B\rangle_{NSNS} \pm i|B\rangle_{RR}\right), \quad N_f = 0 \mod 8. \tag{4.110}$$

The factor $\pm i$ between the NS-NS and the R-R components are both allowed to satisfy the Cardy condition, which also fixes the normalization factor $\mathcal{N}$.

Finally for odd number of flavors of real fermion, there would always be one singlet, which is not paired up. Thus it is impossible to construct a fermion parity invariant boundary state. Therefore the classification is indeed $\mathbb{Z}_8$.

4.5.3 Boundary conditions, gapping potentials and triality

So far, we have only discussed the transformation of boundary states under symmetry operation. But what would happen to the gapping potential? Is it also invariant under symmetry operation? Here we would like to clarify two points: (1) if we can find a symmetry invariant boundary state, then there should exist a set of boundary conditions that is also invariant under the symmetry transformation; (2) symmetry invariant gapping potentials do not guarantee that the corresponding boundary state is also symmetry invariant.

The case of $N_f = 8$ As we have shown before, for eight copies of Majorana fermions, we can construct a fermion parity invariant boundary state, which also satisfies the Cardy condition. We will now try to identify the corresponding boundary conditions following the triality used in Ref. [156].

The boundary conditions and the fermion representation we are using in the notes are given in the vector representation of SO(8) algebra. For this algebra, we know that it has an important property–the triality.

In the vector representation, we can bosonize the (complex) fermions as

$$\psi_{\alpha j} = e^{-i\phi_{\alpha j}}, \quad \psi^{\dagger \alpha j} = e^{i\phi_{\alpha j}}, \tag{4.111}$$

where $\alpha, j = 1, 2$. Then under the fermion parity operator $(-1)^F$, the boson fields change as

$$(-1)^F \phi_{\alpha j} (-1)^F = \phi_{\alpha j} + \pi. \tag{4.112}$$

Thus for each individual complex fermion, the boundary condition is not invariant under this $\mathbb{Z}_2$ symmetry. Now let us use triality to write the fermions in the spinor (c) representation. In this representation, we use a new set of boson fields to bosonize the (complex) fermions.

$$\begin{aligned}
\phi^{\text{ch}} &= \frac{1}{2} \sum_{\alpha,j=1,2} \phi_{\alpha j}, \\
\phi^{\text{sp}} &= \frac{1}{2} \sum_{\alpha,j=1,2} (\sigma^z)^{\alpha}_{\alpha} \phi_{\alpha j}, \\
\phi^{\text{fl}} &= \frac{1}{2} \sum_{\alpha,j=1,2} (\tau^z)^{j}_{j} \phi_{\alpha j}, \\
\phi^{\text{X}} &= \frac{1}{2} \sum_{\alpha,j=1,2} (\sigma^z)^{\alpha}_{\alpha} \, (\tau^z)^{j}_{j} \phi_{\alpha j}.
\end{aligned} \tag{4.113}$$

In this basis, with the transformation (4.112), we can easily check that

$$(-1)^F \phi^i (-1)^F = \phi^i \mod 2\pi, \quad i = \text{ch,sp,fl,X}. \tag{4.114}$$

A similar analysis can be used for the $(-1)^{\tilde{F}}$ operator. Then, by adding gapping potentials, ϕ^i defined in Eq. (4.113) can be pinned at their ground state values simultaneously. Furthermore, by fermionizing these bosons to define new fermion operators, $C_i, i = \text{ch,sp,fl,X}$ via

$$C_i = e^{-i\phi^i}, \tag{4.115}$$

the boundary conditions can be expressed in terms of C_i, namely,

$$\begin{aligned}
&C_{L,ch} = C_{R,ch}, \quad C_{L,fl} = C_{R,fl}, \\
&C_{L,sp} = -C_{R,sp}, \quad C_{L,X} = C^{\dagger}_{R,X} \quad \text{at the boundary.}
\end{aligned} \tag{4.116}$$

Then it is manifest that these boundary conditions are invariant under the transformations defined in Eq. (4.112).

The case of $N_f = 4$ Let us make the relation between boundary conditions, boundary states and gapping potentials clear. Given a boundary condition, we can obtain a boundary state as the solution to the boundary condition. In this sense, there is a one-to-one correspondence between boundary conditions and boundary states. On the other hand, different gapping potentials can correspond to the same boundary condition. In terms of gapping vectors, it means that primitive and non-primitive lattice vectors can represent the same boundary condition. In this sense, the correspondence between gapping vectors and boundary conditions or boundary states is many to one. Therefore, the symmetry invariance of a specific set of gapping potentials does not imply the symmetry invariance of the boundary condition or the boundary state. Let us take an example to clarify this point. In Ref. [157], the authors show that for two copies of Dirac fermions, which is equivalent to four copies of Majorana fermions, there exists a set of symmetry invariant gapping potential, which is equivalent to the boundary condition. Specifically, in their language of Dirac fermions, the gapping potentials

$$\begin{aligned} V_1 &\propto \psi_{1R}^\dagger \psi_{2R}^\dagger \psi_{2L} \psi_{1L} + \text{H.c.} = \cos\left(2\theta_1 + 2\theta_2\right), \\ V_2 &\propto \psi_{1R}^\dagger \psi_{2L}^\dagger \psi_{1L} \psi_{2R} + \text{H.c.} = \cos\left(2\theta_1 - 2\theta_2\right) \end{aligned} \tag{4.117}$$

are invariant under fermion parity projection. Here $\theta_a = \frac{1}{2}\left(\phi_{a,R} - \phi_{a,L}\right), a = 1, 2$ where $\psi_{a,R}^\dagger \propto e^{i\phi_{a,R}}$ and $\psi_{a,L}^\dagger \propto e^{i\phi_{a,L}}$. However, the $\mathbb{Z}_2 \times \mathbb{Z}_2$ symmetry is spontaneously broken, namely, the single-particle backscattering terms do not have vanishing vacuum expectation values (vev), $\langle \psi_{1R}^\dagger \psi_{1L} \rangle \neq 0$, $\langle \psi_{2R}^\dagger \psi_{2L} \rangle \neq 0$. In their language, the boundary condition corresponds to the vev. Even if the gapping potential is symmetry invariant, the vev is not invariant. This is consistent with our analysis that there is no fermion parity invariant boundary state for four copies of Majorana fermions.

Chapter 5

Conclusions and outlook

In this dissertation, we have discussed some applications of conformal field theories in topological phases of matter.

In Chapter 2, we have constructed new quantum Hall states via coupled wire models. We would like to suggest some possible experimental signatures of such quantum Hall states here. As mentioned, the most evident phenomenological distinction of the E_8, G_2 and F_4 states are modified Wiedemann-Franz laws with distinct c/ν ratios. Their presence in low temperature at filling $\nu = 16$ or 8 could be verified by thermal Hall transport measurements. Similar thermal conductance observations have recently been recently performed for other fractional quantum Hall states [158, 159]. Moreover, all three quantum Hall states proposed in this chapter carry bosonic edge modes that only support even charge gapless quasiparticles. This gives rise to a distinct shot noise signature across a point contact below the energy gap. The anyonic statistics of the Fibonacci excitations in the G_2 and F_4 states can be detected by Fabry-Perot interferometry.

In Chapter 3, we systematically studied Abelian surface topological orders that fall under the ADE classification of simply-laced Lie algebras, as well as their symmetries and dualities properties via coupled wire models. A summary was given in section 3.1 in the introduction. Here, we further elaborate on particular results that were not covered in section 3.1. The SPT/SET surface degrees of freedom were first projected onto an array of wires with alternating propagating directions by a generic symmetry-breaking surface stripe order. These chiral wires were then decomposed and backscattered to neighboring wires, thereby obtaining a finite excitation energy gap. We derived the exactly solvable ground state structures as well as the properties quasiparticle excitations by studying the inter-wire sine-Gordon Hamiltonians of the bosonized variables. Specifically, for the D-series, the antiferromagnetic time-reversal symmetry defined in Ref. [21] was dualized to a particle-hole-like symmetry. For the A-series, the mixing between the $U(1)$

charge and the neutral $SU(N)$ sectors allowed us to construct a theory that supports π-fluxes that mimics a $\mathbb{Z}_2$ orbifold/gauge theory. Throughout the ADE discussions, we noticed that all the current backscattering interactions were self-dual in the sense that their dualized gapping terms had the same form as their original ones, except for the special D-series case of $SO(4)$ which required alternative treatment and was out of the scope of this chapter.

We provides several future directions along the discussion in Chapter 3. (1) Based on the ADE classifications that are explored here as parent states, it is interesting to study the descendant topological states, for instance, E_8 quantum Hall state. [42] (2) Our analysis can be systematically generalized to non-simply-laced affine Lie algebras. There has already been some specific progress in this direction [21, 22]. (3) The general ground state degeneracy (GSD) and modular properties when the model is compactified on a closed surface need to be carefully addressed in future works. This is especially the case for the non-Abelian theories. GSD of orbifold structures that support π-fluxes, similar to those appeared in the A series, should also be explicitly analysed. (4) The duality analysis suggests the coupled wire models are particular exact solvable points that belong in a moduli space of surface states that bridges between different dual phases through phase transitions. It would be interesting to explore these moduli spaces of surface states in a controlled but perhaps non-exactly solvable coupled wire manner. Moreover, it would be interesting to utilize the coupled wire constructions to establish the dualities between non-Abelian gauge theories proposed recently [108, 109]. (5) Topological phases and dualities in $3+1$D systems can also be studied using the coupled wire construction. There have already been several attempts [24, 96, 97] in particular situations, and it would be interesting to perform a systematically exploration that encompasses and classifies phases with similar properties.

In Chapter 4, we have discussed the $(1+1)d$ edge theories of $(2+1)d$ SPT phases from the perspective of boundary CFT. We argue that, if a $(1+1)d$ CFT is realized as an edge theory of a $(2+1)d$ SPT phase, it is not possible to find a Cardy boundary state preserving the symmetry of the SPT phase. And vice versa: when it is not possible to find a symmetry-preserving Cardy boundary state in a $(1+1)d$ CFT, the CFT must be realized as an edge theory of a $(2+1)d$ SPT phase. In short, boundaries of SPT phases are not "edgeable," and, conversely, "nonedgeable" CFTs must be realized as an edge theory of a bulk theory in one higher dimension.

We also observed that the edgeablity condition in CFTs are naturally related to the gappability condition. This can be seen most straightforwardly if one invokes the identification between boundary states and gapped ground states (states obtained from a CFT by adding a massive perturbation). Thus, (in)ability to find a symmetry-preserving boundary state means (in)ability to find a symmetry-preserving gapped state. In turn, this also provides an alternative point of view on the relation between BCFT and the modular invariance. It

should be noted that, in higher-dimensional SPT phases, the gappability condition is replaced by a "weaker" condition; $(2+1)d$ boundaries of $(3+1)d$ nontrivial SPT phases are either ingappable or topologically ordered, if the symmetry of SPT phases is preserved. Nevertheless, the edgeablity condition is still valid even for boundaries of higher-dimensional SPT phases. Thus, the edgeablity condition has some precedence over the gappability condition in general, although they seem equivalent in $(1+1)d$ edges of bulk $(2+1)d$ SPT phases.

In the following, let us make a few more comments before closing.

Symmetry actions on boundary states

First, let us summarize the way symmetries act on boundary states in CFTs. In particular, we contrast physics of $(2+1)d$ and $(1+1)d$ SPT phases. Let us consider a CFT with a global unitary symmetry G (spatial and time-reversal symmetries may be discussed in a similar fashion). We consider conformally invariant boundary states $\{|B_a\rangle\}$ realized in the CFT, where a labels the boundary states. Then, for a symmetry operation $g \in G$, one expects the following possible behaviors of $\{|B_a\rangle\}$ under g: In the first case, the action of g on boundary states is given by

$$g|B_a\rangle_h = \varepsilon_a(g|h)|B_a\rangle_h. \tag{5.1}$$

Here, $|B_a\rangle_h$ is a boundary state in the sector twisted by $h \in G$, and $\varepsilon_a(g|h)$ is a phase factor. namely, boundary states are invariant under the symmetry, up to a phase factor. As claimed in Ref. [137], this case is relevant to the physics of boundaries of $(1+1)d$ SPT phases. In Ref. [137], the correspondence between gapped ground states of $(1+1)d$ SPT phases and boundary states in CFTs was made. These boundary states are anomalous in the sense that when acted with symmetry they give rise to anomalous U(1) phases, Eq. (5.1). Furthermore, the anomalous phase $\varepsilon(g|h)$ is related to the two cocycles in $H^2(G, \mathrm{U}(1))$, which gives the classification of $(1+1)d$ SPT phases protected by G. (These phases, however, only appear in boundary states in twisted sectors, namely, the sectors with twisted boundary conditions by a group element in G.)

On the other hand, there are cases in which a boundary state $|B_a\rangle$ is mapped to another boundary state $|B_{a'}\rangle$, which can be different from the original one:

$$g|B_a\rangle = |B_{a'}\rangle. \tag{5.2}$$

We further distinguish the following two cases: (a) There is a subset of boundary states which are mapped

to themselves for all symmetry operations $g \in G$. (b) None of the boundary states remain invariant under $g \in G$. Case (a) is a typical situation when the $(1+1)d$ CFT can be realized on its own right, without referring to higher-dimensional bulk systems. On the other hand, Case (b) is relevant to $(2+1)d$ SPT phases, as we have discussed for the bulk of the chapter.

Boundary states and locality

In Eq. (5.2), it should be noted that the right-hand side is not given by a superposition of $|B_a\rangle$, but by a single boundary state. In fact, superpositions of $|B_a\rangle$ in general do not satisfy the Cardy condition, and are disqualified as a physical boundary state. [In this respect, the symmetry transformation law in Eq. (5.2) is analogous to anyonic symmetry which acts on $(2+1)d$ topologically ordered phases by permuting anyons.] In the present context, this is in perfect agreement with the standard theory of spontaneous symmetry breaking. When spontaneous symmetry breaking happens, ground states having different expectation values of an order parameter should not be superposed in the thermodynamic limit. (These states are "superselected.") The overlap of these states vanishes in the thermodynamic limit, and hence a given ground state with a definite value of the order parameter cannot be mixed by any physical (local) operation. (However, the overlap between different boundary states may not be zero, and defines the Affleck-Ludwig g function.)

In some sense, one can think of Cardy states setting the notion of locality. It should be noted that there are multiple sets of solution to the Cardy equations, which correspond to different modular invariant bulk partition functions.

Let us further illustrate the notion of locality set by the Cardy states: As we demonstrated through various examples, when none of the boundary states are invariant under symmetry G, the CFT must be realized as an edge theory of a bulk nontrivial SPT phase protected by on-site unitary symmetry G. In the edge theory, the criticality (gapless spectrum) is enforced by the symmetry G. This is quite different from criticalities (conformal field theories) that occur in isolated $(1+1)d$ systems; there are typically perturbations at a critical point which are G symmetric. By perturbing the critical point by such perturbation, it may be possible to flow into a gapped phase where the G symmetry is preserved. This suggests that the symmetry G acting within the edge theory of a nontrivial SPT phase is not an ordinary symmetry. In fact, as noted in Ref. [136], the symmetry G is realized non-locally or as a non-on-site symmetry within the edge theory.

Duality and triality

Another canonical example is provided by the $\mathbb{Z}_2$ symmetric topological superconductor discussed in Sec. 4.5. The edge theory in this case is described by the action (4.88). Here, the $\mathbb{Z}_2$ symmetry flips the sign of

the mass term, and hence enforces the criticality. In the language of the $(1+1)d$ transverse-field quantum Ising model (or the $2d$ Ising model), this is nothing but the Kramers-Wannier duality. It is a non-local operation which exchanges the Ising spin operator σ and the disorder operator μ.

Let us have a look at how this $\mathbb{Z}_2$ symmetry acts on boundary states. In the critical Ising model, there are three physical conformal boundary conditions: the free condition $|f\rangle$, and the fixed ones $|+\rangle$ and $|-\rangle$. The periodic (R) sector contains three scalar fields: the identity, the spin field σ, and the energy density ε, of chiral conformal weight 0, 1/16, and 1/2 respectively. They lead to three Ishibashi states $|0\rangle\!\rangle_{\rm R}$, $|\frac{1}{16}\rangle\!\rangle_{\rm R}$, and $|\frac{1}{2}\rangle\!\rangle_{\rm R}$. The second, antiperiodic (NS) sector contains a single scalar field, the disorder field μ, with the same conformal weight 1/16 as the spin field, and gives rise to one Ishibashi state $|\frac{1}{16}\rangle\!\rangle_{\rm NS}$. The Cardy boundary states are given in terms of these Ishibashi states as

$$
\begin{aligned}
|\pm\rangle &= \frac{1}{\sqrt{2}}\left[|0\rangle\!\rangle_{\rm R} \pm \sqrt{2}^{4}|\frac{1}{16}\rangle\!\rangle_{\rm R} + |\frac{1}{2}\rangle\!\rangle_{\rm R}\right], \\
|f\rangle &= |0\rangle\!\rangle_{\rm R} + \sqrt{2}^{4}|\frac{1}{16}\rangle\!\rangle_{\rm NS} - |\frac{1}{2}\rangle\!\rangle_{\rm R},
\end{aligned}
\tag{5.3}
$$

which, in terms of the Ising spin variables, correspond to the fixed boundary condition with spin pointing up/down at the boundary, and the free boundary condition. The Kramers-Wannier duality exchanges the free boundary condition $|f\rangle$ and one of the fixed boundary conditions ($|+\rangle$). This is so since the duality transformation exchanges σ and μ, and hence the Ishibashi states $|1/16\rangle\!\rangle_{\rm R}$ and $|1/16\rangle\!\rangle_{\rm NS}$. (In fact, Ref. [160] proposed a method to diagnose the existence of the Kramers-Wannier duality, for a given CFT, by using boundary states.)

Let us next consider N_f copies of $(2+1)d$ topological superconductors protected by $\mathbb{Z}_2$ symmetry, as discussed. We will focus on the cases where N_f is even. In these cases, spin operators (analog of σ and μ in the critical Ising model) in the edge theory are given by

$$
\Theta^{\boldsymbol{s}}_R = e^{i\sum_a s_a \phi^a_R}, \quad s_a = \pm\frac{1}{2}
\tag{5.4}
$$

in the bosonized language (in the right-moving sector). These operators are an intertwining (vertex) operator that maps the untwisted sector to the twisted sectors specified by $\boldsymbol{s}$. By state-operator correspondence, these operators are identified with a state in the corresponding twisted sector. (Note that there is ground-state degeneracy for the R sectors.) Thus, we have a set of states $\{|0\rangle_{\rm NS}, |\boldsymbol{s}\rangle_{\rm R}\}$. These states appear when one constructs boundary states, and are exchanged under the action of the unitary $\mathbb{Z}_2$ symmetry. (Here, this is

not the $\mathbb{Z}_2^f$ symmetry.) The spin operators satisfy

$$\Theta_R^{\boldsymbol{s}}(z)\Theta_R^{\boldsymbol{s}'}(w) = e^{2\pi i \boldsymbol{s}\cdot\boldsymbol{s}'\mathrm{sgn}(x-x')}\Theta_R^{\boldsymbol{s}'}(w)\Theta_R^{\boldsymbol{s}}(z), \tag{5.5}$$

where $\boldsymbol{s}\cdot\boldsymbol{s}' = (1/4)\sum_a(\pm 1)$. This phase can be made an integer when the number of complex fermions is a multiple of 4 (namely, the number of real fermions is a multiple of 8, $N_f = 8n$) and if we choose

$$\boldsymbol{s} = (1/2, 1/2, \cdots) \quad \text{or} \quad \boldsymbol{s}' = (-1/2, -1/2, \cdots). \tag{5.6}$$

The unitary $\mathbb{Z}_2$ symmetry can exchange spin operators $\Theta_R^{\boldsymbol{s}}$, as the Kramers-Wannier duality of the critical Ising model exchanges σ and μ. However when $N_f = 8n$, the spin operators are mutually local. Hence in this case, the $\mathbb{Z}_2$ symmetry is not a duality (or non-local) symmetry. Rather, it is a (part of) triality symmetry.

Finally, recall that the presence of boundary breaks the Kramers-Wannier duality. This is another indication that the Kramers-Wannier duality is nonlocal.

Appendix A

Details of Chapter 2

In this appendix, we provide further details about the results quoted in Chapter 2. We start in Section A.1 by detailing the momentum conservation conditions of the backscattering interactions of our E_8 model described in the main text. This assigns the corresponding Fermi momenta $k_{F,a}$ of the 11 electronic channels in each bundle in this phase, importantly fixing the filling fraction of the E_8 quantum Hall state to be $\nu = 16$. In the following Section A.2, we provide the details for extending the E_8 model by decomposing the $(E_8)_1$ current algebra into $(G_2)_1 \times (F_4)_1$, also known as a conformal embedding. With the explicitly built operators, transformations between the original electronic momenta and the G_2 or F_4 currents can be again arranged. With these currents, the coupled-wire model for the G_2 and F_4 Fibonacci phases of the main text can be considered explicitly. The necessary backscattering current interactions again constrain the momentum distributions, as shown in Section A.3; both G_2 and F_4 phases Fibonacci are found to exist at magnetic filling fractions $\nu = 8$. Finally, in Section A.4, we focus on the relationship between Fibonacci topological order and G_2 and F_4 current algebras. Using the bulk-boundary correspondence, this is achieved by presenting the modular content of the chiral $(G_2)_1$ and $(F_4)_1$ WZW edge CFTs. Finally, we finish by exploring the relationship between the G_2 and F_4 groups and Fibonacci anyons, illustrating also their irreducible transformation properties as fundamental representations of their corresponding Lie algebras.

A.1 E8 Quantum Hall state and momentum commensurability conditions

We explore in more details the properties of the emergent E_8 WZW current algebra at level 1 in each of the 11-wire bundle. The E_8 currents were introduced in the main text using the unimodular matrix U defined

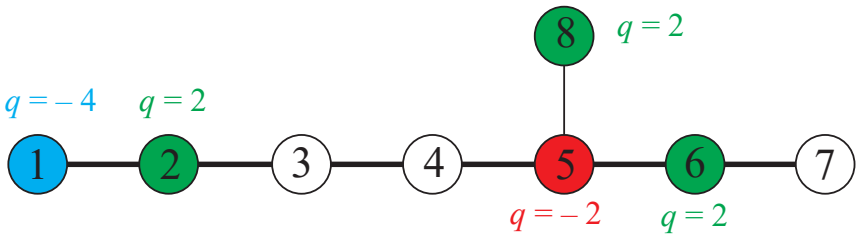

Figure A.1: The Dynkin diagram of E_8 and the charge assignment q (in units of e) of the simple roots $(E_{E_8})^{\sigma}_{y\boldsymbol{\alpha}_I}$, for $I = 1, \ldots, 8$. Uncolored entries are electrically neutral.

in (2.6) and (2.5). The bosonized variables Φ^{σ}_{ya} of the electron operators (2.1) are related to the $\tilde{\Phi}^{\sigma}_{yI}$ of the E_8 simple roots operators (2.3) by the linear transformation $\tilde{\Phi}^{\sigma}_{yI} = U^{\sigma\sigma'}_{Ia}\Phi^{\sigma'}_{ya}$. This transformation induces a linear mapping between the associated charges and momenta of the fundamental electrons and of the E_8 simple roots, given by

$$\tilde{q}^{\sigma}_{I} = U^{\sigma\sigma'}_{Ia} q^{\sigma'}_{a}, \quad \tilde{k}^{\sigma}_{yI} = U^{\sigma\sigma'}_{Ia} k^{\sigma'}_{ya}. \tag{A.1}$$

For instance, the electric charge assignments q_I of the 8 simple roots in the Dynkin diagram in Fig A.1 can be derived using the above formula by substituting the unit electric charge $q^{\sigma'}_{a} = 1$ for all electronic channels.

As mentioned in the main text, a principal step in building the coupled wire model relies in demanding commensurability conditions in the intra- and inter-bundle backscattering interactions (2.9) and (2.10). This requirement takes the form of 11 vanishing (mod 2π) linear equations for the 11 unknown momenta, with coefficients that are also linear in the inverse of the filling fraction ν; these equations are given by

$$\left(U^{++}_{I,a} - U^{+-}_{I,a}\right)\left(k^{R}_{ya} - k^{L}_{y+1a}\right) = 0 \;\; I = 1, ..., 8 \tag{A.2}$$

$$\left(U^{++}_{I,a} - U^{+-}_{I,a}\right)\left(k^{R}_{ya} - k^{L}_{ya}\right) = 0 \quad I = 9, 10, 11. \tag{A.3}$$

From the Fermi momenta $k^{\sigma}_{ya} = (eB/\hbar c)\mathrm{y} + \sigma k_{F,a}$ of the 11 electronic channels (see Eq. (2.7)), one sees that the magnetic filling fraction appears only in the E_8 inter-bundle terms. Equating the determinant of this linear system to zero, so that a non-trivial solution to $k_{F,a}$ exist, we fully fix the filling ν as

$$\frac{2048(\nu - 16)}{\nu} = 0 \implies \nu = 16. \tag{A.4}$$

This result could have been alternatively obtained from a corresponding effective Chern-Simons field theory,

which determines $\nu = \tilde{\mathbf{q}}^T (K^{E_8})^{-1} \tilde{\mathbf{q}} = 16$, where the charge assignments $\tilde{\mathbf{q}} = (-4, 2, 0, 0, -2, 2, 0, 2)$ were given in Fig. A.1, for both chiralities, and where K^{E_8} is the Cartan matrix of E_8. Enforcing this filling fraction, the momentum commensurability condition has a unique solution (up to a single free Fermi-momentum parameter k_F). The momenta of the 11 bare electrons are given by

$$k^\sigma_{y,1} = k^\sigma_{y,2} = \frac{1}{2} y k_F,\ k^\sigma_{y,3} = k^\sigma_{y,7} = \frac{1}{2}(y - \sigma) k_F, \tag{A.5}$$

$$k^\sigma_{y,4} = k^\sigma_{y,5} = k^\sigma_{y,6} = k^\sigma_{y,8} = k^\sigma_{y,9} = \frac{1}{2}(y + 2\sigma) k_F, \tag{A.6}$$

$$k^\sigma_{y,10} = \frac{1}{2}(y + 3\sigma) k_F,\ k^\sigma_{y,11} = \frac{1}{2}(y - 3\sigma) k_F. \tag{A.7}$$

With these, the $\sigma = L$ and R channels of any of the three recombined fermions f^σ_{yn}, for $n = 1, 2, 3$, share the same momentum, and therefore the oscillatory terms in the intra-bundle backscattering interactions (2.9) cancel. Similarly, the inter-bundle terms in (2.10) also conserve momentum, as $\tilde{k}^R_{y,I} = \tilde{k}^L_{y+1,I}$ for $I = 1, \ldots, 8$.

A.2 A G2 x F4 conformal embedding into E8

A.2.1 From E_8 to $SO(16)$

The exceptional E_8 Lie algebra has dimension 248, which separates into 8 Cartan generators and 240 roots in the root lattice Δ_{E_8}. The Cartan generators are mutually commuting operators while the roots are raising and lowering operators of the "spin" eigenvalues. Here, we present a full bosonized description of the E_8 WZW current algebra at level 1 based on the 8 aforementioned simple roots in (2.3) and relate this description to an SO(16) embedding. This will later facilitate the $G_2 \times F_4 \subseteq E_8$ embedding.

We begin by *fermionizing* the 8 simple roots operators. This expresses each E_8 root as either a pair or a half-integral combination of a set of 8 *non-local* Dirac fermions $d^\sigma_{yI} \sim \exp\left[i(\phi^\sigma_{yI}(\mathsf{x}) + k^\sigma_{yI}\mathsf{x})\right]$. The bosonized variables and momenta are related to that of the 8 simple roots by

$$\tilde{\Phi}^\sigma_{yI} = R^{I'}_I \phi^\sigma_{yI'}, \quad \tilde{k}^\sigma_{yI} = R^{I'}_I k^\sigma_{yI'}, \tag{A.8}$$

where the 8×8 R matrix is

$$R=\begin{pmatrix} 1 & -1 & & & & & & \\ & 1 & -1 & & & & & \\ & & 1 & -1 & & & & \\ & & & 1 & -1 & & & \\ & & & & 1 & -1 & & \\ & & & & & 1 & 1 & \\ -\frac{1}{2} & -\frac{1}{2} & -\frac{1}{2} & -\frac{1}{2} & -\frac{1}{2} & -\frac{1}{2} & -\frac{1}{2} & -\frac{1}{2} \\ & & & & & 1 & -1 & \end{pmatrix} \tag{A.9}$$

The lines of the R matrix form a set of primitive basis vectors that are commonly adopted to generate the E_8 root lattice in $\mathbb{R}^8$.

The R-matrix decomposes the Cartan matrix K^{E_8} of E_8 into $K^{E_8}=RR^T$. Consequently, under the transformation (A.8), the equal-time commutation relation (2.4) becomes $\left[\partial_{\mathsf{x}}\phi^{\sigma}_{yI}(\mathsf{x}),\phi^{\sigma'}_{y'I'}(\mathsf{x}')\right]=2\pi i\sigma\delta^{\sigma\sigma'}\delta_{II'}\delta_{yy'}\delta(\mathsf{x}-\mathsf{x}')$. This ensures the vertex operators $d^{\sigma}_{yI}\sim\exp\left[i(\phi^{\sigma}_{yI}(\mathsf{x})+k^{\sigma}_{yI}\mathsf{x})\right]$ to represent spin 1/2 Dirac fermions. As we argue next, these fermions do not associate to natural excitations in the bulk or the edge of the quantum Hall states. Inverting the matrix (A.9) and multiplying by our original unimodular transformation U, one sees that all ϕ^{σ}_{yI} expressed in terms of the original electronic bosonized variables Φ^{σ}_{ya} involve half-integral coefficients. The non-locality is also revealed by their even charge assignments $q=0,\pm 2$. The pair creation of such non-local Dirac fermions requires a linearly divergent energy in the coupled wire model and, as a result, these fermions do not arise as deconfined bulk excitations or gapless edge primary field. They should only be treated as artificial fields introduced to describe the WZW current algebra. Henceforth, where it leads to no confusion, we are suppressing the σ,y indices for conciseness.

By decomposing the 8 Dirac fermions into 16 Majorana fermions as $d_I=(\psi_{2I-1}+i\psi_{2I})/\sqrt{2}$, the E_8 WZW current algebra can be related to an $SO(16)_1$ WZW current algebra. In terms of root systems, Δ_{E_8} is shown to be an extension of $\Delta_{SO(16)}$, as follows. The root lattice of $SO(16)_1$, $\Delta_{SO(16)}$, contains $2^2\times C_2^8=112$ elements, with C_n^k being the binomial coefficient. The elements are given by bosonic spin 1 fermion pairs $d_I^{\pm}d_{I'}^{\pm}\sim e^{i(\pm\phi_I\pm\phi_{I'})}$, where $1\le I<I'\le 8$. Besides the root system of $SO(16)_1$, to generate the root system of Δ_{E_8}we include the SO(16) $128=2^7$ even spinors. The even spinors can be represented by bosonic spin 1 half-integral combinations $d_I^{\epsilon^I/2}\sim e^{i\epsilon^I\phi_I/2}$, where $\epsilon^I=\pm 1$ and $\prod_{I=1}^{8}\epsilon^I=+1$. By combining the even spinors with root lattice of $SO(16)$, the $112+128=240$ roots of E_8 can be represented by the vertex operators

$$[E_{E_8}]^{\sigma}_{y\boldsymbol{\alpha}}\sim\exp\left[i\alpha^I(\phi^{\sigma}_{yI}(\mathsf{x})+k^{\sigma}_{yI}\mathsf{x})\right]=\exp\left[i\alpha^I(R^{-1})^{I'}_{I}U^{\sigma\sigma'}_{I'a}(\Phi^{\sigma'}_{ya}(\mathsf{x})+k^{\sigma'}_{ya}\mathsf{x})\right], \tag{A.10}$$

where the root vectors $\boldsymbol{\alpha} = (\alpha^1, \ldots, \alpha^8)$ are

$$\Delta_{E_8} = \left\{\boldsymbol{\alpha} \in \mathbb{Z}^8 : |\boldsymbol{\alpha}|^2 = 2\right\} \cup \left\{\boldsymbol{\alpha} = \frac{\boldsymbol{\epsilon}}{2} : \epsilon^I = \pm 1, \prod_{I=1}^{8} \epsilon^8 = 1\right\}. \tag{A.11}$$

Each root vector $\boldsymbol{\alpha}$ can be expressed as a linear combination $\alpha^J = a^I R_I^J$, with the R matrix given in (A.9) and a^I integer coefficients, which are the entries of the root vectors in the Chevalley basis. This integer combination ensures that every E_8 root operator in (A.11) is an integral combination of local electrons (2.1). Since each of these vertex operators is a spin-1 boson, it must be an even product of electron operators and therefore must carry an even electric charge.

The fermionization of the E_8 presented above allows us to represent each and every E_8 root using a vertex operator $[E_{E_8}]^\sigma_{y\boldsymbol{\alpha}} \sim \exp\left[i\alpha^I(\phi^\sigma_{yI} + k^\sigma_{yI}\mathsf{x})\right]$ (see (A.10)), where $d^\sigma_{yI} \sim \exp\left[i(\phi^\sigma_{yI} + k^\sigma_{yI}\mathsf{x})\right]$ are 8 non-local Dirac fermions and $\boldsymbol{\alpha}$ are Cartan-Weyl root vectors in Δ_{E_8} (recall (A.8) and (A.11)). To complete the algebra structure, the 8 Cartan generators of E_8, which are identical to the Cartan generators of $SO(16)$, are given by the number density operators $[H_{E_8}]^\sigma_{yI} \sim i\partial\phi^\sigma_{yI} \sim (d^\sigma_{yI})^\dagger d^\sigma_{yI}$. This also allows an explicit conformal embedding of the G_2 and F_4 WZW CFTs in the E_8 theory at level 1.

A.2.2 From $SO\,(16)$ to $G_2 \times F_4$

The embedding $(G_2)_1 \times (F_4)_1 \subseteq (E_8)_1$ can be intuitively understood as follows. First, $G_2 \subseteq SO\,(7) \subseteq SO\,(16) \subseteq E_8$. By decomposing the Dirac fermions into Majorana components $d_I = (\psi_{2I-1} + i\psi_{2I})/\sqrt{2}$, the $SO(16)_1$ currents are bilinear combinations of the 16 Majorana fermions. The $(G_2)_1$ current operators have free field representations using $\psi_1, ..., \psi_7$, which generate the $SO(7)_1$. Second, $SO(9) \subseteq F_4 \subseteq E_8$. The root system of F_4 composes of (i) the 24 (long) roots, (ii) the 8 vectors, and (iii) the 16 (even and odd) spinors of $SO(8)$, all of which act on $\psi_9, ..., \psi_{16}$. As we will see, accompanying the $SO(8)$ vectors with the remaining Majorana ψ_8 in $SO(9)$ and the $SO(8)$ spinors with two special emergent fermions, we are able to to embed the F_4 currents in E_8 in a way that is fully decoupled from G_2. To abridge, G_2 is a bit smaller than $SO(7)$ while F_4 is a bit bigger than $SO(9)$, and the two WZW algebras at level 1 completely decomposes $(E_8)_1$.

To construct the embedding explicitly, we start by representing the SO(7) Kac-Moody currents with Majorana fermions as $J^a_{SO(7)} = -i : \psi_i \Lambda^a_{ij} \psi_j : /2$, where Λ^a are generators of the SO(7) Lie algebra. We introduce the complex fermion combinations and bosonized representations, $c_j = (\psi_{2j-1} + i\psi_{2j})/\sqrt{2} = e^{i\phi^j}$ where the bosons obey

$$\left\langle \phi^j(z)\, \phi^{j'}(w) \right\rangle = -\delta^{jj'} \log(z-w) + \frac{i\pi}{2} \mathrm{sgn}\,(j-j'), \tag{A.12}$$

with the sgn accounting for mutual fermionic exchange statistics. We then follow reference [161] to embed G_2 generators into $SO(7)$. The resulting Cartan generators $H^{1,2}_{G_2}$ of G_2 are

$$H^1_{G_2}(z) = i\sqrt{\frac{1}{6}}\left(-2\partial\phi^1 + \partial\phi^2 + \partial\phi^3\right), \quad H^2_{G_2}(z) = i\sqrt{\frac{1}{2}}\left(\partial\phi^2 - \partial\phi^3\right). \tag{A.13}$$

while the positive long roots are

$$E^1_{G_2}(z) = -e^{i(\phi_2-\phi_3)}, \quad E^2_{G_2}(z) = -e^{i(\phi_3-\phi_1)}, \quad E^3_{G_2}(z) = -e^{i(\phi_2-\phi_1)}. \tag{A.14}$$

To bosonize the positive short roots, we need $\psi_7 = \left(e^{i\phi_4} + e^{-i\phi_4}\right)/\sqrt{2}$, yielding

$$\begin{aligned}
E^4_{G_2}(z) &= \frac{1}{\sqrt{3}}\left[-e^{-i(\phi_1+\phi_2)} - i\left(e^{i(\phi_3+\phi_4)} - e^{i(\phi_3-\phi_4)}\right)\right], \\
E^5_{G_2}(z) &= \frac{1}{\sqrt{3}}\left[-e^{-i(\phi_1+\phi_3)} + i\left(e^{i(\phi_2+\phi_4)} - e^{i(\phi_2-\phi_4)}\right)\right], \\
E^6_{G_2}(z) &= \frac{1}{\sqrt{3}}\left[-e^{i(\phi_2+\phi_3)} - i\left(e^{-i(\phi_1-\phi_4)} - e^{-i(\phi_1+\phi_4)}\right)\right].
\end{aligned} \tag{A.15}$$

The negative roots can be obtained by simple Hermitian conjugation.

Now we move on to F_4. Our goal is to define the F_4 currents in terms of $SO(16)$ degrees of freedom in a way that the operators decoupled from G_2, in the OPE sense. Since we used the $SO(7)$ part, generated by fermions $\psi_{1,\ldots,7}$ to define the G_2 operators, we may facilitate the decoupling of the currents by using the remaining $SO(8)$ subalgebra, generated by $\psi_{9,\ldots,16}$. This is achieved by carefully sewing F_4 into the full degrees of freedom of $SO(16)$. The Cartan generators can be chosen to be the ones in the $SO(8)$ subalgebra

$$H^a_{F_4}(z) = i\partial\phi_{4+a}, \ a = 1, \ldots, 4. \tag{A.16}$$

The group F_4 has 48 roots, 24 short and 24 long. The 24 long roots are identical to those of $SO(8)$, and may be written in bosonized form as

$$E^{\boldsymbol{\alpha}}_{F_4}(z) = e^{i\boldsymbol{\alpha}\cdot\boldsymbol{\phi}}, \tag{A.17}$$

where $\alpha_1 = \ldots = \alpha_4 = 0$ and $(\alpha_5, \ldots, \alpha_8) \in \mathbb{Z}^4 | \, |(\alpha_5, \ldots, \alpha_8)|^2 = 2$. The 24 short roots of F_4 correspond to 8 vector and 16 spinor representations of $SO(8)$. To write the 8 vector roots, we increment the vertex operators with fermion ψ_8, obtaining

$$E^{\pm a}_{F_4} \sim \psi_8 e^{\pm i\phi_{4+a}} \sim \frac{1}{\sqrt{2}}\left(e^{i(\phi_4 \pm \phi_{4+a})} + e^{i(-\phi_4 \pm \phi_{4+a})}\right). \tag{A.18}$$

Finally, the 16 spinors read

$$E_{F_4}^{\mathbf{s}_\pm} \sim \psi_\pm e^{i\mathbf{s}_\pm\cdot\boldsymbol{\phi}/2}, \tag{A.19}$$

where the spinor labels are $\mathbf{s}_\pm = (0,0,0,0,s_5,s_6,s_7,s_8)$ with $s_5s_6s_7s_8 = \pm 1$; the critical step here lies in the inclusion of the Majorana fermions

$$\psi_+ = \frac{1}{\sqrt{2}}\left(\omega_+ e^{i(\phi_1+\phi_2+\phi_3+\phi_4)/2} + h.c.\right), \quad \psi_- = \frac{1}{\sqrt{2}}\left(\omega_- e^{i(\phi_1+\phi_2+\phi_3-\phi_4)/2} + h.c.\right) \tag{A.20}$$

where $\omega_\pm$ are $U(1)$ phases to be determined. Combining the vertices with the fermions,

$$E_{F_4}^{\mathbf{s}_+} \sim \frac{1}{\sqrt{2}}\left(\omega_+ e^{i(\phi_1+\phi_2+\phi_3+\phi_4+\mathbf{s}_+\cdot\boldsymbol{\phi})/2} + \omega_+^* e^{i(-\phi_1-\phi_2-\phi_3-\phi_4+\mathbf{s}_+\cdot\boldsymbol{\phi})/2}\right), \tag{A.21}$$

$$E_{F_4}^{\mathbf{s}_-} \sim \frac{i}{\sqrt{2}}\left(\omega_- e^{i(\phi_1+\phi_2+\phi_3-\phi_4+\mathbf{s}_-\cdot\boldsymbol{\phi})/2} - \omega_-^* e^{i(-\phi_1-\phi_2-\phi_3+\phi_4+\mathbf{s}_-\cdot\boldsymbol{\phi})/2}\right). \tag{A.22}$$

Our goal is to decouple the G_2 and F_4 currents in the SO(16) embedding. Computing the OPEs between all G_2 and F_4 operators, one recognizes that singular terms only arise between G_2 short roots and F_4 short roots from $SO(8)$ spinors. These singular terms, however, can be made to vanish with an appropriate choice of $\omega_\pm$ following

$$\omega_+ + e^{-i\pi/4}\omega_+^* = \omega_- - e^{-i\pi/4}\omega_-^* = 0. \tag{A.23}$$

Distinct solutions only differ by a sign, which can be absorbed in the Majorana fermion $\psi_\pm$. We pick

$$\omega_+ = e^{i3\pi/8}, \quad \omega_- = e^{-i\pi/8}. \tag{A.24}$$

This completes the proof that the G_2 and F_4 embeddings decouple and act on distinct Hilbert spaces.

As a non-trivial check of the conformal embedding, one may compute the energy-momentum tensors, seeing that the E_8 tensor decouples identically into those of G_2 and F_4 under the construction above. By definition, WZW energy momentum tensors at level 1 read [54]

$$T(z) = \frac{(\mathbf{J}\cdot\mathbf{J})(z)}{2(1+g)}, \tag{A.25}$$

with J^a a Sugawara current, g dual coxeter number, and the normal ordering defined as

$$(J^aJ^a)(z) = \frac{1}{2\pi i}\oint_z \frac{dw}{w-z} J^a(w)\,J^a(z). \tag{A.26}$$

The contraction of the Sugawara currents can be written in the Cartan-Weyl basis

$$(\mathbf{J}\cdot\mathbf{J})(z)=\sum_j\left(H^jH^j\right)(z)+\sum_{\boldsymbol{\alpha}}\left(E^{-\boldsymbol{\alpha}}E^{\boldsymbol{\alpha}}\right)(z)\,, \tag{A.27}$$

where the $\boldsymbol{\alpha}$ sum is over the full root lattice, while j sums over the generators of the Cartan subalgebra. We have absorbed the normalization factors into the root operators.

We are then ready to verify the energy-momentum tensor decoupling via the conformal embedding. Under the $SO(16)$ embedding, the E_8 tensor reduces to

$$T_{E_8}(z)=-\frac{\partial\boldsymbol{\phi}\cdot\partial\boldsymbol{\phi}}{2}, \tag{A.28}$$

which is, in fact, of the same form of the $SO(16)$ energy-momentum tensor.

To fully verify the conformal embedding, one may compute the energy momentum tensors of the G_2 and F_4 CFTs. This calculation requires lengthy but straightforward bookkeeping, and will not be presented in here. The operators T_{G_2} and T_{F_4} are found to be

$$\begin{aligned}T_{G_2}(z)=&-\frac{1}{2}\left[\left(\sum_{j=1}^{3}\partial\phi_j\partial\phi_j\right)(z)-\frac{1}{5}\left(\sum_{j=1}^{3}\partial\phi_j\right)^2(z)\right]-\frac{1}{5}\left(\partial\phi_4\partial\phi_4\right)(z)\\&+\frac{2}{5}\left\{\cos\left[2\left(\frac{\pi}{8}-\phi_+(z)\right)\right]-\cos\left[2\left(\frac{\pi}{8}-\phi_-(z)\right)\right]+\cos\left[2\phi_4(z)\right]\right\},\end{aligned} \tag{A.29}$$

and

$$\begin{aligned}T_{F_4}(z)=&-\frac{1}{2}\left[\sum_{j=5}^{8}\left(\partial\phi_j\partial\phi_j\right)(z)+\frac{1}{5}\left(\sum_{j=1}^{3}\partial\phi_j\right)^2(z)\right]-\frac{3}{10}\left(\partial\phi_4\partial\phi_4\right)(z)\\&-\frac{2}{5}\left\{\cos\left[2\left(\frac{\pi}{8}-\phi_+(z)\right)\right]-\cos\left[2\left(\frac{\pi}{8}-\phi_-(z)\right)\right]+\cos\left[2\phi_4(z)\right]\right\},\end{aligned} \tag{A.30}$$

where $\phi_\pm\equiv\phi_1+\phi_2+\phi_3\pm\phi_4$. The sum of these two expressions returns T_{E_8}, as it should, finishing the verification of the conformal embedding.

A.3 G2 and F4 quantum Hall states momentum commensurability conditions

To stabilize the G_2 and F_4 Fibonacci phases, a process of fixing a distribution of Fermi momenta for the 11 electronic channels (2.1) in the coupled wire model is necessary. This is analogous to the one used for the E_8 Quantum Hall state. Applying the process for the F_4 Fibonacci phase, i.e. demanding commensurability conditions on the momenta so that oscillatory terms cancel from interactions in (2.13), results in the unique non-trivial solution (up to the single free parameter k_F)

$$\begin{aligned} k^{\sigma}_{y,1} = k^{\sigma}_{y,2} = k^{\sigma}_{y,7} = (y-\sigma)\,k_F,\ k^{\sigma}_{y,3} = (y-2\sigma)\,k_F, \\ k^{\sigma}_{y,4} = k^{\sigma}_{y,5} = k^{\sigma}_{y,6} = k^{\sigma}_{y,8} = k^{\sigma}_{y,9} = (y+2\sigma)\,k_F, \\ k^{\sigma}_{y,10} = (y+3\sigma)\,k_F,\ k^{\sigma}_{y,11} = (y-4\sigma)\,k_F,\ \nu = 8. \end{aligned} \tag{A.31}$$

Similarly, demanding momentum commensurability in (2.14), one obtain the Fermi momentum distribution for the coupled wire model for the G_2 Fibonacci quantum Hall state.

$$\begin{aligned} k^{\sigma}_{y,1} = k^{\sigma}_{y,2} = k^{\sigma}_{y,3} = k^{\sigma}_{y,11} = (\sigma+y)\,k_F, \\ k^{\sigma}_{y,4} = k^{\sigma}_{y,5} = k^{\sigma}_{y,6} = k^{\sigma}_{y,7} = k^{\sigma}_{y,8} = k^{\sigma}_{y,9} = k^{\sigma}_{y,10} = yk_F,\ \nu = 8. \end{aligned} \tag{A.32}$$

A.4 Fibonacci primary field representations in the G2 and F4 WZW CFTs at level 1

Our prime motivation for studying $(G_2)_1$ and $(F_4)_1$ WZW theories stems from the claim that both carry excitations in the form of Fibonacci anyons. Here we will provide a short demonstration of that, and then follow with a coset construction that allows us to profit from the embeddings discussed up to now to explicitly build the corresponding Fibonacci primary fields.

To see that the only excitations in $(G_2)_1$ and $(F_4)_1$ are Fibonacci anyons, we can start by noticing that at level 1, these theories contain only 1 non-trivial primary field besides the vacuum $\mathbb{I}$. We name these fields τ for $(G_2)_1$ and $\bar{\tau}$ for $(F_4)_1$. Following, we invoke the Gauss-Milgram formula; this formula is an avatar of the bulk-boundary correspondence. It connects quantities that point to the bulk anyon excitations of a topological phase to the CFT degrees of freedom that live at its boundary. Stating the formula explicitly,

we have

$$\sum_a d_a^2 \theta_a = \mathcal{D} e^{i2\pi \frac{c}{8}}, \tag{A.33}$$

where $\mathcal{D}^2 \equiv \sum_a d_a^2$ is the total quantum order and d_a are called quantum dimensions, quantities that characterize bulk anyons, while $\theta_a = e^{i2\pi h_a}$ are conformal spins, determined quantum dimentions h_a, and c is the chiral central charge; the latter two quantities characterize the CFT at the edge of the topological phase. The sum is over all primary fields of the CFT or, correspondingly, all anyons. By definition $d_{\mathbb{I}} = 1$ and $h_{\mathbb{I}} = 0$. Furthermore, the conformal dimension of a primary field a of a WZW theory is completely determined by its Lie algebra content by $h_a = \frac{C_a}{2(k+g)}$, [54] where k is the level, g is the dual coxeter number and C_τ is the quadratic Casimir of the representation. Collecting these numbers, $h_\tau = 2/5$ and $h_{\bar{\tau}} = 3/5$, leaving a single unknown in the Gauss-Milgram formula, namely d_τ or $d_{\bar{\tau}}$ for G_2 or F_4. Solving for these,

$$d_\tau = d_{\bar{\tau}} = \frac{1+\sqrt{5}}{2}, \tag{A.34}$$

which is the Golden ratio expected for Fibonacci anyons. Since the quantum dimensions obey a algebraic version of the fusion rulesy, these follow imediately as $\tau \times \tau = \mathbb{I} + \tau$. Equivalently, the fusion rules can be explicitly determined by the modular (2×2) S-matrices of the theory using the Verlinde formula.

We thus established that the chiral $(G_2)_1$ and $(F_4)_1$ WZW edge CFTs contain primary fields that obey the Fibonacci fusion rules. They correspond to Fibonacci anyonic excitations in the 2D bulk, and thus we refer to them as Fibonacci primary fields. Let us now construct explicit expressions for them based on our conformal embedding here developed.

The non-trivial primary fields $[\tau]$ and $[\bar{\tau}]$ are associated with the fundamental irreducible representations of their respective exceptional Lie algebras. Each of them consists of a super-selection sector of fields, $[\tau] = \text{span}\{\tau_m\}_{m=1,\dots,7}$ and $[\bar{\tau}] = \text{span}\{\bar{\tau}_l\}_{l=1,\dots,26}$, that rotate into each other by the WZW algebraic actions

$$[E_{G_2}(\mathsf{z})]_{\boldsymbol{\gamma}}\, \tau_m(\mathsf{w}) = \frac{1}{\mathsf{z}-\mathsf{w}} \rho_{G_2}(\boldsymbol{\gamma})_m^{m'} \tau_{m'}(\mathsf{w}) + \dots, \quad [E_{F_4}(\mathsf{z})]_{\boldsymbol{\beta}}\, \bar{\tau}_l(\mathsf{w}) = \frac{1}{\mathsf{z}-\mathsf{w}} \rho_{F_4}(\boldsymbol{\beta})_l^{l'} \bar{\tau}_{l'}(\mathsf{w}) + \dots, \tag{A.35}$$

where $\mathsf{z}, \mathsf{w} \sim e^{\tau + i\mathsf{x}}$ are radially ordered holomorphic space-time parameters, $\boldsymbol{\gamma}$ and $\boldsymbol{\beta}$ are the roots of G_2 and F_4, and ρ_{G_2} and ρ_{F_4} are the 7- and 26-dimensional irreducible matrix representation of the G_2 and F_4 algebras. Here, we provide a parafermionic representations of these fields that constitute the Fibonacci super-sectors. Using the coset construction, each Fibonacci field τ_m, $\bar{\tau}_l$ can be expressed as a product of two components: (1) a non-Abelian primary field of the $\mathbb{Z}_3$ parafermion CFT or the tricritical Ising CFT,

respectively, and (2) a vertex operator of bosonized variables.

The $(G_2)_1$ WZW CFT can be decomposed into two decoupled sectors using its $SU(3)_1$ sub-algebra.

$$(G_2)_1 \simeq SU(3)_1 \times \frac{(G_2)_1}{SU(3)_1} = SU(3)_1 \times \mathbb{Z}_3 \text{ parafermion.} \tag{A.36}$$

For instance, the decomposition agrees with the partition of the energy-momentum tensors $T_{\mathbb{Z}_3} = T_{(G_2)_1/SU(3)_1} \equiv T_{(G_2)_1} - T_{SU(3)_1}$ and central charges $c((G_2)_1) = 14/5 = c(SU(3)_1) + c(\mathbb{Z}_3) = 2 + 4/5$. First, we focus on the $SU(3)_1$ sub-algebra. Using the aforementioned fermionization of E_8, the six roots of $SU(3)$ coincide with the long roots of G_2, $e^{\pm i(\phi_1-\phi_2)}$, $e^{\pm i(\phi_2-\phi_3)}$, $e^{\pm i(\phi_1-\phi_3)}$. The $SU(3)_1$ WZW sub-algebra has three primary fields, $\mathbb{I}$, $[\mathcal{E}]$ and $[\mathcal{E}^{-1}]$, with conformal dimensions $h_{\mathbb{I}} = 0$ and $h_{\mathcal{E}} = h_{\mathcal{E}^{-1}} = 1/3$. $\mathbb{I}$ denotes the trivial vacuum, while $[\mathcal{E}]$ and $[\mathcal{E}^{-1}]$ are three-dimensional super-selection sectors of fields

$$\begin{aligned}
[\mathcal{E}] &= \text{span}\left\{e^{i(\phi_1+\phi_2-2\phi_3)/3}, e^{i(\phi_2+\phi_3-2\phi_1)/3}, e^{i(\phi_3+\phi_1-2\phi_2)/3}\right\}, \\
[\mathcal{E}^{-1}] &= \text{span}\left\{e^{-i(\phi_1+\phi_2-2\phi_3)/3}, e^{-i(\phi_2+\phi_3-2\phi_1)/3}, e^{-i(\phi_3+\phi_1-2\phi_2)/3}\right\},
\end{aligned} \tag{A.37}$$

that rotate according to the two fundamental representations of $SU(3)$. For example, under the $SU(3)_1$ roots,

$$e^{i[\phi_a(\mathsf{z})-\phi_b(\mathsf{z})]} e^{i[\phi_b(\mathsf{w})+\phi_c(\mathsf{w})-2\phi_a(\mathsf{w})]} \sim e^{i[\phi_a(\mathsf{w})+\phi_c(\mathsf{w})-2\phi_b(\mathsf{w})]}/(\mathsf{z}-\mathsf{w}) + \dots . \tag{A.38}$$

The 7-dimensional fundamental representation of G_2 decomposes into $1 + 3 + 3$ under $SU(3)$ and each component is associated to a distinct $SU(3)_1$ primary field.

Next, we focus on the $(G_2)_1/SU(3)_1$ coset, which is identical to the $\mathbb{Z}_3$ parafermionic CFT. It supports three Abelian primary fields $\mathbb{I}, \Psi, \Psi^{-1}$ and three non-Abelian ones $\tau, \varepsilon, \varepsilon^{-1}$. They have conformal dimensions $h_{\mathbb{I}} = 0$, $h_\Psi = h_{\Psi^{-1}} = 2/3$, $h_\tau = 2/5$ and $h_\varepsilon = h_{\varepsilon^{-1}} = 1/15$. They obey the fusion rules

$$\Psi \times \Psi = \Psi^{-1},\ \Psi \times \Psi^{-1} = \mathbb{I},\ \tau \times \Psi = \varepsilon,\ \tau \times \Psi^{-1} = \varepsilon^{-1},\ \tau \times \tau = \mathbb{I} + \tau. \tag{A.39}$$

The Fibonacci primary field of $(G_2)_1$ is the 7-dimensional super-selection sector

$$\begin{aligned}
[\tau] &= (\tau \otimes \mathbb{I}) \oplus (\varepsilon \otimes [\mathcal{E}]) \oplus (\varepsilon^{-1} \otimes [\mathcal{E}^{-1}]) \\
&= \text{span}\left\{ \begin{array}{c} \tau, \varepsilon e^{i(\phi_1+\phi_2-2\phi_3)3}, \varepsilon e^{i(\phi_2+\phi_3-2\phi_1)/3}, \varepsilon e^{i(\phi_3+\phi_1-2\phi_2)/3}, \\ \varepsilon^{-1} e^{-i(\phi_1+\phi_2-2\phi_3)/3}, \varepsilon^{-1} e^{-i(\phi_2+\phi_3-2\phi_1)/3}, \varepsilon^{-1} e^{-i(\phi_3+\phi_1-2\phi_2)/3} \end{array} \right\}
\end{aligned} \tag{A.40}$$

All seven fields share the same conformal dimension $h_\tau = 2/5$. For example, $h_{\varepsilon\otimes[\mathcal{E}]} = 1/15+1/3 = 2/5$. The super-sector splits into three components under $SU(3)$. However, they rotate irreducibly into each other under G_2.

The Fibonacci primary field of $(F_4)_1$ can be described in a similar manner. First, using the $SO(9)_1$ sub-algebra, the WZW CFT can be factored into two decoupled sectors

$$(F_4)_1 \simeq SO(9)_1 \times \frac{(F_4)_1}{SO(9)_1} = SO(9)_1 \times (\text{tricritical Ising}). \tag{A.41}$$

Like the previous G_2 coset decomposition, here the energy-momentum tensor and central charge also decompose accordingly: $c((F_4)_1) = 26/5 = 9/2 + 7/10$, where $9/2$ and $7/10$ are the central charges for $SO(9)_1$ and the tricritical Ising CFTs. The Fibonacci super-selection sector of $(F_4)_1$ consists of fields, which are linear combinations of products of primary fields in $SO(9)_1$ and the tricritical Ising CFTs.

We first concentrate on $SO(9)_1$. It supports three primary fields $\mathbb{I}$, $[\psi]$ and $[\Sigma]$ with conformal dimensions $h_{\mathbb{I}} = 0$, $h_\psi = 1/2$ and $h_\Sigma = 9/16$ and respectively associate to the trivial, vector and spinor representations of $SO(9)$. Using the fermionization convention of E_8, the $SO(9)_1$ theory is generated by the 9 Majorana fermions $\psi_8, \ldots, \psi_{16}$, where the last 8 Majorana fermions are paired into the 4 Dirac fermions $d_I = (\psi_{2I-1} + i\psi_{2I})/\sqrt{2} \sim e^{i\phi_I}$, for $I = 5, 6, 7, 8$. The vector primary field consists of any linear combinations of these 9 fermions $[\psi] = \text{span}\{\psi_8, \ldots, \psi_{16}\}$. We arbitrarily single out the first Majorana fermion ψ_8, which is not paired with any of the others, and associate it to an Ising CFT. This further decomposes

$$SO(9)_1 = \text{Ising} \times SO(8)_1. \tag{A.42}$$

The spinor primary field of $SO(9)_1$ decomposes into a product between the Ising twist field σ and the $SO(8)_1$ spinors.

$$[\Sigma] = \text{span}\left\{\sigma \exp\left(\frac{i}{2}\sum_{I=5}^{8}\epsilon^I\phi_I\right) : \epsilon^5, \ldots, \epsilon^8 = \pm 1\right\}. \tag{A.43}$$

The conformal dimension of σ is $1/16$ and that of the $SO(8)_1$ spinors are $1/2$. Thus, they combine to the appropriate conformal dimension of $h_\Sigma = 9/16$ for each field in the set. The dimension of the $SO(9)$ spinor representation is $2^4 = 16$. The 26-dimensional fundamental representation of F_4 decomposes into $1 + 9 + 16$ under the $SO(9)$ sub-algebra, and each component is associated to a unique $SO(9)_1$ primary field.

We now focus on the $(F_4)_1/SO(9)_1$ coset, which is identical to the tricritical Ising CFT, or equivalently,

the minimal theory $\mathcal{M}(5,4)$. The theory has six primary fields arranged in the following conformal grid

$$\begin{array}{|c|c|c|} \hline f & s & \mathbb{I} \\ \hline \bar{\tau} & s\bar{\tau} & f\bar{\tau} \\ \hline f\bar{\tau} & s\bar{\tau} & \bar{\tau} \\ \hline \mathbb{I} & s & f \\ \hline \end{array} = \begin{array}{|c|c|c|} \hline \Phi_{3,1} & \Phi_{2,1} & \Phi_{1,1} \\ \hline \Phi_{3,2} & \Phi_{2,2} & \Phi_{1,2} \\ \hline \Phi_{1,2} & \Phi_{2,2} & \Phi_{3,2} \\ \hline \Phi_{1,1} & \Phi_{2,1} & \Phi_{3,1} \\ \hline \end{array} \xrightarrow{\text{conformal dimensions}} \begin{array}{|c|c|c|} \hline 3/2 & 7/16 & 0 \\ \hline 3/5 & 3/80 & 1/10 \\ \hline 1/10 & 3/80 & 3/5 \\ \hline 0 & 7/16 & 3/2 \\ \hline \end{array} \tag{A.44}$$

They obey the fusion rules

$$f \times f = \mathbb{I},\ s \times f = s,\ s \times s = 1 + f, f \times \bar{\tau} = f\bar{\tau},\ s \times \bar{\tau} = s\bar{\tau},\ \bar{\tau} \times \bar{\tau} = \mathbb{I} + \bar{\tau}. \tag{A.45}$$

The Fibonacci primary field of $(F_4)_1$ is the 26-dimensional super-selection sector

$$\begin{aligned} [\bar{\tau}] &= (\bar{\tau} \otimes \mathbb{I}) \oplus (f\bar{\tau} \otimes [\psi]) \oplus (s\bar{\tau} \otimes [\Sigma]) \\ &= \text{span} \left\{ \bar{\tau}, f\bar{\tau}\psi_j, s\bar{\tau}\sigma \exp\left(\frac{i}{2} \sum_{I=5}^{8} \epsilon^I \phi_I \right) : \begin{array}{l} j = 8, \ldots, 16 \\ \epsilon^5, \ldots, \epsilon^8 = \pm 1 \end{array} \right\}. \end{aligned} \tag{A.46}$$

Each of these fields carry the identical conformal dimension $h_{\bar{\tau}} = 3/5$. For example, the second field $f\bar{\tau}[\psi]$ has the combined conformal dimension $1/10 + 1/2 = 3/5$, and the third $s\bar{\tau}[\Sigma]$ has $3/80 + 9/16 = 3/5$. Although the super-sector splits into three under $SO(9)_1$, it is irreducible under $(F_4)_1$.

Appendix B

Details of Chapter 3

B.1 Gapping conditions for K-matrix formalism

B.1.1 Gapping terms for the general K-matrix theory

We briefly review the gapping condition and the gapping term for the general K-matrix theory. Assume we have two effective Lagrangians on the boundary of a (2+1)d system:

$$\begin{aligned}\mathcal{L}_L &= -\frac{1}{4\pi}K^L_{IJ}\partial_t\phi^L_I\partial_x\phi^L_J + V^L_{IJ}\partial_x\phi^L_I\partial_x\phi^L_J,\\ \mathcal{L}_R &= \frac{1}{4\pi}K^R_{IJ}\partial_t\phi^R_I\partial_x\phi^R_J + V^R_{IJ}\partial_x\phi^R_I\partial_x\phi^R_J,\end{aligned} \tag{B.1}$$

where K^R and K^L have the same dimension N and signature, and V^R and V^L are some symmetric non-universal potentials. Define $\mathsf{K} \equiv K^R \oplus (-K^L)$. The completely gapping condition or Haldane's nullity condition [112] is that there exists N 2N-component linearly independent integer vectors $\boldsymbol{\ell}_i = (\boldsymbol{\ell}^R_i, \boldsymbol{\ell}^L_i)^T$, called null vectors, satisfying

$$\boldsymbol{\ell}_i^T\mathsf{K}\boldsymbol{\ell}_j = 0, \quad i,j = 1,\ldots,N. \tag{B.2}$$

Then the whole gapping term is written as

$$\mathcal{H}_{gapping} = \sum_{i=1}^{N} C_i \cos\left(\boldsymbol{\ell}_i^T\mathsf{K}\boldsymbol{\Phi} + \alpha_i\right), \tag{B.3}$$

where $\boldsymbol{\Phi} = (\boldsymbol{\phi}^R, \boldsymbol{\phi}^L)^T$ and α_i are some undetermined variables, which can be fixed by the specific theory.

Actually if we only impose that we can pin the gapping terms simultaneously to their minima, we only need $\boldsymbol{n}_i^T \mathsf{K}^{-1} \boldsymbol{n}_j = 0$ for $i, j = 1, \ldots, N$, where $\boldsymbol{n}_i$ are integer vectors. However, if we further require that the gapping terms are composed of local operators, we need $\boldsymbol{n}_i = \mathsf{K}\boldsymbol{\ell}_i$, which gives Eq.(B.2).

One corollary is that when $K^R = K^L$, then we can always choose $\mathbf{l}_i^R = \mathbf{l}_i^L$ to gap out the whole system, as long as there are enough linearly independent N-component integer vectors $\mathbf{l}_i^R$.

B.1.2 Gapping conditions in different basis

For a general K-matrix theory with simply-laced algebra, we can write the kinetic term in two equivalent ways

$$\mathcal{L}_0 = \frac{1}{4\pi} \int dxdt \; K_{IJ} \partial_x \phi'^I \partial_t \phi'^J, \tag{B.4}$$

with the canonical quantization

$$[\phi'^I(x), \partial_{x'} \phi'^J(x')] = 2\pi i K^{-1}_{IJ} (x - x'). \tag{B.5}$$

We can choose simple roots for the current algebra α_I such that $\alpha_I \cdot \alpha_J = K_{IJ}$. We denote

$$R = \begin{pmatrix} - - - - & \alpha_1 & - - - - \\ & \vdots & \\ - - - - & \alpha_r & - - - - \end{pmatrix} \tag{B.6}$$

as the matrix formed by these simple roots, where r is the rank of the Lie algebra. Then we have $RR^T = K$. Now we make a basis transformation

$$\phi^I = \sum_J R_{JI} \phi'^J. \tag{B.7}$$

Then we can check that Eq. (B.5) becomes

$$[\phi^I(x), \partial_{x'} \phi^J(x')] = 2\pi i \delta^{IJ} \delta(x - x'), \tag{B.8}$$

where we have used $R^T K^{-1} R = 1$, which is obvious. If $\boldsymbol{\ell}^i = (\boldsymbol{\ell}^i_R, \boldsymbol{\ell}^i_L)$ is a set of $2r$-component Haldane null vectors, they should satisfy the nullity condition

$$(\boldsymbol{\ell}^i)^T \mathsf{K} \boldsymbol{\ell}^j = 0, \quad \forall i, j = 1, \ldots, r, \tag{B.9}$$

in the ϕ'^I basis, where $\mathsf{K} = K \oplus (-K)$, or

$$\boldsymbol{\ell}^i_R \cdot \boldsymbol{\ell}^j_R - \boldsymbol{\ell}^i_L \cdot \boldsymbol{\ell}^j_L = 0, \quad \forall i, j = 1, \ldots, r, \tag{B.10}$$

in the ϕ^I basis.

B.2 Simply-laced Lie algebras and their representations

We review the simpled-laced Lie algebras, namely, *ADE* classifications, and their representations here. [54] "Simply-laced" means that all roots $\boldsymbol{\alpha}$ of the corresponding algebras have identical length, which are usually normalized to be $|\boldsymbol{\alpha}| = \sqrt{2}$. Let r be the rank of an algebra G, namely, the maximal number of mutually commuting generators of G. Then in *Cartan-Weyl* basis, we have

$$\begin{aligned}
\left[H^i, E^{\boldsymbol{\alpha}}\right] &= \alpha^i E^{\boldsymbol{\alpha}}, \\
\left[E^{\boldsymbol{\alpha}}, E^{-\boldsymbol{\alpha}}\right] &= \frac{2}{|\boldsymbol{\alpha}|^2} \sum_{i=1}^{r} \alpha^i H^i = \sum_{i=1}^{r} \alpha^i H^i, \\
\left[E^{\boldsymbol{\alpha}}, E^{\boldsymbol{\beta}}\right] &\propto \begin{cases} E^{\boldsymbol{\alpha}+\boldsymbol{\beta}} & \text{if } \boldsymbol{\alpha}+\boldsymbol{\beta} \in \Delta, \\ 0 & \text{otherwise} \end{cases} \qquad \text{for } \boldsymbol{\alpha} \neq \boldsymbol{\beta}.
\end{aligned} \tag{B.11}$$

All roots of G can be obtained from r simple roots $\boldsymbol{\alpha}_1, \ldots, \boldsymbol{\alpha}_r$ by linear combinations. The choice of simple roots is not unique. For $SU(r+1)$ algebras, it can be chosen as

$$\boldsymbol{\alpha}_I = \mathbf{e}_I - \mathbf{e}_{I+1}, \quad I = 1, \ldots, r, \tag{B.12}$$

where $\boldsymbol{e}_I$ are unit basis vectors of $\mathbb{R}^{r+1}$. For $SO(2r)$ algebras, it can be chosen as

$$\boldsymbol{\alpha} = \begin{cases} \mathbf{e}_I - \mathbf{e}_{I+1} & \text{for } I = 1, \ldots, r-1, \\ \mathbf{e}_{r-1} + \mathbf{e}_r & \text{for } I = r, \end{cases} \tag{B.13}$$

where $\boldsymbol{e}_I$ are unit basis vectors of $\mathbb{R}^r$. For E-series, simple roots are usually taken at one's convenience. We have shown some particular choices in the main text.

The fundamental representation t^a of $SU(r+1)$ algebra have properties

$$\begin{aligned} \mathrm{Tr}(t^a t^b) &= \delta^{ab}, \\ \sum_a t^a_{ij} t^a_{kl} &= \delta_{il}\delta_{jk} - \frac{1}{r+1}\delta_{ij}\delta_{kl}, \\ \sum_{a,b} f_{abc} f_{abd} &= 2(r+1)\delta_{cd}, \end{aligned} \tag{B.14}$$

where f_{abc} are the structure constants of the $SU(r+1)$ algebra. The vector representation of $SO(2r)$ Lie algebra has an explicit matrix representation

$$t^a_{ij} \equiv t^{rs}_{ij} = i(\delta^r_i \delta^s_j - \delta^r_j \delta^s_i), \quad 1 \le r < s \le 2r,$$

$$\mathrm{Tr}(t^a t^b) = 2\delta_{ab}, \tag{B.15}$$

$$\sum_a t^a_{ij} t^a_{kl} = 2(-\delta_{ik}\delta_{jl} + \delta_{il}\delta_{jk}), \tag{B.16}$$

and the structure constant can be written as

$$\begin{aligned} f_{abc} \equiv f_{(rs)(pq)(mn)} = &(\delta_{rm}\delta_{nq}\delta_{sp} - \delta_{ms}\delta_{nq}\delta_{rp}) \\ &+ (\delta_{mp}\delta_{sq}\delta_{nr} - \delta_{np}\delta_{sq}\delta_{rm}) \\ &+ (\delta_{pr}\delta_{ns}\delta_{mq} - \delta_{rq}\delta_{ns}\delta_{mp}). \end{aligned} \tag{B.17}$$

The Cartan matrix K of the algebra G is an $r \times r$ matrix defined by

$$K_{IJ} = \frac{2\boldsymbol{\alpha}_I^T \boldsymbol{\alpha}_J}{|\boldsymbol{\alpha}_J|^2} = \sum_{i=1}^{r} \frac{2\alpha^i{}_I \alpha^i{}_J}{|\boldsymbol{\alpha}_J|^2} = \sum_{i=1}^{r} \alpha^i{}_I \alpha^i{}_J. \tag{B.18}$$

It is easy to see that the Cartan matrix for simply-laced algebras are symmetric. Cartan matrices for simply-laced algebras are listed below.

$$K_{SU(r+1)} = \begin{pmatrix} 2 & -1 & 0 & \cdots & 0 & 0 \\ -1 & 2 & -1 & \cdots & 0 & 0 \\ 0 & -1 & 2 & \cdots & 0 & 0 \\ \vdots & \vdots & \vdots & \ddots & \vdots & \vdots \\ 0 & 0 & 0 & \cdots & 2 & -1 \\ 0 & 0 & 0 & \cdots & -1 & 2 \end{pmatrix}, \; K_{SO(2r)} = \begin{pmatrix} 2 & -1 & 0 & \cdots 0 & 0 & 0 \\ -1 & 2 & -1 & \cdots 0 & 0 & 0 \\ 0 & -1 & 2 & \cdots 0 & 0 & 0 \\ \vdots & \vdots & \vdots & \ddots & \vdots & \vdots \\ 0 & 0 & 0 & \cdots 2 & -1 & -1 \\ 0 & 0 & 0 & \cdots -1 & 2 & 0 \\ 0 & 0 & 0 & \cdots -1 & 0 & 2 \end{pmatrix}, \quad (r \geq 4),$$

$$K_{E_8} = \begin{pmatrix} 2 & -1 & 0 & 0 & 0 & 0 & 0 & 0 \\ -1 & 2 & -1 & 0 & 0 & 0 & 0 & 0 \\ 0 & -1 & 2 & -1 & 0 & 0 & 0 & 0 \\ 0 & 0 & -1 & 2 & -1 & 0 & 0 & 0 \\ 0 & 0 & 0 & -1 & 2 & -1 & 0 & -1 \\ 0 & 0 & 0 & 0 & -1 & 2 & -1 & 0 \\ 0 & 0 & 0 & 0 & 0 & -1 & 2 & 0 \\ 0 & 0 & 0 & 0 & -1 & 0 & 0 & 2 \end{pmatrix}, \; K_{E_7} = \begin{pmatrix} 2 & -1 & 0 & 0 & 0 & 0 & 0 \\ -1 & 2 & -1 & 0 & 0 & 0 & 0 \\ 0 & -1 & 2 & -1 & 0 & 0 & 0 \\ 0 & 0 & -1 & 2 & -1 & 0 & -1 \\ 0 & 0 & 0 & -1 & 2 & -1 & 0 \\ 0 & 0 & 0 & 0 & -1 & 2 & 0 \\ 0 & 0 & 0 & -1 & 0 & 0 & 2 \end{pmatrix},$$

$$K_{E_6} = \begin{pmatrix} 2 & -1 & 0 & 0 & 0 & 0 \\ -1 & 2 & -1 & 0 & 0 & 0 \\ 0 & -1 & 2 & -1 & 0 & -1 \\ 0 & 0 & -1 & 2 & -1 & 0 \\ 0 & 0 & 0 & -1 & 2 & 0 \\ 0 & 0 & -1 & 0 & 0 & 2 \end{pmatrix}. \tag{B.19}$$

Sometimes it is convenient to use *Chevalley* basis as it is directly related to the Cartan matrix:

$$h^I = \frac{2}{|\boldsymbol{\alpha}_I|^2} \sum_{i=1}^{r} \alpha^i{}_I H^i = \sum_{i=1}^{r} \alpha^i{}_I H^i, \tag{B.20}$$

with the commutation relations

$$\left[h^I, E^{\pm \boldsymbol{\alpha}_J}\right] = \pm K_{IJ} E^{\pm \boldsymbol{\alpha}_J}, \quad \left[E^{\boldsymbol{\alpha}_J}, E^{-\boldsymbol{\alpha}_J}\right] = \delta^{IJ} h^J. \tag{B.21}$$

In Chapter 3, we are focused on the level-1 algebras of ADE classifications, in which there exist free

field representations. To be specific, $SO(2r)_1$ algebras (D-series), can be constructed by $2r$ independent Majorana fermions ψ^i with operator product expansions (OPEs)

$$\psi_i(z)\psi_j(w) \sim \frac{\delta_{ij}}{z-w}, \quad i,j = 1,\ldots,2r. \tag{B.22}$$

The current operators can be constructed with these free Majorana fermions as

$$J^a(z) = \frac{1}{2}\sum_{i,j}(\psi_i t^a_{ij}\psi_j)(z), \tag{B.23}$$

where normal ordering is assumed. One can check that these currents satisfy the current algebra

$$J^a(z)J^b(w) \sim \frac{k\delta_{ab}}{(z-w)^w} + \sum_c \frac{if_{abc}J^c(w)}{(z-w)}, \tag{B.24}$$

where f_{abc} are called structure constants.

For $SU(r+1)_1$ algebras (A-series), we can use r independent free bosons ϕ^i with OPEs

$$\phi^i(z)\phi^j(w) \sim -\delta_{ij}\ln(z-w), \quad i,j = 1,\ldots,r. \tag{B.25}$$

The currents in Cartan-Weyl basis can be constructed as

$$\begin{aligned} H^j(z) &= i\partial\phi^j(z), \\ E^{\boldsymbol{\alpha}}(z) &= c_{\boldsymbol{\alpha}} e^{i\boldsymbol{\alpha}\cdot\boldsymbol{\phi}(z)}, \end{aligned} \tag{B.26}$$

where $c_{\boldsymbol{\alpha}}$ is a correction factor ensuring the correct OPEs. This bosonic construction also works for D-series if we pair up Majorana fermions and then bosonize them.

For $(E_8)_1$ algebras (E-series), we can follow the same construction as in A-series with 8 independent free bosons to construct the currents, with the vector and spinor representations of $SO(16)$ algebra introduced in the main text. E_7 and E_6 algebras can be constructed from the corresponding conformal embeddings, respectively.

References

[1] M. E. Cage, R. F. Dziuba, and B. F. Field. A test of the quantum hall effect as a resistance standard. *IEEE Transactions on Instrumentation and Measurement*, IM-34(2):301–303, June 1985.

[2] W. Pan, H. L. Stormer, D. C. Tsui, L. N. Pfeiffer, K. W. Baldwin, and K. W. West. Fractional quantum hall effect of composite fermions. *Phys. Rev. Lett.*, 90:016801, Jan 2003.

[3] H. A. Feritg. Viewpoint: A view from the edge. *Physics*, 2:15, Feb 2009.

[4] J. C. Y. Teo and C. L. Kane. From luttinger liquid to non-abelian quantum hall states. *Phys. Rev. B*, 89:085101, Feb 2014.

[5] X. L. Qi and S. C. Zhang. Topological insulators and superconductors. *Rev. Mod. Phys.*, 83:1057, 2011.

[6] M. Z. Hasan and C. L. Kane. Topological insulators. *Rev. Mod. Phys.*, 82:3045, 2010.

[7] S. Murakami. Phase transition between the quantum spin hall and insulator phases in 3d: emergence of a topological gapless phase. *New J. Phys.*, 9:356, 2007.

[8] Y. Xia, D. Qian, D. Hsieh, L. Wray, A. Pal, H. Lin, A. Bansil, D. Grauer, Y. S. Hor, R. J. Cava, and M. Z. Hasan. Observation of a large-gap topological-insulator class with a single dirac cone on the surface. *Nat. Phys.*, 5:398–402, 06 2009.

[9] E. Witten. Quantum field theory and the jones polynomial. *Comm. Math. Phys.*, 121:351, 1989.

[10] G. Moore and N. Seiberg. Classical and quantum conformal field theory. *Comm. Math. Phys.*, 123:177, 1989.

[11] E. Witten. Global aspects of current algebra. *Nuclear Physics B*, 223(2):422 – 432, 1983.

[12] K. v. Klitzing, G. Dorda, and M. Pepper. New Method for High-Accuracy Determination of the Fine-Structure Constant Based on Quantized Hall Resistance. *Phys. Rev. Lett.*, 45(6):494–, August 1980.

[13] D. C. Tsui, H. L. Stormer, and A. C. Gossard. Two-dimensional magnetotransport in the extreme quantum limit. *Phys. Rev. Lett.*, 48:1559, 1982.

[14] R. E. Prange and S. M. Girvin. *The Quantum Hall Effect*. Springer, New York, 1987.

[15] X. G. Wen. *Quantum field theory of many-body systems: from the origin of sound to an origin of light and electrons*. Oxford University Press Oxford, 2004.

[16] T. H. Hansson, M. Hermanns, S. H. Simon, and S. F. Viefers. Quantum hall physics: Hierarchies and conformal field theory techniques. *Rev. Mod. Phys.*, 89:025005, May 2017.

[17] X. G. Wen. Topological orders and edge excitations in fractional quantum hall states. *Advances in Physics*, 44(5):405, 1995.

[18] C. L. Kane, R. Mukhopadhyay, and T. C. Lubensky. Fractional quantum hall effect in an array of quantum wires. *Phys. Rev. Lett.*, 88:036401, Jan 2002.

[19] D. F. Mross, J. Alicea, and O. I. Motrunich. Explicit derivation of duality between a free dirac cone and quantum electrodynamics in $(2+1)$ dimensions. *Phys. Rev. Lett.*, 117:016802, Jun 2016.

[20] D. F. Mross, J. Alicea, and O. I. Motrunich. Symmetry and duality in bosonization of two-dimensional dirac fermions. *Phys. Rev. X*, 7:041016, Oct 2017.

[21] S. Sahoo, Z. Zhang, and J. C. Y. Teo. Coupled wire model of symmetric majorana surfaces of topological superconductors. *Phys. Rev. B*, 94:165142, Oct 2016.

[22] M. Cheng. Microscopic theory of surface topological order for topological crystalline superconductors. *Phys. Rev. Lett.*, 120:036801, Jan 2018.

[23] S. Hong and L. Fu. Topological order and symmetry anomaly on the surface of topological crystalline insulators.

[24] S. Raza, A. Sirota, and J. C. Y. Teo. From dirac semimetals to topological phases in three dimensions: A coupled-wire construction. *Phys. Rev. X*, 9:011039, Feb 2019.

[25] C. L. Kane and E. J. Mele. Quantum spin hall effect in graphene. *Phys. Rev. Lett.*, 95:226801, 2005.

[26] C. L. Kane and E. J. Mele. Z2 topological order and the quantum spin hall effect. *Phys. Rev. Lett.*, 95:146802, 2005.

[27] L. Fu, C. L. Kane, and E. J. Mele. Topological insulators in three dimensions. *Phys. Rev. Lett.*, 98:106803, 2007.

[28] R. Roy. Topological phases and the quantum spin hall effect in three dimensions. *Phys. Rev. B*, 79:195322, 2009.

[29] J. E. Moore and L. Balents. Topological invariants of time-reversal-invariant band structures. *Phys. Rev. B*, 75(12):121306–, March 2007.

[30] A. P. Schnyder, S. Ryu, A. Furusaki, and A. W. W. Ludwig. Classification of topological insulators and superconductors in three spatial dimensions. *Phys. Rev. B*, 78:195125, 2008.

[31] S. Ryu, A. P. Schnyder, A. Furusaki, and A. W. W. Ludwig. Topological insulators and superconductors: tenfold way and dimensional hierarchy. *New J. Phys.*, 12:065010, 2010.

[32] A. Kitaev. Periodic table for topological insulators and superconductors. *AIP Conf. Proc.*, 1134(1):22–30, May 2009.

[33] C. K. Chiu, J. C. Y. Teo, A. P. Schnyder, and S. Ryu. Classification of topological quantum matter with symmetries. *Rev. Mod. Phys.*, 88:035005, Aug 2016.

[34] L. Fidkowski and A. Kitaev. Effects of interactions on the topological classification of free fermion systems. *Phys. Rev. B*, 81:134509, Apr 2010.

[35] T. Morimoto, A. Furusaki, and C. Mudry. Breakdown of the topological classification $\mathbb{Z}$ for gapped phases of noninteracting fermions by quartic interactions. *Phys. Rev. B*, 92:125104, Sep 2015.

[36] S. Ryu, J. E. Moore, and A. W. W. Ludwig. Electromagnetic and gravitational responses and anomalies in topological insulators and superconductors. *Phys. Rev. B*, 85(4):045104, January 2012.

[37] E. Witten. Fermion path integrals and topological phases. *Rev. Mod. Phys.*, 88:035001, July 2016.

[38] Z. C. Gu and X. G. Wen. Tensor-entanglement-filtering renormalization approach and symmetry-protected topological order. *Phys. Rev. B*, 80(15):155131–, October 2009.

[39] X. Chen, Z. C. Gu, Z. X. Liu, and X. G. Wen. Symmetry protected topological orders and the group cohomology of their symmetry group. *Phys. Rev. B*, 87:155114, 2013.

[40] A. Kapustin, R. Thorngren, A. Turzillo, and Z. Wang. Fermionic symmetry protected topological phases and cobordisms. *Journal of High Energy Physics*, 2015(12):1–21, Dec 2015.

[41] Y. M. Lu and A. Vishwanath. Theory and classification of interacting 'integer' topological phases in two dimensions: A Chern-Simons approach. *Phys. Rev. B*, 86:125119, 2012.

[42] P. L. e S. Lopes, V. Quito, B. Han, and J. C. Y. Teo. A non-abelian twist to integer quantum hall states.

[43] F. Wilczek. *Fractional Statistics and Anyon Superconductivity*. World Scientific, 1990.

[44] X. G. Wen. *Quantum Field Theory of Many Body Systems*. Oxford Univ. Press, Oxford, 2004.

[45] C. Nayak, S. H. Simon, A. Stern, M. Freedman, and S. Das Sarma. Non-abelian anyons and topological quantum computation. *Rev. Mod. Phys.*, 80:1083–1159, Sep 2008.

[46] R. Franz and G. Wiedemann. Ueber die wärme-leitungsfähigkeit der metalle. *Annalen der Physik*, 165(8):497–531, 1853.

[47] S. Trebst, M. Troyer, Z. Wang, and A. W. W. Ludwig. A short introduction to fibonacci anyon models. *Progress of Theoretical Physics Supplement*, 176:384–407, 2008.

[48] N. Read and E. Rezayi. Beyond paired quantum hall states: Parafermions and incompressible states in the first excited landau level. *Phys. Rev. B.*, 59:8084, 1999.

[49] R. S. K. Mong, D. J. Clarke, J. Alicea, N. H. Lindner, P. Fendley, C. Nayak, Y. Oreg, A. Stern, E. Berg, K. Shtengel, and M. P.A. Fisher. Universal topological quantum computation from a superconductor-abelian quantum hall heterostructure. *Phys. Rev. X*, 4:011036, Mar 2014.

[50] Y. Hu and C. L. Kane. Fibonacci topological superconductor. *Phys. Rev. Lett.*, 120:066801, Feb 2018.

[51] E. Rowell, R. Stong, and Z. Wang. On classification of modular tensor categories. *Communications in Mathematical Physics*, 292(2):343–389, Dec 2009.

[52] F. A. Bais and P. G. Bouwknegt. A classification of subgroup truncations of the bosonic string. *Nuclear Physics B*, 279(3):561 – 570, 1987.

[53] S. Garibaldi. E8 the most exceptional lie group. *Bulletin of the American Mathematical Society*, 53(4):643–671, 2016.

[54] P. Di Francesco, P. Mathieu, and D. Senechal. *Conformal Field Theory*. Springer, New York, 1999.

[55] J. Wess and B. Zumino. Consequences of anomalous ward identities. *Physics Letters B*, 37(1):95 – 97, 1971.

[56] E. Fradkin. *Field Theories of Condensed Matter Physics*. Cambridge University Press, second edition, 2013.

[57] F. D. M. Haldane. Stability of chiral luttinger liquids and abelian quantum hall states. *Phys. Rev. Lett.*, 74:2090–2093, Mar 1995.

[58] B. I. Halperin. Quantized hall conductance, current-carrying edge states, and the existence of extended states in a two-dimensional disordered potential. *Phys. Rev. B*, 25:2185–2190, Feb 1982.

[59] X. G. Wen. Chiral luttinger liquid and the edge excitations in the fractional quantum hall states. *Phys. Rev. B*, 41:12838, 1990.

[60] C. L. Kane and M. P. A. Fisher. Quantized thermal transport in the fractional quantum hall effect. *Phys. Rev. B*, 55:15832–15837, Jun 1997.

[61] A. Cappelli, M. Huerta, and G. R. Zemba. Thermal transport in chiral conformal theories and hierarchical quantum hall states. *Nuclear Physics B*, 636(3):568 – 582, 2002.

[62] A. Kitaev. Anyons in an exactly solved model and beyond. *Annals of Physics*, 321(1):2 – 111, 2006. January Special Issue.

[63] A. Vishwanath and T. Senthil. Physics of three-dimensional bosonic topological insulators: Surface-deconfined criticality and quantized magnetoelectric effect. *Phys. Rev. X*, 3:011016, 2013.

[64] C. Wang, A. C. Potter, and T. Senthil. Classification of interacting electronic topological insulators in three dimensions. *Science*, 343(6171):629–631, 2014.

[65] M. Z. Hasan and J. E. Moore. Three-dimensional topological insulators. *Annual Review of Condensed Matter Physics*, 2(1):55–78, 2011.

[66] J. Cano, M. Cheng, M. Mulligan, C. Nayak, E. Plamadeala, and J. Yard. Bulk-edge correspondence in $(2+1)$-dimensional abelian topological phases. *Phys. Rev. B*, 89:115116, Mar 2014.

[67] A. Sirota, S. Sahoo, G. Y. Cho, and J. C. Y. Teo. Paired parton quantum Hall states: a coupled wire construction. *arXiv e-prints*, page arXiv:1812.01642, December 2018.

[68] D. F. Mross, J. Alicea, and O. I. Motrunich. Bosonic analogue of dirac composite fermi liquid. *Phys. Rev. Lett.*, 117:136802, Sep 2016.

[69] Y. Fuji and A. Furusaki. Quantum hall hierarchy from coupled wires.

[70] A. N. Schellekens. Meromorphic c=24 conformal field theories. *Communications in Mathematical Physics*, 153(1):159–185, Apr 1993.

[71] A.N. Schellekens and S. Yankielowicz. Curiosities at c=24. *Physics Letters B*, 226(3):285 – 290, 1989.

[72] B. Han and J. C. Y. Teo. Coupled-wire description of surface *ade* topological order. *Phys. Rev. B*, 99:235102, Jun 2019.

[73] C. Wang, A. C. Potter, and T. Senthil. Gapped symmetry preserving surface state for the electron topological insulator. *Phys. Rev. B*, 88:115137, Sep 2013.

[74] M. A. Metlitski, C. L. Kane, and M. P. A. Fisher. Symmetry-respecting topologically ordered surface phase of three-dimensional electron topological insulators. *Phys. Rev. B*, 92:125111, Sep 2015.

[75] X. Chen, L. Fidkowski, and A. Vishwanath. Symmetry enforced non-abelian topological order at the surface of a topological insulator. *Phys. Rev. B*, 89:165132, Apr 2014.

[76] P. Bonderson, C. Nayak, and X. L. Qi. A time-reversal invariant topological phase at the surface of a 3d topological insulator. *Journal of Statistical Mechanics: Theory and Experiment*, 2013(09):P09016, 2013.

[77] M. N. Khan, J. C. Y. Teo, and T. L. Hughes. Anyonic symmetries and topological defects in abelian topological phases: An application to the *ade* classification. *Phys. Rev. B*, 90:235149, Dec 2014.

[78] M. N. Khan, J. C. Y. Teo, T. L. Hughes, and S. Vishveshwara. Fermion parity flips and majorana bound states at twist defects in superconducting fractional topological phases. *arXiv:1603.04427*, 2016.

[79] Y. Ando and L. Fu. Topological crystalline insulators and topological superconductors: From concepts to materials. *Annual Review of Condensed Matter Physics*, 6(1):361–381, 2015.

[80] J. Maciejko, X. L. Qi, A. Karch, and S. C. Zhang. Fractional topological insulators in three dimensions. *Phys. Rev. Lett.*, 105:246809, 2010.

[81] C. S. O'Hern, T. C. Lubensky, and J. Toner. Sliding phases in XY models, crystals, and cationic lipid-dna complexes. *Phys. Rev. Lett.*, 83:2745–2748, Oct 1999.

[82] V. J. Emery, E. Fradkin, S. A. Kivelson, and T. C. Lubensky. Quantum theory of the smectic metal state in stripe phases. *Phys. Rev. Lett.*, 85:2160–2163, Sep 2000.

[83] A. Vishwanath and D. Carpentier. Two-dimensional anisotropic non-fermi-liquid phase of coupled luttinger liquids. *Phys. Rev. Lett.*, 86:676–679, Jan 2001.

[84] S. L. Sondhi and K. Yang. Sliding phases via magnetic fields. *Phys. Rev. B*, 63:054430, Jan 2001.

[85] R. Mukhopadhyay, C. L. Kane, and T. C. Lubensky. Crossed sliding luttinger liquid phase. *Phys. Rev. B*, 63:081103, Feb 2001.

[86] R. B. Laughlin. Anomalous quantum hall effect: An incompressible quantum fluid with fractionally charged excitations. *Phys. Rev. Lett.*, 50:1395–1398, May 1983.

[87] F. D. M. Haldane. Fractional quantization of the hall effect: A hierarchy of incompressible quantum fluid states. *Phys. Rev. Lett.*, 51:605, 1983.

[88] B. I. Halperin. Statistics of quasiparticles and the hierarchy of fractional quantized hall states. *Phys. Rev. Lett.*, 52:1583, 1984.

[89] E. Sagi, Y. Oreg, A. Stern, and B. I. Halperin. Imprint of topological degeneracy in quasi-one-dimensional fractional quantum hall states. *Phys. Rev. B*, 91:245144, Jun 2015.

[90] C. L. Kane, A. Stern, and B. I. Halperin. Pairing in luttinger liquids and quantum hall states. *Phys. Rev. X*, 7:031009, Jul 2017.

[91] C. L. Kane and A. Stern. Coupled wire model of Z_4 orbifold quantum hall states. *Phys. Rev. B*, 98:085302, Aug 2018.

[92] J. Klinovaja and D. Loss. Integer and fractional quantum hall effect in a strip of stripes. *The European Physical Journal B*, 87:171, 2014.

[93] Y. Oreg, E. Sela, and A. Stern. Fractional helical liquids in quantum wires. *Phys. Rev. B*, 89:115402, Mar 2014.

[94] T. Meng, T. Neupert, M. Greiter, and R. Thomale. Coupled-wire construction of chiral spin liquids. *Phys. Rev. B*, 91:241106, Jun 2015.

[95] T. Meng. Fractional topological phases in three-dimensional coupled-wire systems. *Phys. Rev. B*, 92:115152, Sep 2015.

[96] T. Iadecola, T. Neupert, C. Chamon, and C. Mudry. Wire constructions of abelian topological phases in three or more dimensions. *Phys. Rev. B*, 93:195136, May 2016.

[97] T. Iadecola, T. Neupert, C. Chamon, and C. Mudry. Non-Abelian topological phases in three spatial dimensions from coupled wires. *ArXiv e-prints*, March 2017.

[98] M. M. Vazifeh. Weyl semimetal from the honeycomb array of topological insulator nanowires. *EPL (Europhysics Letters)*, 102(6):67011, 2013.

[99] M. J. Park, S. Raza, M. J. Gilbert, and J. C. Y. Teo. Coupled Wire Models of Interacting Dirac Nodal Superconductors. *ArXiv e-prints*, June 2018.

[100] T. Meng, A. G. Grushin, K. Shtengel, and J. H. Bardarson. Theory of a 3+1d fractional chiral metal: Interacting variant of the weyl semimetal. *Phys. Rev. B*, 94:155136, Oct 2016.

[101] D. F. Mross, A. Essin, and J. Alicea. Composite dirac liquids: Parent states for symmetric surface topological order. *Phys. Rev. X*, 5:011011, Feb 2015.

[102] J. C. Y. Teo and C. L. Kane. Topological defects and gapless modes in insulators and superconductors. *Phys. Rev. B*, 82:115120, Sep 2010.

[103] S. Sahoo, A. Sirota, G. Y. Cho, and J. C. Y. Teo. Surfaces and slabs of fractional topological insulator heterostructures. *Phys. Rev. B*, 96:161108, Oct 2017.

[104] F. J. Burnell, X. Chen, L. Fidkowski, and A. Vishwanath. Exactly soluble model of a three-dimensional symmetry-protected topological phase of bosons with surface topological order. *Phys. Rev. B*, 90:245122, Dec 2014.

[105] I. Affleck, T. Kennedy, E. H. Lieb, and H. Tasaki. Rigorous results on valence-bond ground states in antiferromagnets. *Phys. Rev. Lett.*, 59:799–802, Aug 1987.

[106] I. Affleck, T. Kennedy, E. H. Lieb, and H. Tasaki. Valence bond ground states in isotropic quantum antiferromagnets. *Comm. Math. Phys.*, 115(3):477–528, 1988.

[107] R. J. Baxter. *Exactly Solved Models in Statistical Mechanics*. Dover Publications, 1982.

[108] P. S. Hsin and N. Seiberg. Level/rank duality and chern-simons-matter theories. *Journal of High Energy Physics*, 2016(9):95, Sep 2016.

[109] O. Aharony, F. Benini, P. S. Hsin, and N. Seiberg. Chern-simons-matter dualities with so and usp gauge groups. *Journal of High Energy Physics*, 2017(2):72, Feb 2017.

[110] N. Seiberg, T. Senthil, C. Wang, and E. Witten. A duality web in 2+1 dimensions and condensed matter physics. *Annals of Physics*, 374:395 – 433, 2016.

[111] A. Karch and D. Tong. Particle-vortex duality from 3d bosonization. *Phys. Rev. X*, 6:031043, Sep 2016.

[112] F. D. M. Haldane. Stability of chiral luttinger liquids and abelian quantum hall states. *Phys. Rev. Lett.*, 74:2090–2093, Mar 1995.

[113] L. Fidkowski, X. Chen, and A. Vishwanath. Non-abelian topological order on the surface of a 3d topological superconductor from an exactly solved model. *Phys. Rev. X*, 3:041016, Nov 2013.

[114] W. P. Su, J. R. Schrieffer, and A. J. Heeger. Soliton excitations in polyacetylene. *Phys. Rev. B*, 22:2099–2111, Aug 1980.

[115] F. D. M. Haldane. Continuum dynamics of the 1-d heisenberg antiferromagnet: Identification with the o(3) nonlinear sigma model. *Physics Letters A*, 93(9):464 – 468, 1983.

[116] F. D. M. Haldane. Nonlinear field theory of large-spin heisenberg antiferromagnets: Semiclassically quantized solitons of the one-dimensional easy-axis néel state. *Phys. Rev. Lett.*, 50:1153–1156, Apr 1983.

[117] E. Witten. The "parity" anomaly on an unorientable manifold. *Phys. Rev. B*, 94:195150, Nov 2016.

[118] N. Seiberg and E. Witten. Gapped boundary phases of topological insulators via weak coupling. *Progress of Theoretical and Experimental Physics*, 2016(12):12C101, 2016.

[119] J. Cardy. *Scaling and Renormalization in Statistical Physics*. Cambridge University Press, 1996.

[120] D. J. Gross and A. Neveu. Dynamical symmetry breaking in asymptotically free field theories. *Phys. Rev. D*, 10:3235–3253, Nov 1974.

[121] J. C. Y. Teo, L. Fu, and C. L. Kane. Surface states and topological invariants in three-dimensional topological insulators: Application to $\mathrm{bi}_{1-x}\mathrm{sb}_x$. *Phys. Rev. B*, 78:045426, Jul 2008.

[122] L. Fu. Topological crystalline insulators. *Phys. Rev. Lett.*, 106:106802, Mar 2011.

[123] B. Han, A. Tiwari, C. T. Hsieh, and S. Ryu. Boundary conformal field theory and symmetry-protected topological phases in $2+1$ dimensions. *Phys. Rev. B*, 96:125105, Sep 2017.

[124] X. Chen, Z. X. Liu, and X. G. Wen. Two-dimensional symmetry-protected topological orders and their protected gapless edge excitations. *Phys. Rev. B*, 84(23):235141–, December 2011.

[125] H. Song, S.J. Huang, L. Fu, and M. Hermele. Topological phases protected by point group symmetry. *Phys.Rev.X*, 7(1):011020, 2017.

[126] X. Chen, Z. C. Gu, Z. X. Liu, and X. G. Wen. Symmetry protected topological orders in interacting bosonic systems. *Science*, 338:1604, 2012.

[127] F. Pollmann, E. Berg, A. M. Turner, and M. Oshikawa. Symmetry protection of topological phases in one-dimensional quantum spin systems. *Phys.Rev.B*, 85(7):075125, 2012.

[128] L. Fidkowski and A. Kitaev. Topological phases of fermions in one dimension. *Phys.Rev.B*, 83(7):075103, 2011.

[129] S. Ryu and S. C. Zhang. Interacting topological phases and modular invariance. *Phys.Rev.B*, 85(24):245132, 2012.

[130] O. M. Sule, X. Chen, and S. Ryu. Symmetry-protected topological phases and orbifolds: Generalized laughlin's argument. *Phys.Rev.B*, 88(7):075125, 2013.

[131] C. T. Hsieh, G. Y. Cho, and S. Ryu. Global anomalies on the surface of fermionic symmetry-protected topological phases in (3+1) dimensions. *Phys.Rev.B*, 93(7):075135, 2016.

[132] E. Witten. Fermion path integrals and topological phases. *Rev. Mod. Phys.*, 88(3):035001, 2016.

[133] X. Chen, A. Tiwari, and S. Ryu. Bulk- correspondence in (3+1)-dimensional topological phases. *Phys.Rev.B*, 94(4):045113, 2016.

[134] R. E. Behrend, P. A. Pearce, V. B. Petkova, and J.-B. Zuber. Boundary conditions in rational conformal field theories. *Nucl.Phys.B*, 570:525–589, March 2000.

[135] N. Sousa and A. N. Schellekens. Orientation matters for nimreps. *Nucl.Phys.B*, 653(3):339–368, 2003.

[136] L. H. Santos and J. Wang. Symmetry-protected many-body aharonov-bohm effect. *Phys.Rev.B*, 89(19):195122, 2014.

[137] G. Y. Cho, K. Shiozaki, S. Ryu, and A. W. W. Ludwig. Relationship between Symmetry Protected Topological Phases and Boundary Conformal Field Theories via the Entanglement Spectrum. June.

[138] M. Miyaji, S. Ryu, T. Takayanagi, and X. Wen. Boundary states as holographic duals of trivial spacetimes. *Journal of High Energy Physics*, 5:152, May 2015.

[139] G. Y. Cho, C. T. Hsieh, T. Morimoto, and S. Ryu. Topological phases protected by reflection symmetry and cross-cap states. *Phys.Rev.B*, 91(19):195142, 2015.

[140] C. T. Hsieh, O. M. Sule, G. Y. Cho, S. Ryu, and R. G. Leigh. Symmetry-protected topological phases, generalized laughlin argument, and orientifolds. *Phys.Rev.B*, 90(16):165134, 2014.

[141] J. L. Cardy. Boundary conditions, fusion rules and the verlinde formula. *Nucl.Phys.B*, 324(3):581–596, 1989.

[142] J. Cardy. Boundary conformal field theory. *arXiv: hep-th/0411189*.

[143] N.Ishibashi. The boundary and crosscap states in conformal field theories. *Mod.Phys.Lett.A*, 4:251, 1989.

[144] Z.X. Liu and X.G. Wen. Symmetry-protected quantum spin hall phases in two dimensions. *Phys.Rev.Lett.*, 110(6):067205, 2013.

[145] X.G. Wen. Classifying gauge anomalies through symmetry-protected trivial orders and classifying gravitational anomalies through topological orders. *Phys.Rev.D*, 88(4):045013, 2013.

[146] M. Levin and Z.C. Gu. Braiding statistics approach to symmetry-protected topological phases. *Phys.Rev.B*, 86(11):115109, 2012.

[147] H. Yao and S. Ryu. Interaction effect on topological classification of superconductors in two dimensions. *Phys.Rev.B*, 88(6):064507, 2013.

[148] M. Gaberdiel. unpublished.

[149] R. Blumenhagen and E. Plauschinn. *Introduction to conformal field theory.* Springer,New York, 2009.

[150] A. Recknagel and V. Schomerus. *Boundary conformal field theory and the worldsheet approach to D-branes.* Cambridge University Press, Cambridge, England, 2013.

[151] K. Hori, S. Katz, A. Klemm, R. Pandharipande, R. Thomas, C. Vafa, R. Vakil, and E. Zaslow. *Mirror Symmetry.* American Mathematical Society, Providence, RI, 2003.

[152] M. Oshikawa. Boundary conformal field theory and entanglement entropy in two-dimensional quantum lifshitz critical point. *arXiv:1007.3739.*

[153] X.-L. Qi. A new class of (2 + 1)-dimensional topological superconductors with {Z}_8 topological classification. *New Journal of Physics*, 15(6):065002, June 2013.

[154] R. Blumenhagen, D. Lust, and S. Theisen. *Basic Concepts of String Theory.* Springer, New York, 2013.

[155] D. E. l Diaconescu and J. Gomis. Fractional branes and boundary states in orbifold theories. *Journal of High Energy Physics*, 2000(10):001, 2000.

[156] J. M. Maldacena and A. W. W. Ludwig. Majorana fermions, exact mapping between quantum impurity fixed points with four bulk fermion species, and solution of the "unitarity puzzle". *Nucl.Phys.B*, 506(3):565–588, 1997.

[157] H. Isobe and L. Fu. Theory of interacting topological crystalline insulators. *Phys.Rev.B*, 92(8):081304, 2015.

[158] M. Banerjee, M. Heiblum, A. Rosenblatt, Y. Oreg, D. E. Feldman, A. Stern, and V. Umansky. Observed quantization of anyonic heat flow. *Nature*, 545:75–79, April 2017.

[159] M. Banerjee, M. Heiblum, V. Umansky, D. E. Feldman, Y. Oreg, and A. Stern. Observation of half-integer thermal hall conductance. *Nature*, 559:205, 2018.

[160] P. Ruelle. Kramers-Wannier dualities via symmetries. *Phys. Rev. Lett.*, 95:225701, 2005.

[161] A. J. Macfarlane. Lie algebra and invariant tensor technology for g2. *International Journal of Modern Physics A*, 16(18):3067–3097, 2001.